#3

346750

General Mills

THE GENERAL MILLS ELECTRONICS GROUP

12-M-3146 R-2

General Mills

[redacted]

This document consists of 129 pages, and is number 2 of 45 copies, series A and the following 2 attachments.

THIRTEENTH QUARTERLY PROGRESS REPORT

ON

DISSEMINATION OF SOLID AND LIQUID BW AGENTS

(Unclassified Title)

For Period 4 June 1963 - 4 September 1963
Contract No. DA-18-064-CML-2745

Prepared for:

U. S. Army Biological Laboratories
Fort Detrick, Maryland

Submitted by: G R Whitnah
G. R. Whitnah
Project Manager

Report No: 2451
Project No: 82408
Date: 24 October 1963

Approved by: G. R Whitnah, for
S. P. Jones, Director
Aerospace Research

AEROSPACE RESEARCH
2295 Walnut Street
St. Paul 13, Minnesota

[redacted]

[redacted]

FOREWORD

Staff members of the Aerospace Research Department and Engineering Department who have participated in directing or performing the work reported herein include Messrs. S. P. Jones, Jr., G. Whitnah, M. Sandgren, A. Anderson, D. Stender, R. Lindquist, J. McGillicuddy, J. Upton, P. Stroom, G. Morfitt, A. T. Bauman, T. Petersen, D. Harrington, R. Ackroyd, D. Kedl, B. Schmidt, G. Lunde, R. Dahlberg, R. Kendall, E. Knutson, J. Ungs, J. Pliney, A. Johnson, G. Leiter, C. A. Morris, and K. Pontinen.

ABSTRACT

This Thirteenth Quarterly Progress Report presents the results of work conducted at General Mills, Inc. under Contract No. DA-18-064-CML-2745, "Dissemination of Solid and Liquid BW Agents" during the period 4 June to 4 September 1963.

Valuable information on the properties of powders, both biological simulants (Sm and Bg) and non-biological simulants (such as dried egg albumin and cornstarch), have aided in the development of the E-41 spray tank for the line-source dissemination of dry solid BW agents.

Tensile strength of powders as a function of bulk density and particle size was studied, using the segmented column method. The sliding-disk shear-strength method was used to measure shear characteristics of a number of powders. A methods study was made to determine the relative merits of pre-shearing or not pre-shearing the powder prior to the shear test.

The fundamental behavior of two categories of powders was studied. The resulting data correlate powder properties in a consistent and logical manner.

The newly designed and built Powder Resistometer was used to measure with great precision interparticulate resistance to flow in a number of powders.

Surface area of powders was measured by the BET adsorption method and a mathematical determination of microspore structure of powders was made from these data.

The electron microscope was used to study shape and structure of one powder.

Effects of electrostatic charge and humidity conditions upon aerosol formation and decay were studied with results sufficiently consistent to define the operating range of relative humidity.

Storage of compacted Sm samples was continued with viability assays being made on 2-month and 4-month samples. There was no significant difference between compacted and uncompacted Sm.

[redacted]

The status of work related to the E-41 spray tank is reported. Weight and center of gravity data are presented for the unit when fitted with the new 4-finned tail section. Experiments on compaction of powder within the experimental unit using the piston-screw mechanism for compaction are discussed. Dry lubricants, principally graphite, were found to cause a small decrease in side wall friction of compacted talc. It was found that parafin and sodium silicate could be removed by the piston nut if these materials are applied to the screw threads to keep out the powder. Successful fit tests of the E-41 on the F-100D and F-105 airplanes at Eglin Air Force Base are reported.

Results of a planning meeting at the Navy Department in preparation for testing the E-41 spray tank on the Mohawk airplane are reported.

[redacted]

TABLE OF CONTENTS

TABLE OF CONTENTS (continued)

LIST OF ILLUSTRATIONS

LIST OF ILLUSTRATIONS (continued)

LIST OF ILLUSTRATIONS (continued)

[redacted]

THIRTEENTH QUARTERLY PROGRESS REPORT ON DISSEMINATION OF SOLID AND LIQUID BW AGENTS

1. INTRODUCTION

General Mills, Inc. has completed the thirteenth quarter of work under contract DA-18-064-CML-2745 with the U.S. Army Biological Laboratories. This document reports the progress during this past quarter on the continuing work related to the dissemination of solid and liquid BW agents. The program covers work areas ranging from experimental and theoretical studies of the properties of finely-divided solids to flight tests with full-scale airborne spray tanks.

A variety of dry powders are being used in the experimental work. Some, such as talc, powdered milk, saccharin, powdered sugar and cornstarch, are nonbiological simulants which are readily available and relatively inexpensive. Much valuable information has been obtained with these materials. The biological simulants, Serratia marcescens (Sm) and baccilus globigii (Bg), have also been used extensively but generally only after techniques and equipment have been developed with the nonbiological simulants. Some of the recent work has been done with dried egg albumin, dried egg embryo simulant, and a special, low-density Bg.

Information derived from the study of the properties of powders has been valuable in the development of the E-41 spray tank for line-source dissemination of dry solid BW agents. With the completion of the second E-41 in August, two of these units are now available for use in the BW field test program. One is presently at Eglin AFB for flight tests on the F-100D and F-105 airplanes. The other will be used in the flight tests using a Mohawk airplane flying out of the Patuxent River Naval Air Test Center.

[redacted]

2. STUDIES OF THE FUNDAMENTAL BEHAVIOR OF DRY POWDERS

A program of study is underway to characterize the behavior of powders in the uncompacted state, their behavior during compaction, their behavior in dispersion and in aerosol decay. Such a study should yield information relative to the manufacture, handling, and dissemination of bulk powders. During the current quarter we have examined the tensile strength of powders as a function of bulk density and of particle size, studied the possible effects of preshearing powders prior to performing the shear-strength test, and determined the shear strengths of a number of powders in comparison with their compaction properties. The particle shapes and particle rugosities of a number of powders have been determined. In addition, a new apparatus, the "Powder Resistometer", is now being used to measure the interparticle resistance to flow in a bed of loose powder. It is gratifying to find good correlation of the data from the various physical tests performed.

2.1 Behavior of Powders in the Compacted State

2.1.1 Tensile Strength of Compacted Powders

As the particle size of a powder is reduced, the powder becomes increasingly difficult to compact. This is a result of the increased number of interparticle contacts per unit cross section. To explore this more fully, the segmented column method was used to determine the tensile strength of a number of powders as a function of bulk density and of particle size. Tensile data on powdered sugar and egg albumin are presented as examples of typical behavior of various powders studied. The highly elastic powders such as talc and dried egg embryo simulant have tensile strengths too low to measure. Powdered sugar is typical of the "well behaved" powders, as shown in Figure 2.1a. Powdered sugar as well as the egg albumin (Figure 2.2) shows a marked increase in tensile strength with decreasing particle size at a given bulk density. The tensile strength of the egg albumin rises more sharply with increasing bulk density. In addition, the bulk tensile strength appears to be a function not only of the bulk density but of the compressive load used to obtain this bulk density. Obviously a different mechanism of compaction is involved here.

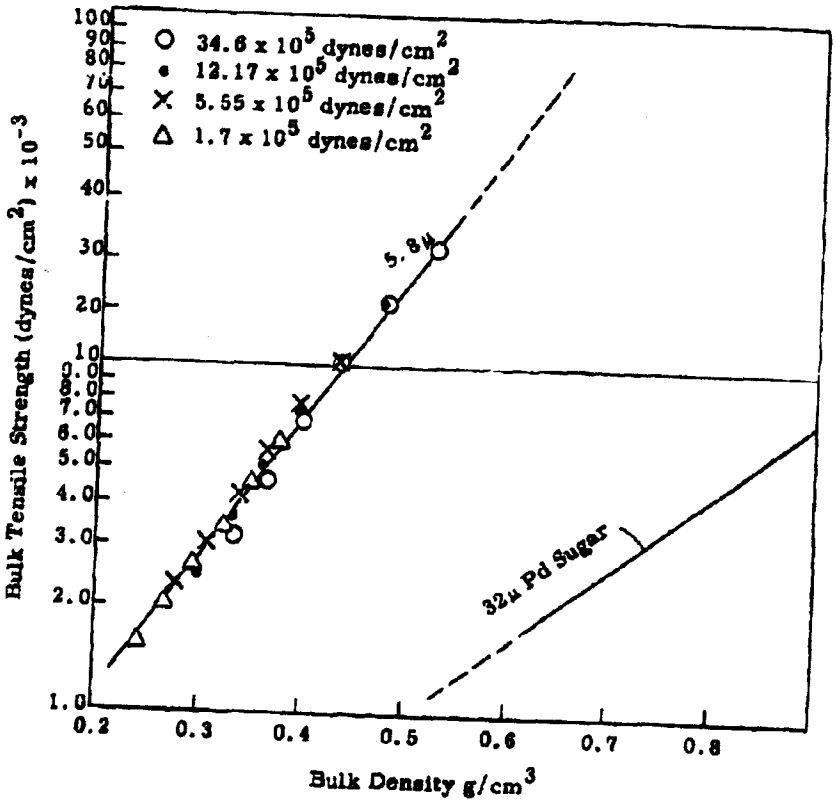

Figure 2.1(a) Bulk Tensile Strength of Powdered Sugar

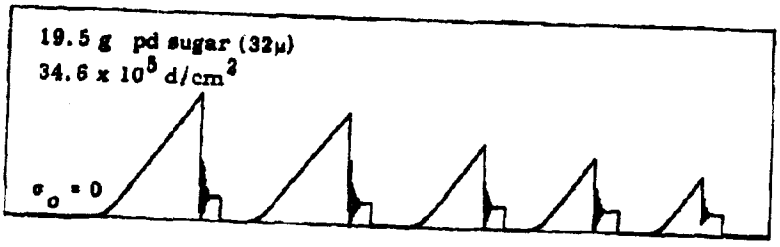

Figure 2.1(b) Sample Record of Data from Sanborn Recorder

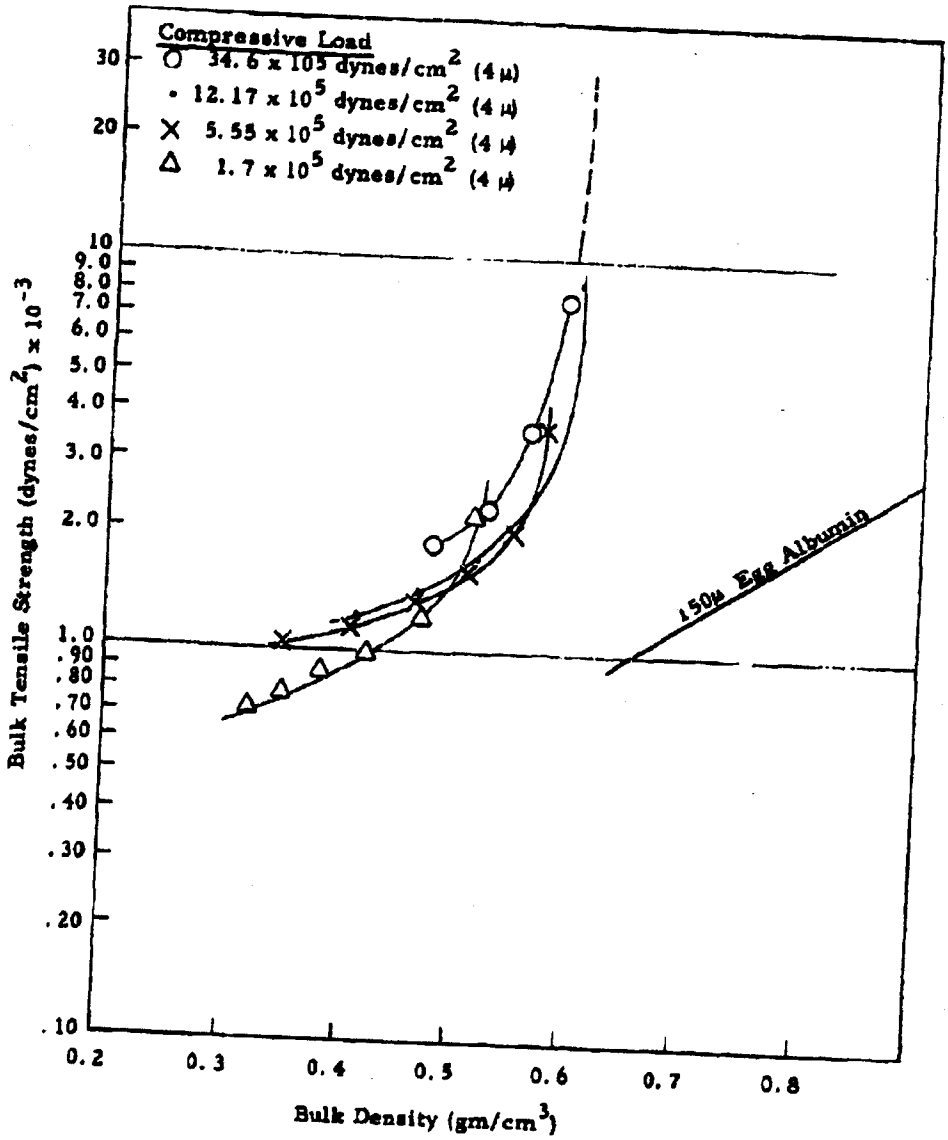

Figure 2.2 Bulk Tensile Strength of Egg Albumin

Auxiliary information routinely obtained in such a study is the variation of bulk density at various compressive loads (Figures 2.3 and 2.4), as well as the column capacity as a function of compressive load (Figure 2.5). This information is useful in comparing differences in degree of compaction and in understanding the mechanisms of compaction. Note the difference in mode of compaction of the two powders as shown in Figures 2.3 and 2.4. Figure 2.1b also includes a simple data recording to show the progressive decrease in tensile strength down the column of powder. The tensile strength of a powder at a given bulk density should relate quite well to its ease of dispersibility. Additionally, it is pertinent to attempt to account for the differences in variation of tensile strength of powdered sugar and egg albumin in relation to other powder properties such as elasticity, particle rugosity, and particle size and shape.

2.1.2 Instron Tensile Method

The segmented-column tensile method has worked so effectively, we have adopted it as our standard method for measuring the tensile strength of powders. The Instron tensile method, developed for comparative purposes, has been abandoned.

2.1.3 Shear Strength of Compacted Powders

2.1.3.1 Method Study

In our use of the sliding-disk method for the measurement of the shear strength of powders it has been routine practice to preshear the powder prior to making the actual shear test. This was adopted in the pioneering stages of test development as a workable procedure to obtain good reproducible results. Since the shear-strength test component of our multipurpose test unit now yields good results even at low compressive loads, a study was recently undertaken to investigate the difference in shear strength of a powder in the preshear and nonpreshear case. It was found that the shear strength could be determined with equal accuracy in either case. The shear strength in the nonpreshear case was uniformly lower than in the preshear case. Interestingly enough, if the

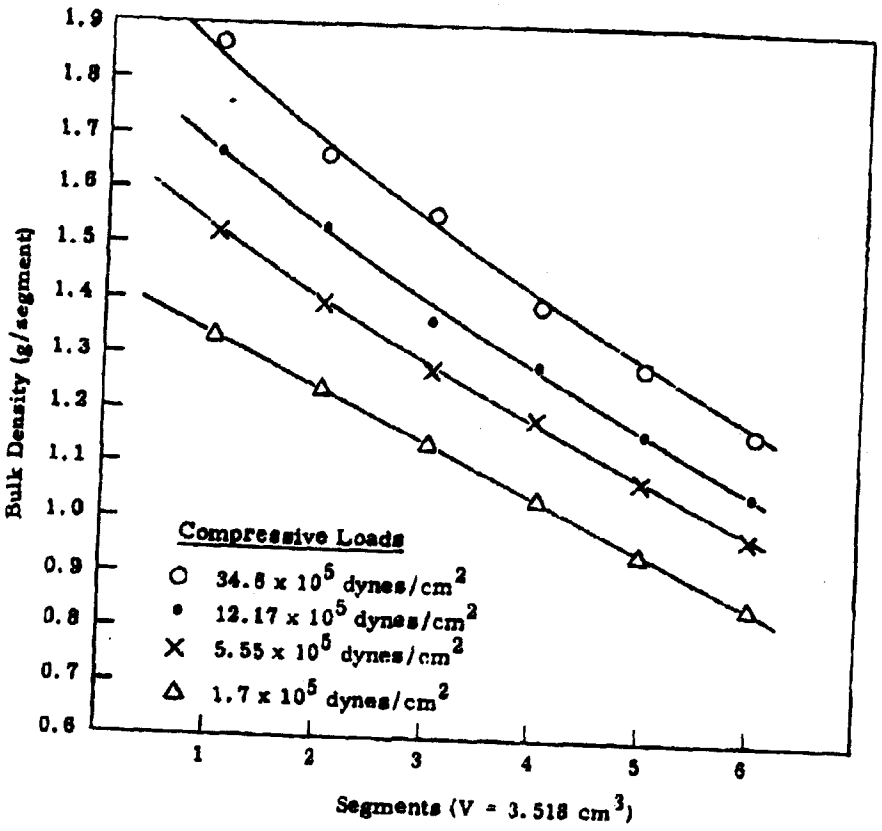

Figure 2.3 Bulk Density Variation of Powdered Sugar (5.8 -)

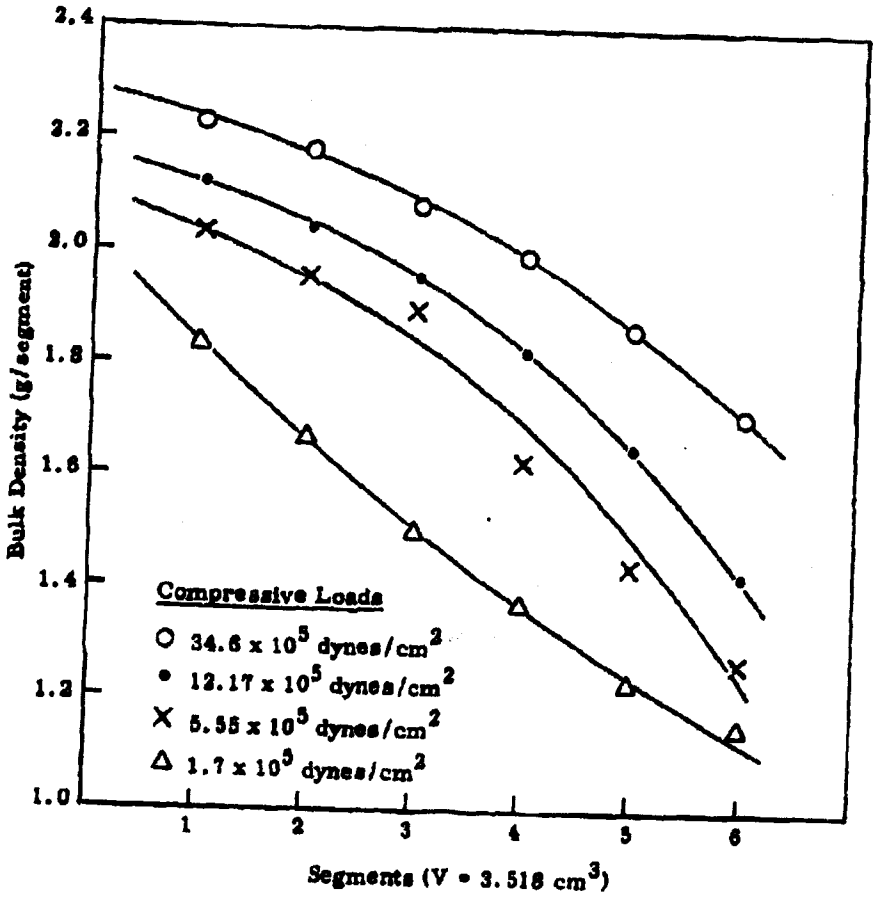

Figure 2.4. Bulk Density Variation of Egg Albumin (4 μ)

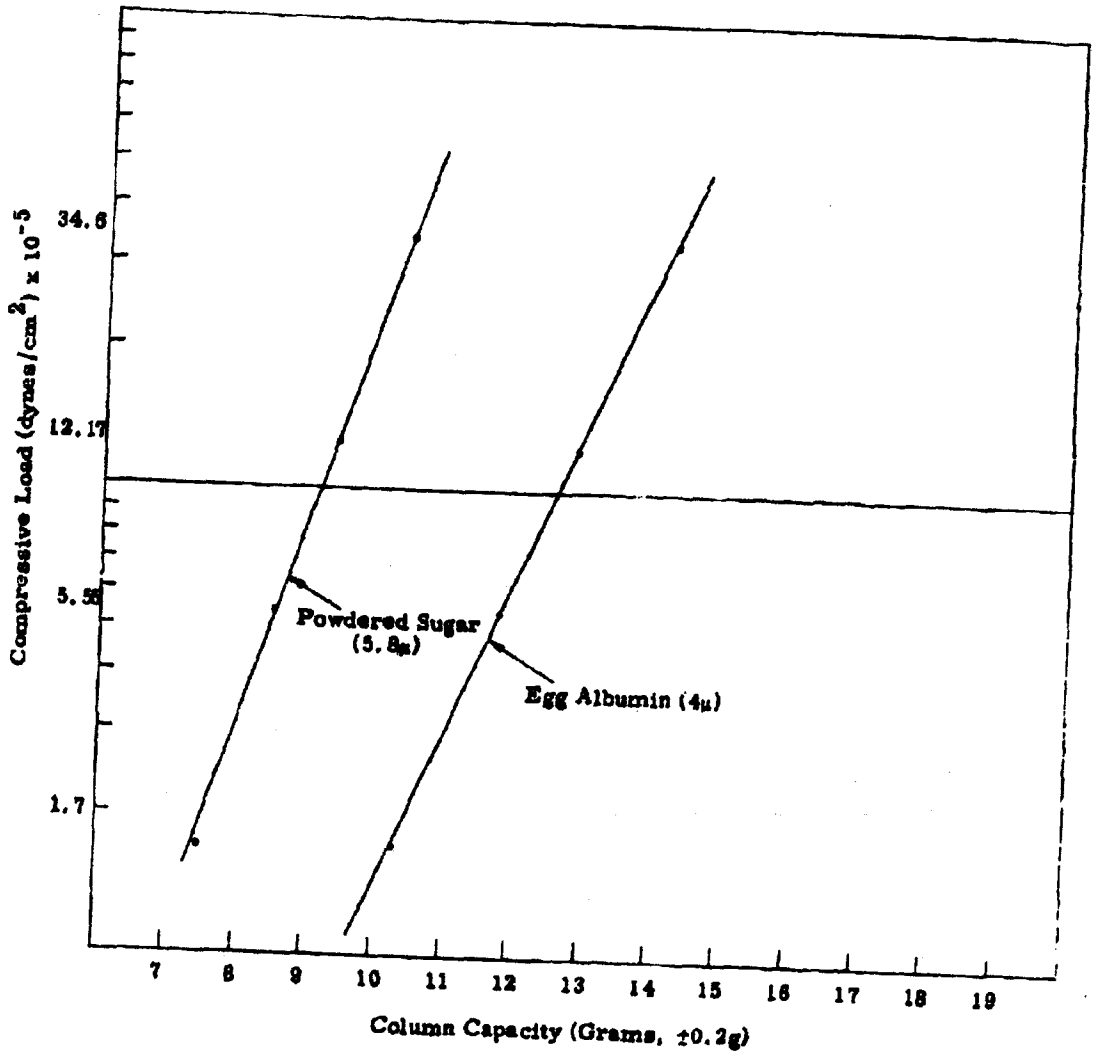

Figure 2.5 Comparative Compaction Characteristics of Powders

disk was allowed to continue to shear following the initial yield point, the shear strength of the nonpreshear case would equilibrate at approximately the same level as the shear strength in the preshear case. Based upon this study and upon previous experience with powders, it is believed that the values obtained from the preshear case are more closely related to the compaction characteristics of powders.

2.1.3.2 Comparative Shear Strength of Powders

In our shear strength studies we are interested in the shear strength of a powder undergoing compaction (compaction shear strength) and in the shear strength of the compacted state. The compaction shear strength is determined by shearing the powder under the same compressive load used to compact it. By contrast, the shear strength of the compacted state is determined by using a certain compressive force to compact the powder to a given bulk density and then measuring its shear strength at successively lower loads. The compressive force levels used are in the range of (0.25 to 8) x 10^4 dynes/cm^2. The compaction of a powder results in a change in the number and energy level of the interparticle contacts, in cohesive strength, in mechanical interlocking of particles, in plastic and/or elastic deformation of particles, and in an increase in the "stored up" elastic energy. When the shear strength of the compacted state is determined, the powder is compacted at a higher load and measured at a lower load as described above. If, as the heavier load is removed, the powder undergoes complete recovery, the shear strength would be identical to that of the lower load, and the two shear strength curves could be superimposed. Therefore, the difference in slope of the two plots becomes a measure of the cohesive strength and elastic-recovery properties of the powder. It has become routine practice to record, for comparative purposes, the compaction shear strength and the shear strength of a powder precompacted at the highest load (8 x 10^4 dynes/cm^2). Typical examples of recent work are shown in Figures 2.8 to 2.10. It is informative to compare the two shear strengths individually as shown on Figures 2.11 and 2.12. The comparative differences in three individual lots of Sm are shown in Figure 2.13. The correlation of these data, as well as the study of the three lots of Sm, will be

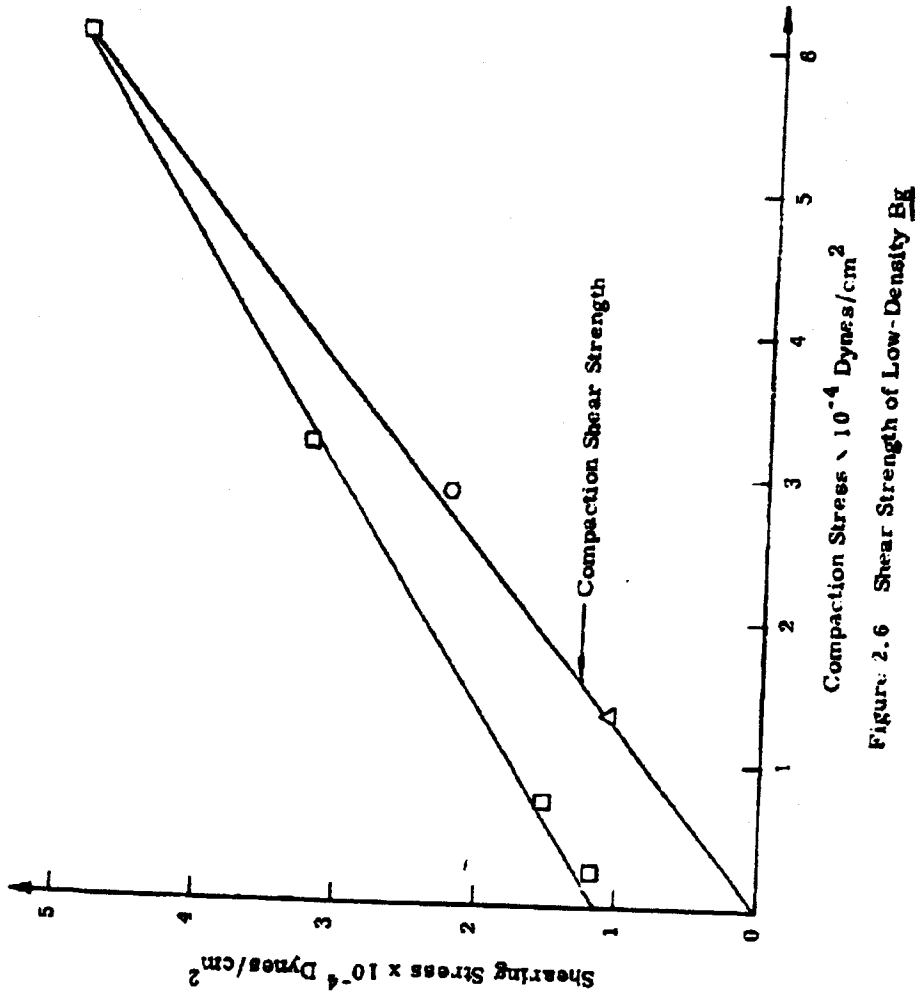

Figure 2.6 Shear Strength of Low-Density Be

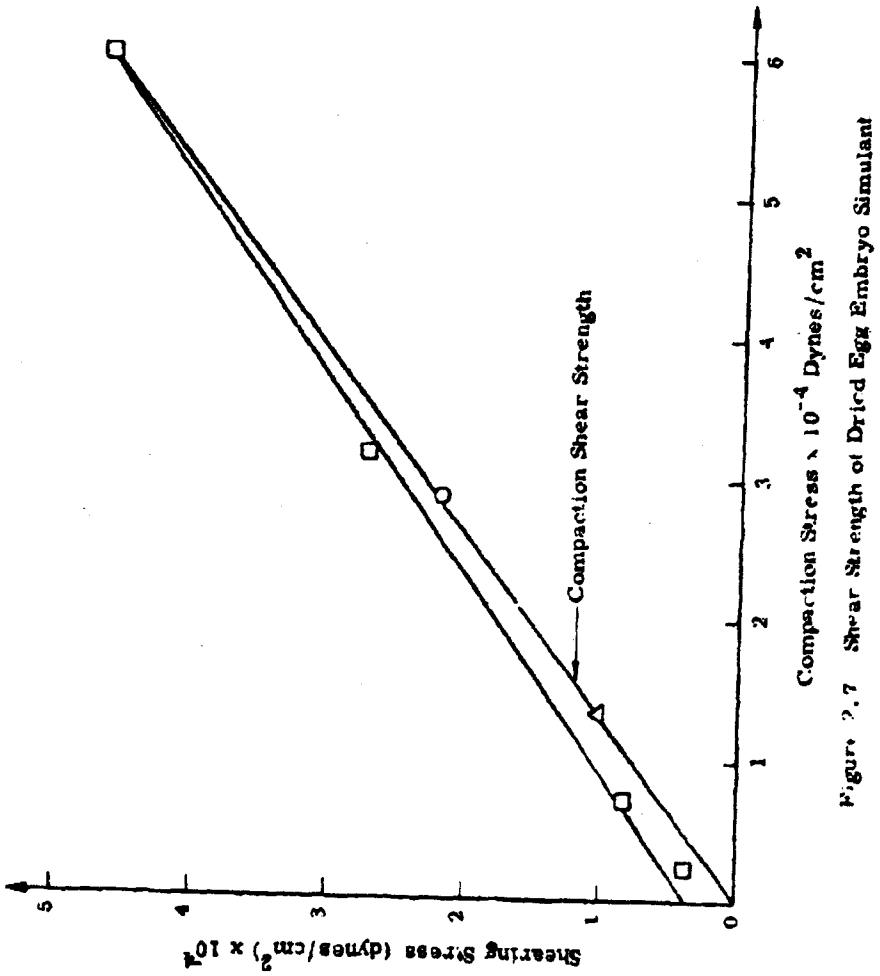

Figure 2.7 Shear Strength of Dried Egg Embryo Simulant

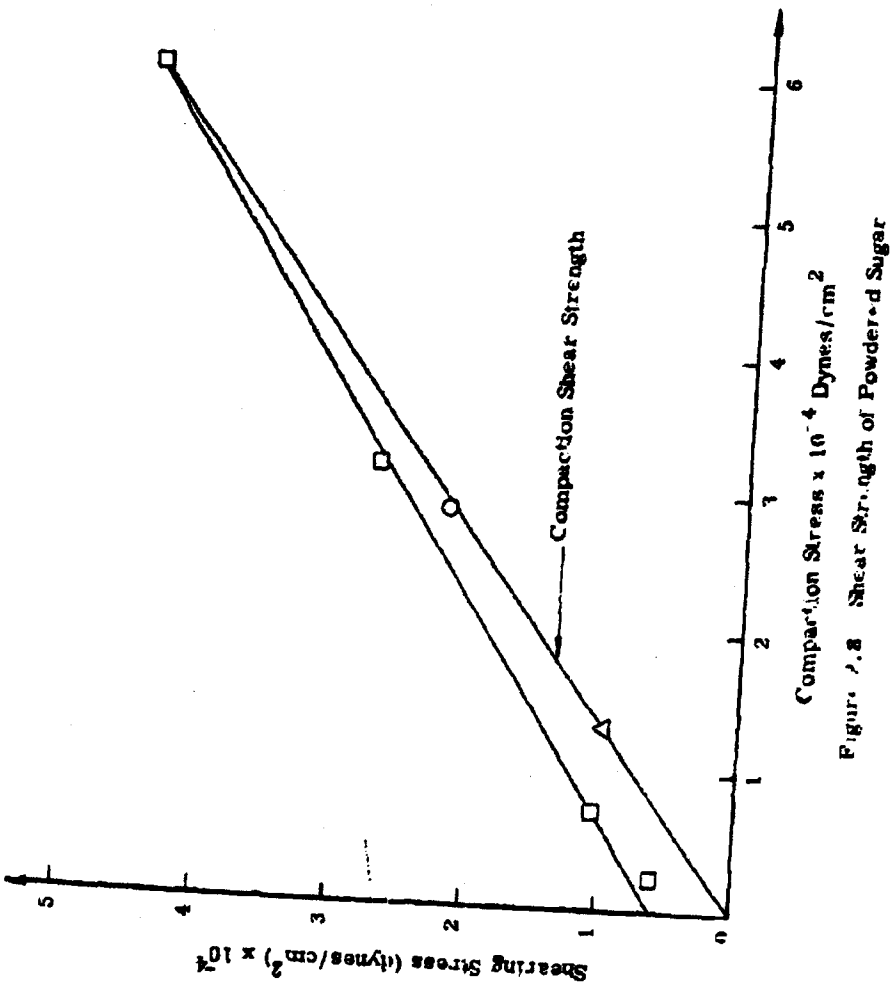

Figure 2.8 Shear Strength of Powdered Sugar

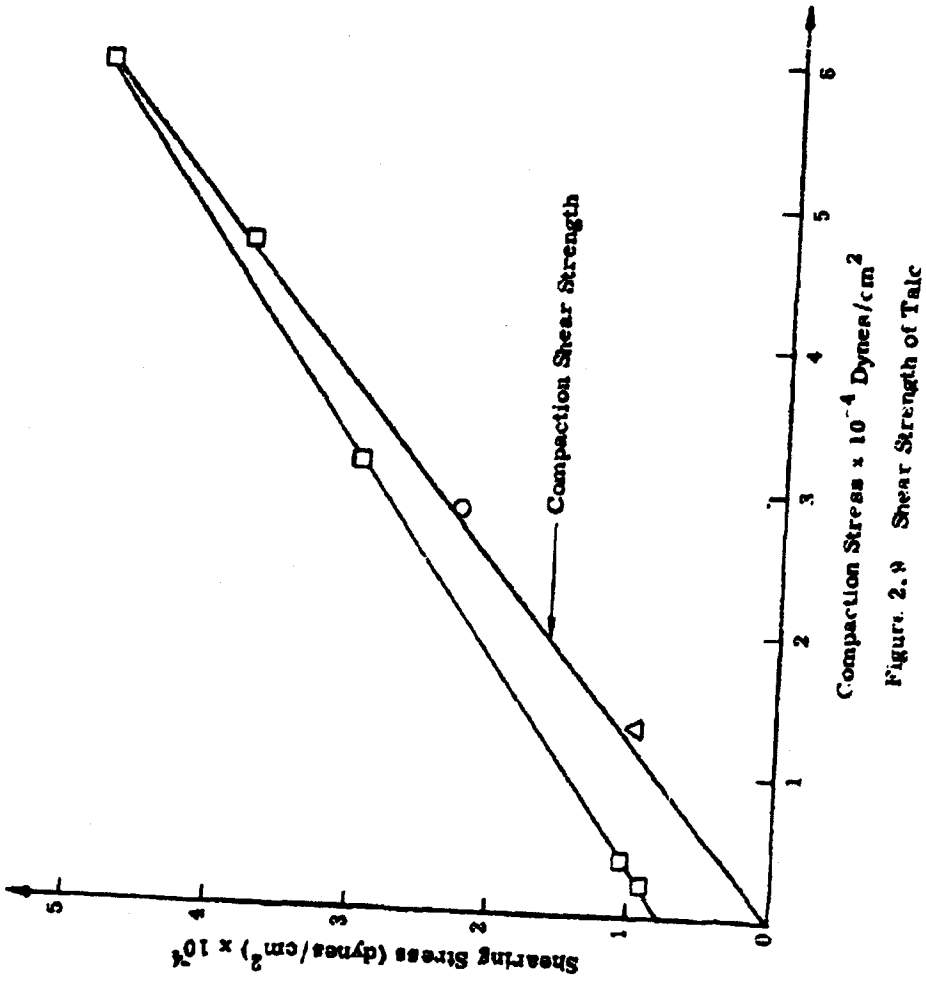

Figure 2.9 Shear Strength of Talc

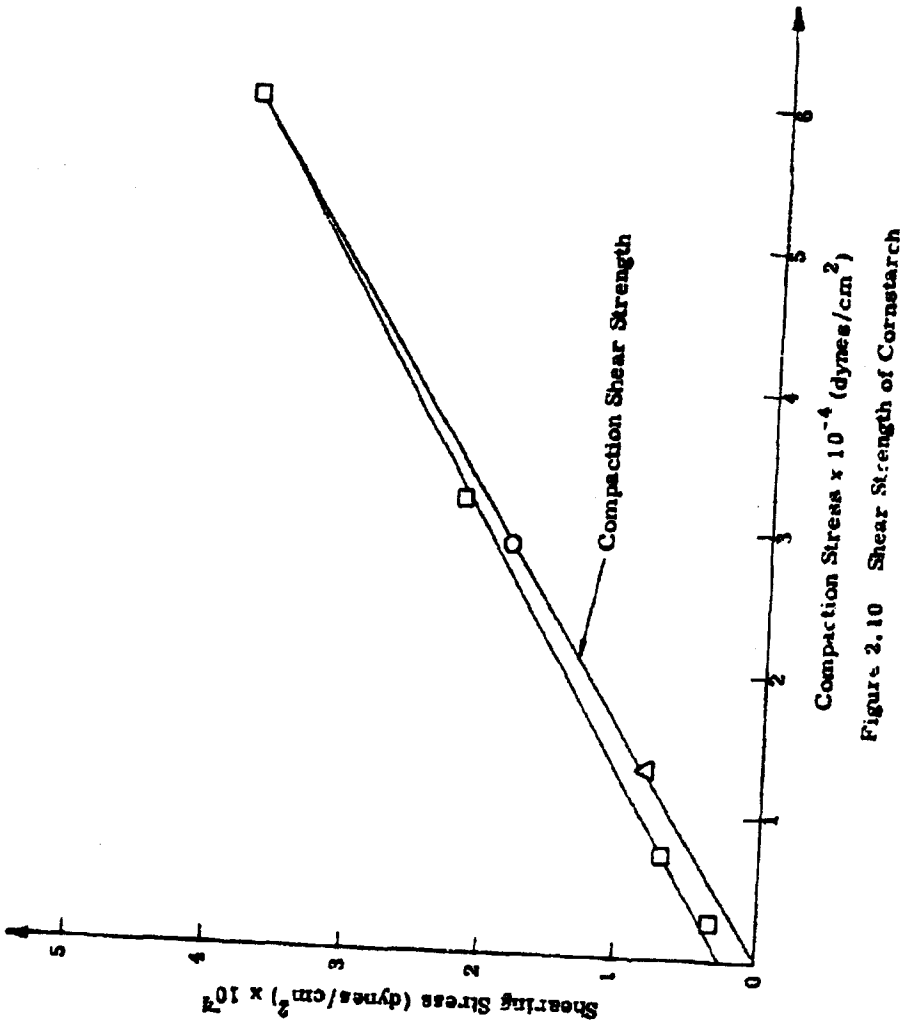

Figure 2.10 Shear Strength of Cornstarch

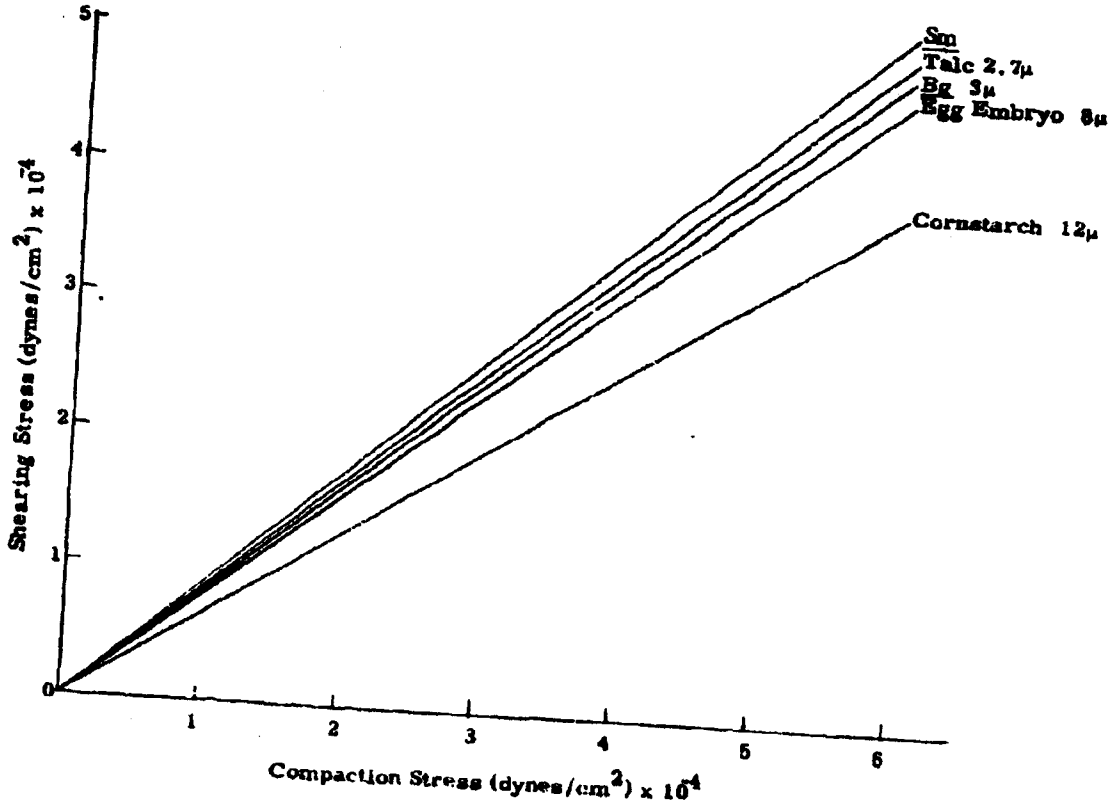

Figure 2.11 Compaction Shear Strength of Powders

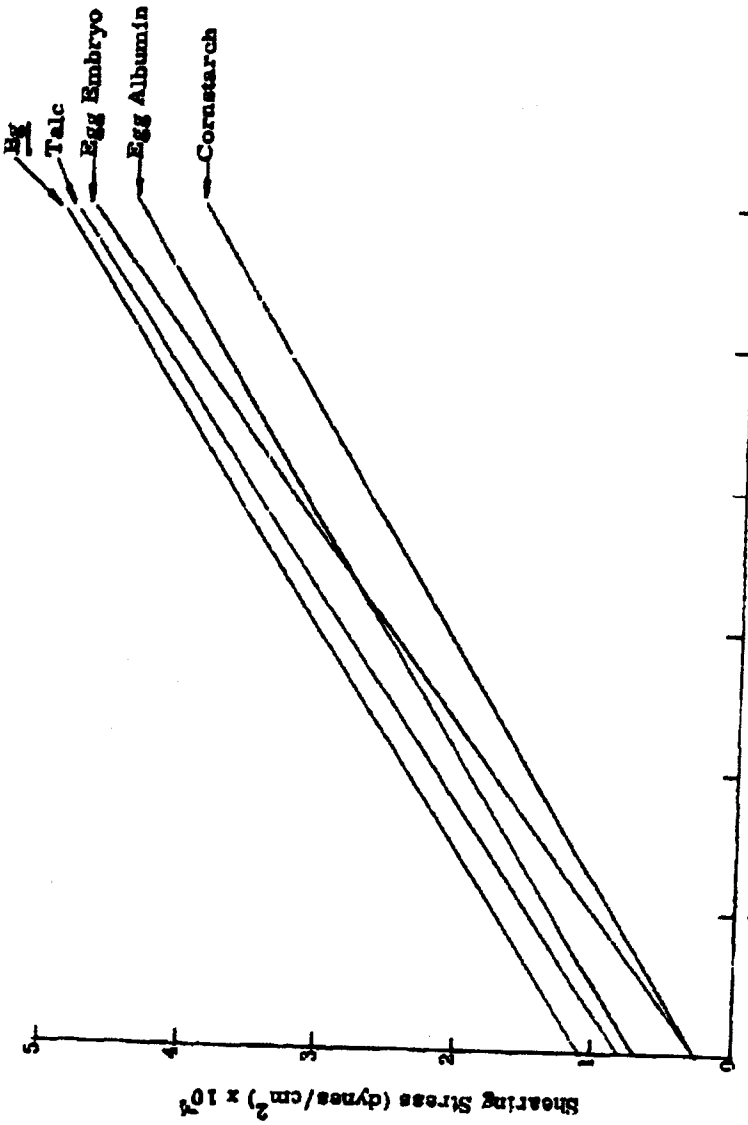

Figure 2.12 Comparison of Shear Strengths of Powders Pre-compacted at 50,820 Dynes/cm^2

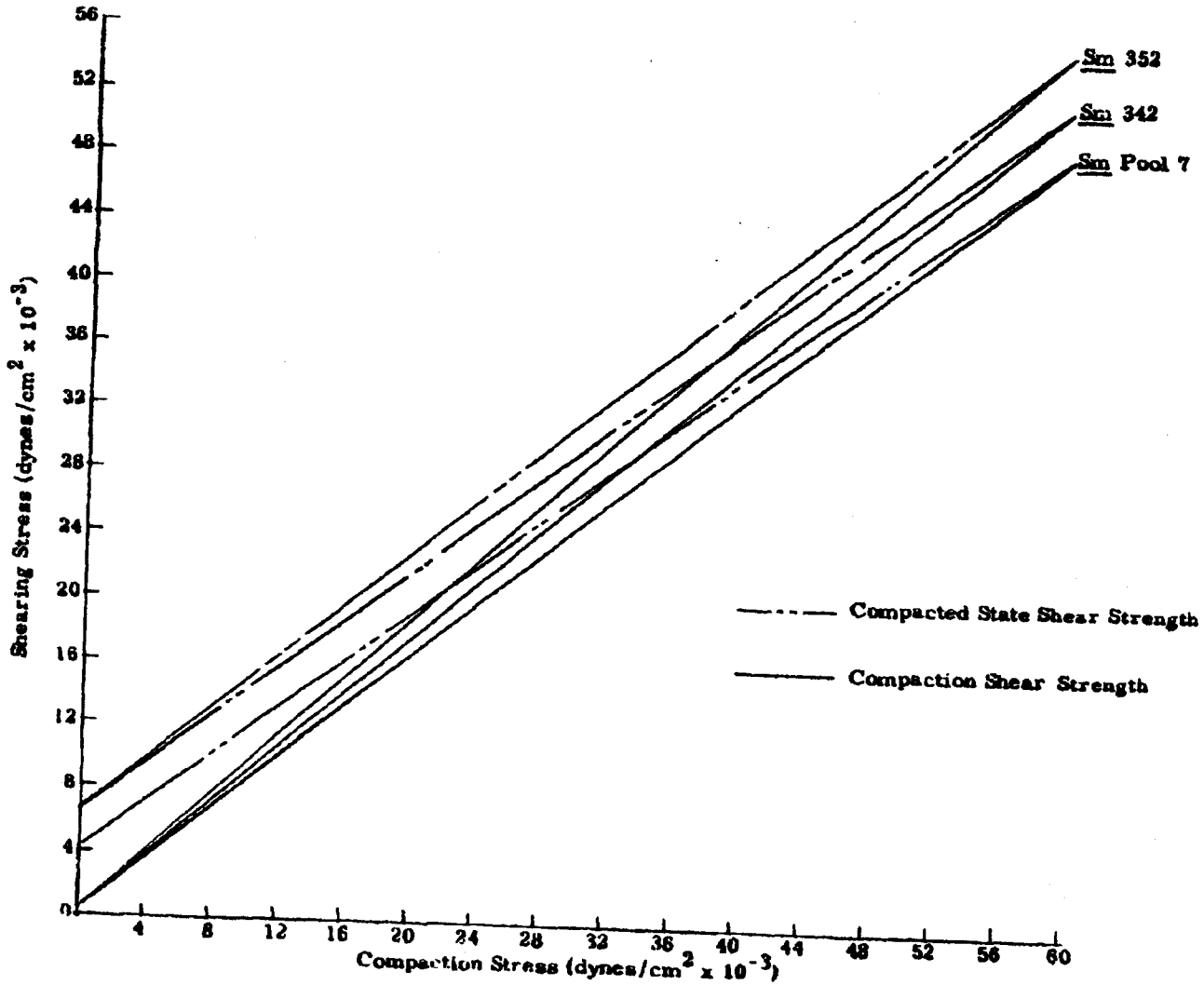

Figure 2.13 Shear Strength of Sm

covered in greater detail in a later section of this report. Under proper conditions there appears to be good correlation between compaction shear strength and other powder properties.

2.1.4 Wall-Stress Distribution

The apparatus designed to measure the distribution of stresses down the wall of the column of compacted powder has been outfitted with temperature-compensating strain gauges. This apparatus is still of importance to our overall study effort. Work in this area has, however, been substantially delayed during this quarter due to work requirements in other areas.

2.1.5 Compaction Characteristics of Powders

2.1.5.1 Dried Egg Embryo and Low-Density Bg

Two new samples have been included in our studies. They are (1) a dried-egg embryo simulant, and (2) a low (bulk)-density Bg simulant. Compaction data on these samples as well as comparative data on Sm and Bg are presented in Figure 2.14. As shown, the low-density Bg is somewhat more difficult to compact by a factor of 10. A more complete discussion is contained in following sections.

2.1.6 Compaction Characteristics in Comparison with Other Powder Properties

2.1.6.1 Egg Embryo Simulant

This material, prepared at Fort Detrick, is a mixture of lactose, silica, and the soluble components of egg embryo, that has been subjected to a freeze-drying process. The resultant product is a nonhomogenous rough-surfaced crystalline product (as shown in micrographs presented in Section 3 of this report) with a particle density of 1.50 g/cc and an MMD of 8.2 microns. It is a highly elastic substance and very difficult to compact. Preliminary evidence

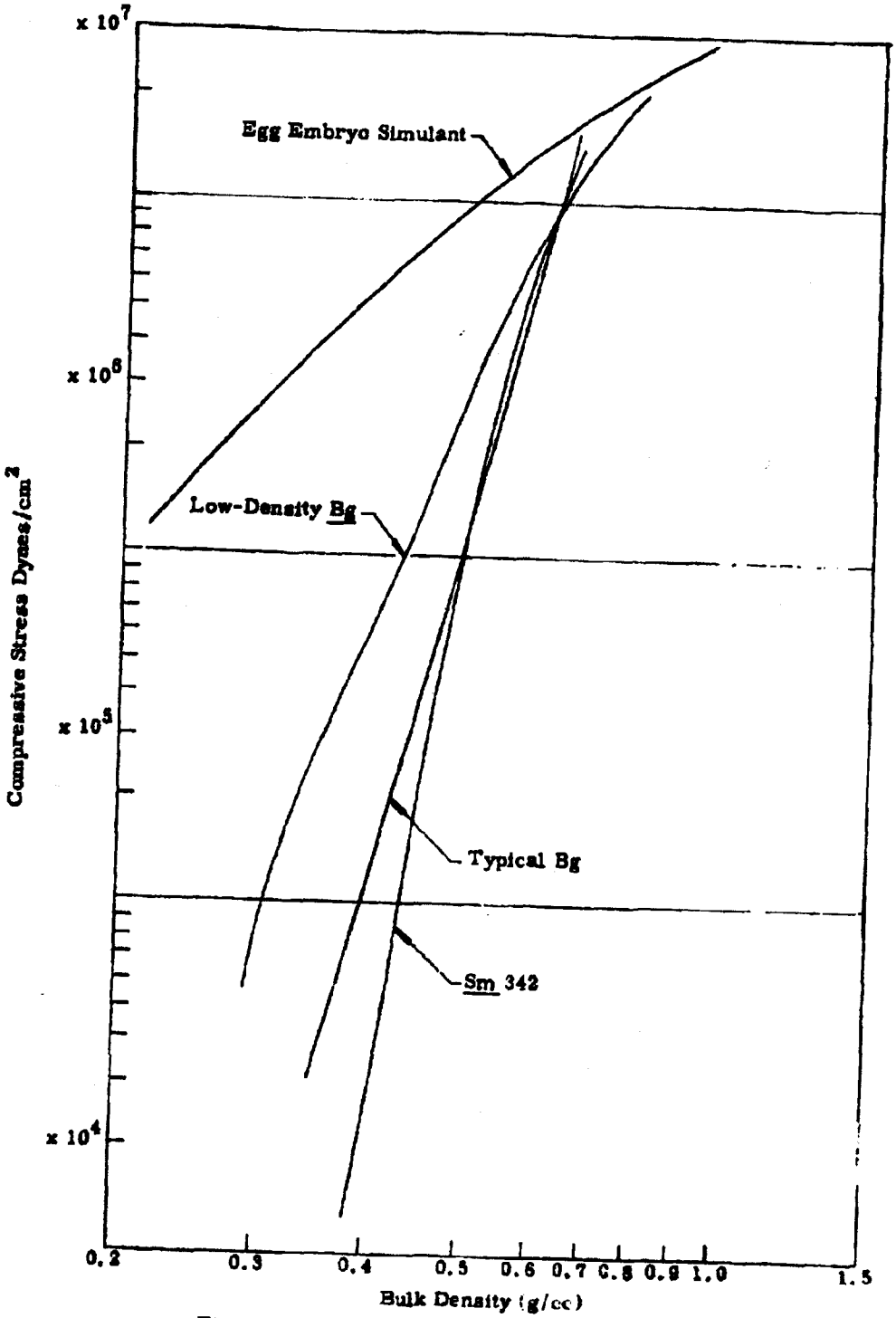

Figure 2.14 Compaction Characteristics of Powders

indicates that this powder seems to lose its elastic character when compacted to a high degree. This may result from the breakdown of the particles made up of submicronspheres. (Figure 3.8 - 3.13). Tests in our aerosol chamber indicate that this forms a stable aerosol and appears not to present any difficulties in that respect. Its compaction shear strength is lower than one would expect from the fact that it is so difficult to compact; however, this emphasizes the importance of proper interpretation of data. Plotting the shear strength as a function of compressive load is correct procedure, but care must be exercised when these data are used for comparing a wide range of materials. Since the egg embryo is so difficult to compact, we are in fact shearing a much lower-bulk density material at a given compressive load. At the moment we tend to restrict ourselves to making comparisons between similar powders such as the three lots of Sm or between samples having the same particle size (to be discussed in the following sections). In the future and as time permits considerably more work will be done utilizing particle density, void volume, and loose-bulk density in order to normalize the data so that more generalized comparisons can be made.

2.1.6.2 Low-Density Bg

Only shear strength and compaction data are available to date for this Bg. Except for being somewhat difficult to compact, it presents no obvious or unique problems.

2.1.6.3 Characteristics of Three Lots of Sm

Three lots of Sm (352, 342, and Pool 7) have distinctly different compaction characteristics, indicating differences in ease of dissemination. We are undertaking a study-in-depth of these materials, not only because the determination of the relative ease of dissemination is essential to the goals of this project but to utilize this as a practical "test case" to demonstrate that the techniques developed on this project will, in fact, characterize the behavior of powders in a meaningful way, so that the various powder properties may be intelligently interrelated.

The compaction characteristics of the three Sm samples are shown in Figure 2.15. Sample 352, for example, is more difficult by a factor of 10 to compact to the same bulk density as Pool 7. This means that when disseminated at the same energy level, a smaller payload is permissible with lot 352. The moisture contents of the three samples are:

Sample	Moisture (percent)
Sm 352	2.78
Sm 342	2.58
Sm Pool 7	4.46

Biological materials are considered relatively stable with moisture contents below five percent. Because this is not a sharp cutoff point, the moisture content of 4.46 percent for Pool 7 is indicative of a possible structural difference due to viability losses. To study the possible effects of the moisture, the samples were dried and compacted as shown in Figures 2.16, 2.17, and 2.18. Plot A is for the original sample, plot B represents sample vacuum-dried 24 hours at 50 C, and in plot C, the sample was vacuum-dried 122 hours at 64 C, reducing the Sm viability to near zero. Whitby size-analysis data for these samples are as follows:

	Plot A		Plot B		Plot C	
Sample	MMD	σ_g	MMD	σ_g	MMD	σ_g
Sm 352	4.9	1.86	5.0	1.72	4.8	1.79
Sm 342	5.3	1.83	7.4	1.63	4.9	1.60
Sm Pool 7	6.2	1.86	6.4	1.75	5.4	1.60

The particle densities of the original samples were:

Sample	Particle Density (g/cc)
Sm 352	1.38
Sm 342	1.38
Sm Pool 7	1.37

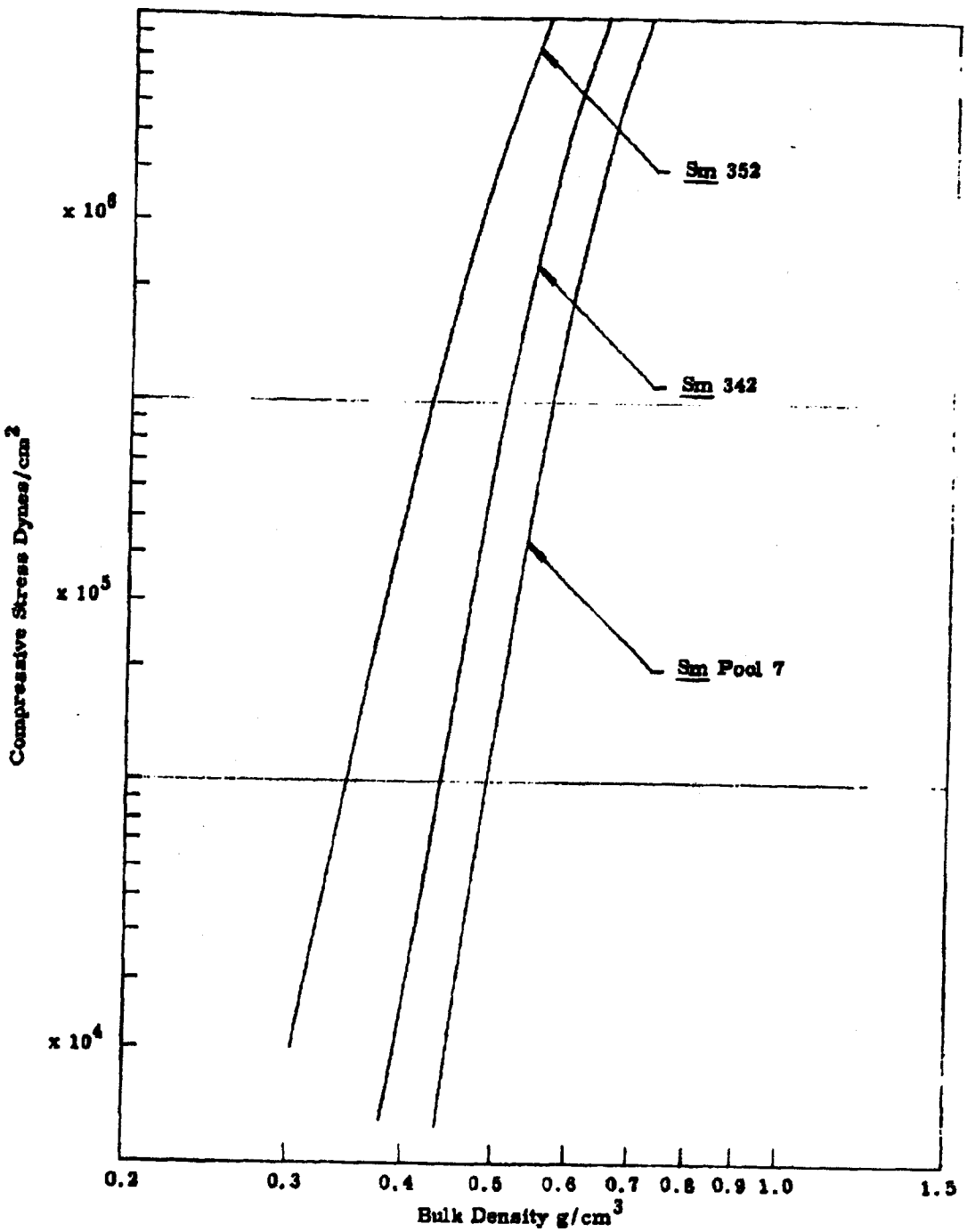

Figure 2.15 Compaction Characteristics of Sm

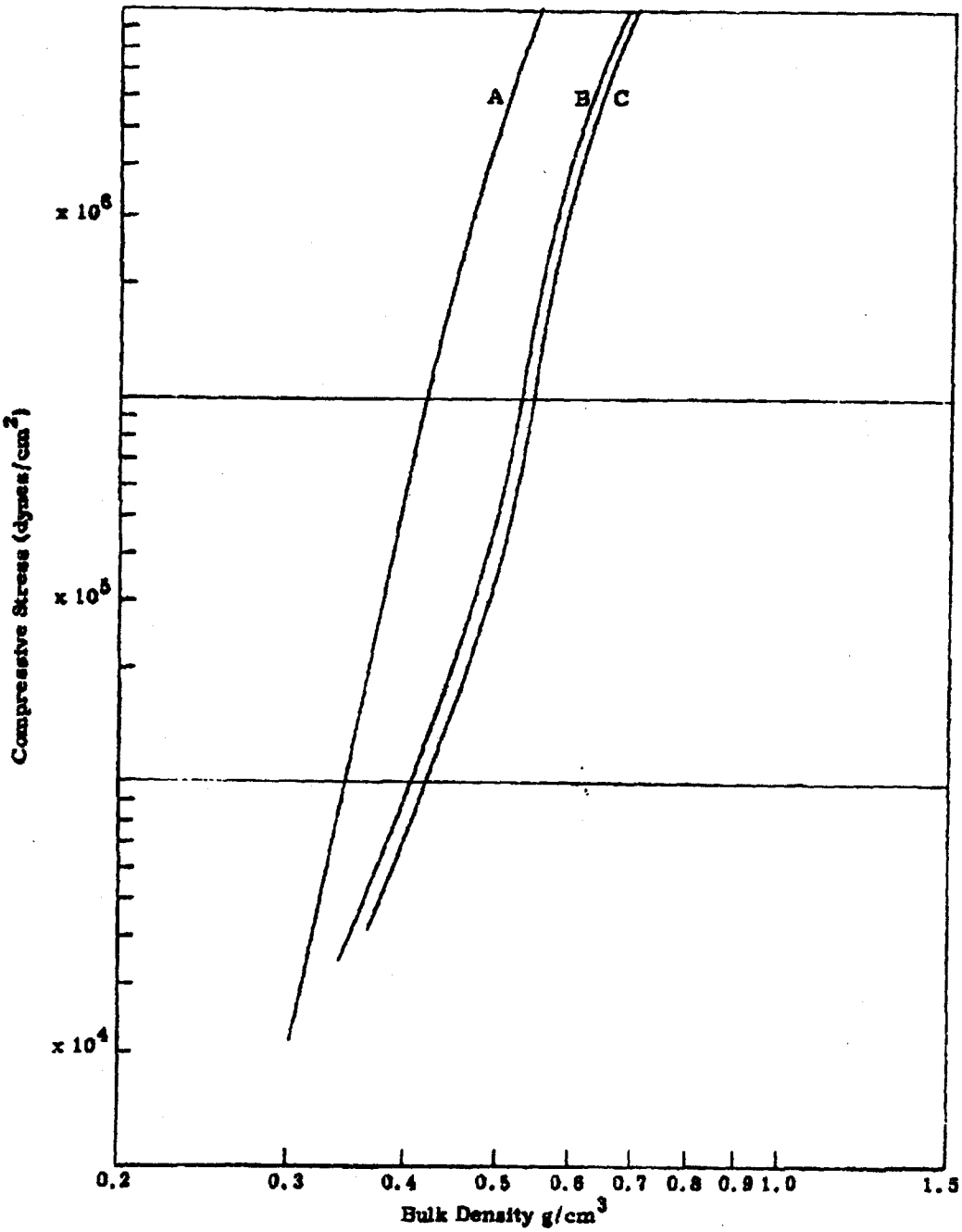

Figure 2.16 Compaction Characteristics of Dried Sm 352

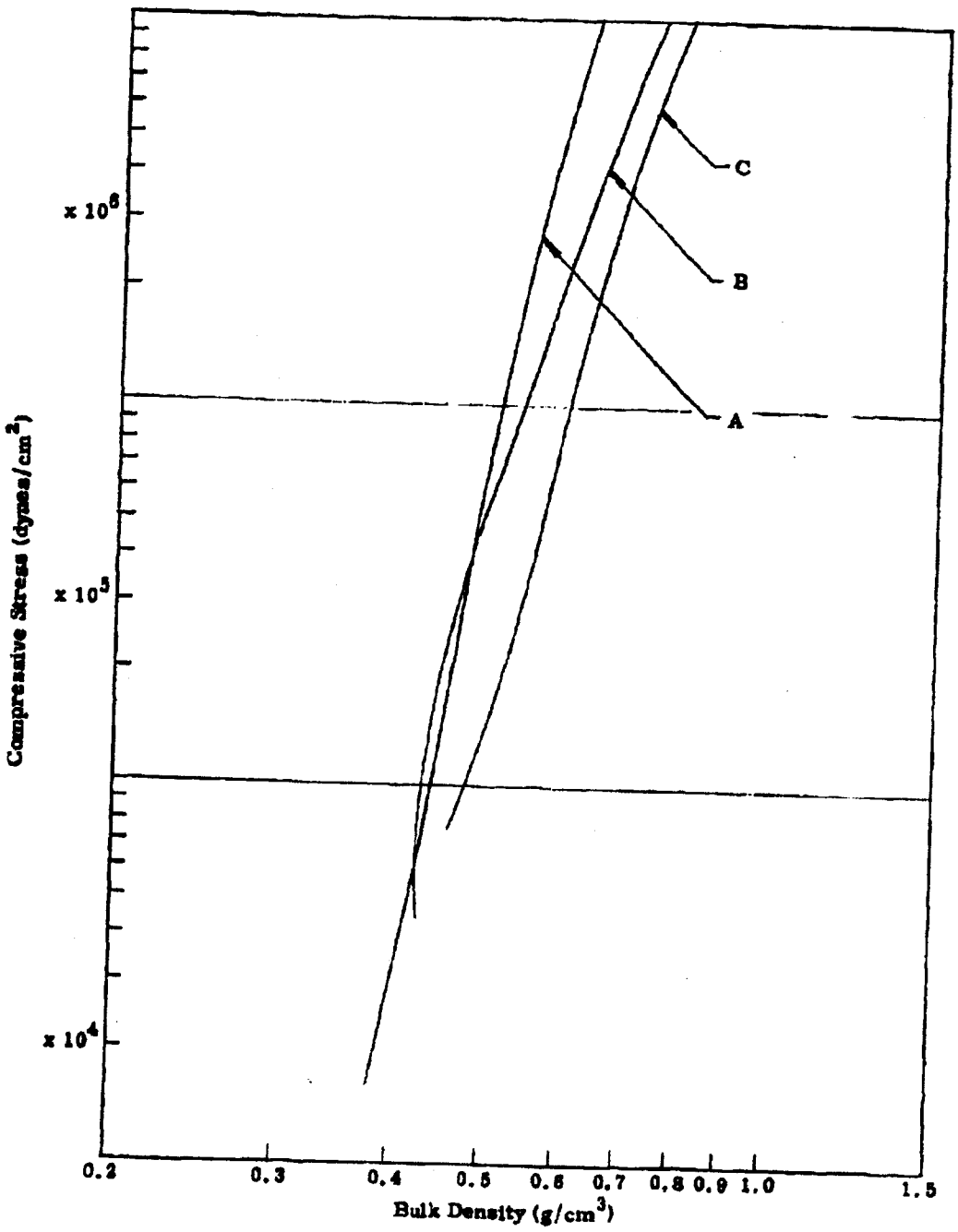

Figure 2.17 Compaction Characteristics of Dried Sm 342

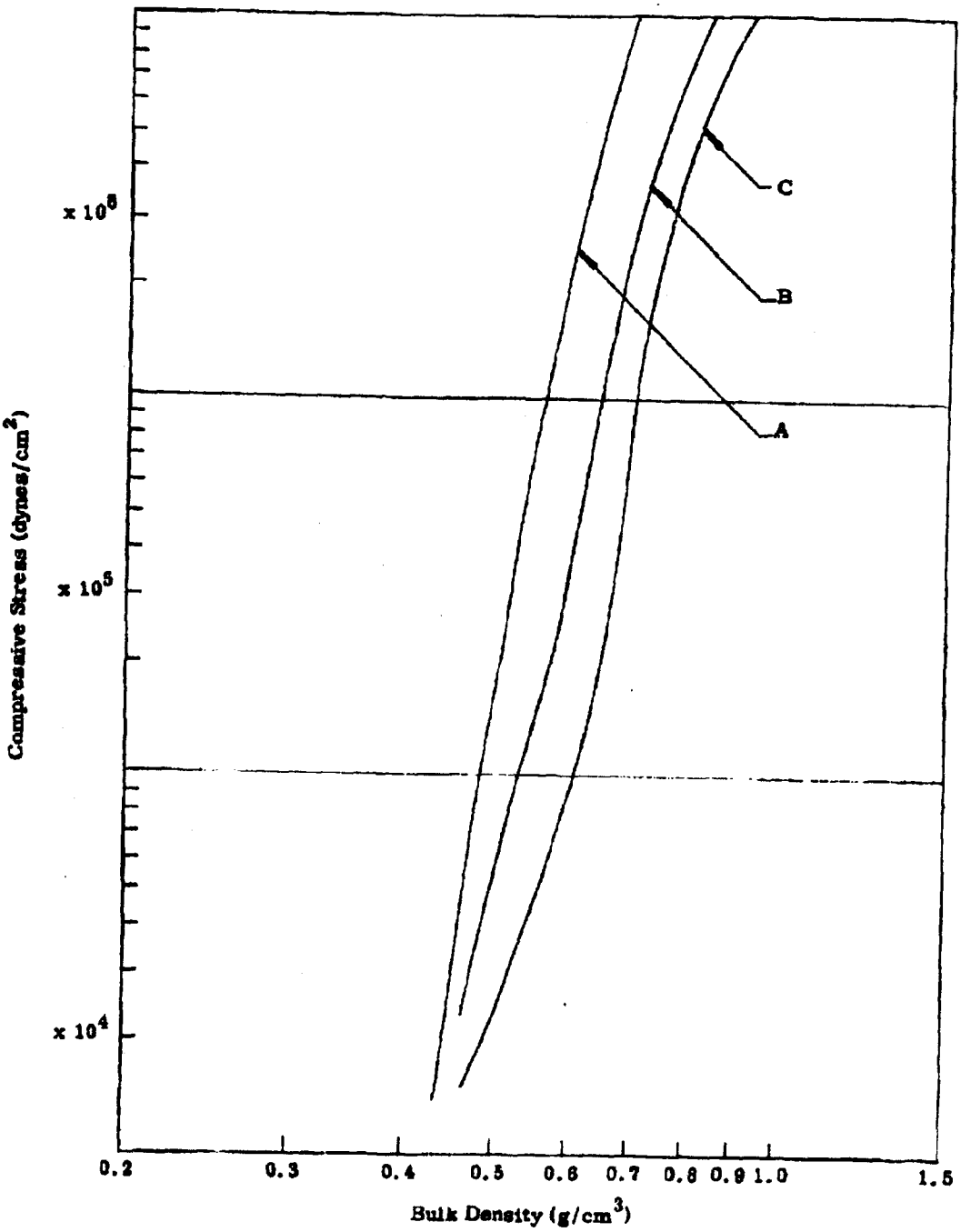

Figure 2.18 Compaction Characteristics of Dried Sm Pool 7

As the data show, the samples become increasingly easy to compact as the drying process is continued. Drying conditions represented by Plot B, Pool 7 did not produce as pronounced an effect since there was more water to remove. A close examination of the plots indicates that the shift in compaction characteristics was somewhat different with sample 342. The interesting point here is that when these three samples were vacuum-dried, Pool 7 and 352 retained their free-flowing characteristics, whereas the 342 sample caked badly on drying, thus indicating the possibility of a residual impurity remaining in this sample. To obtain a measure of the relative roughness of the surface of the particles, the rugosities (discussed later in this report) were determined on three powders. As would be expected, the rugosities of the powders increased with increasing difficulty to compact. Another interesting point is that Pool 7 was somewhat more difficult to compact than would be expected from MMD. Pool 7 had unusually high moisture content and was the only powder found to be somewhat porous -- further evidence that some structural change may have taken place. A comparison of the compaction shear data reported earlier in this report with the compaction data given here shows a direct correlation between increasing compaction-shear strength and increasing difficulty to compact. The differences observed here are all self-consistent and logical in the light of the real differences in the samples themselves.

2.1.6.4 Comparison of Samples Having the Same MMD

In the previous section a study of the compaction characteristics of three lots of the same type of powder was made. In contrast to this, a study was recently completed in cooperation with another project in which three powders, all 12 microns in diameter, were compared. The three powders were (1) spray-dried (soluble) saccharin -- a spherical powder with a relatively rough surface, (2) ground (insoluble) saccharin -- irregular in shape, and (3) cornstarch -- not completely spherical but quite smooth-surfaced. The compaction, tensile strength, and shear strength characteristics obtained to date are summarized in Figures 2.19 through 2.24. Preliminary tensile strength data on the ground saccharin is shown by the broken line in Figure 2.20. Again there appears to be a direct correlation between increasing tensile strength, increasing compaction-shear strength, and increasing difficulty to compact. It should be kept in mind

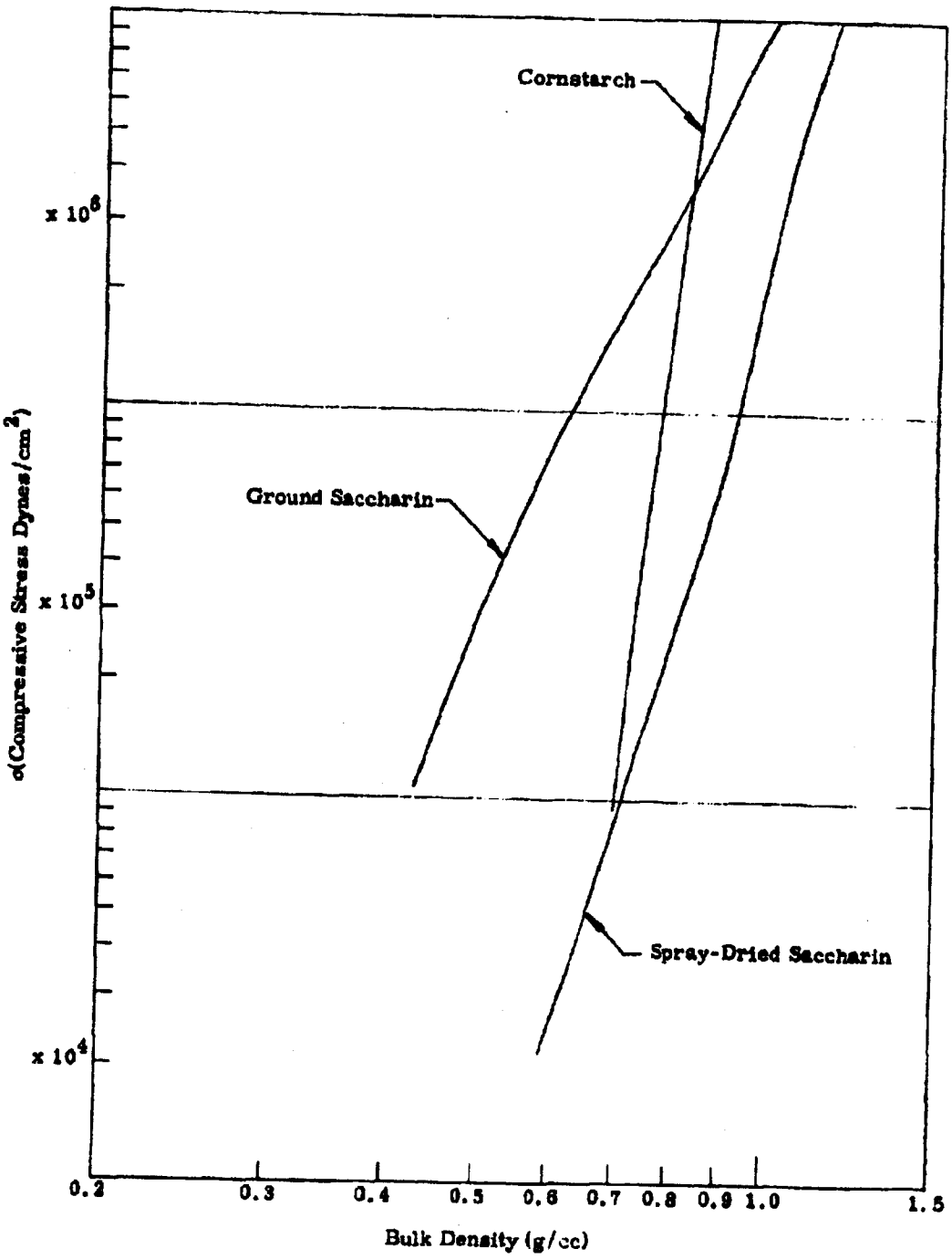

Figure 2.19 Compaction Characteristics of 12 Powders

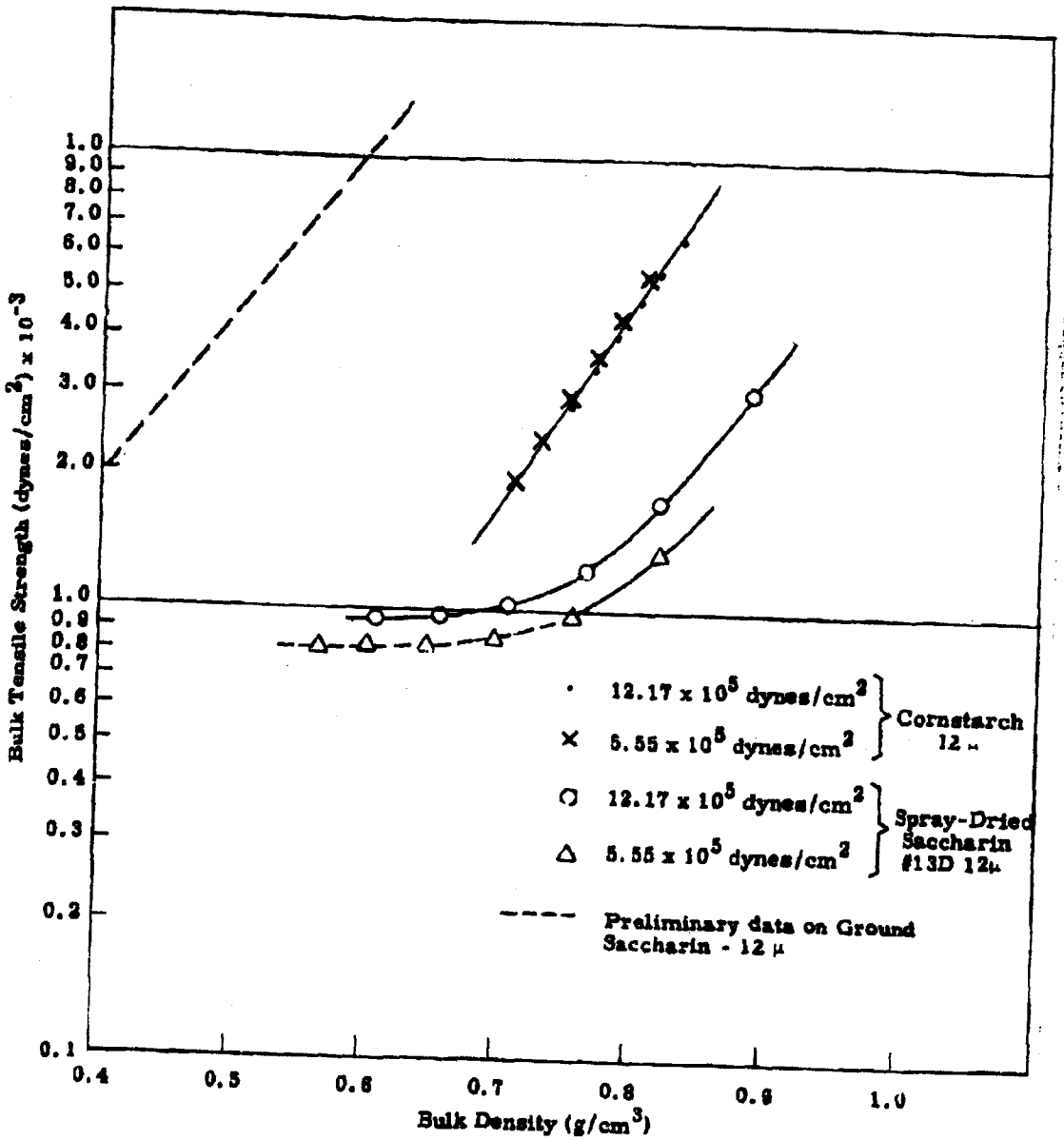

Figure 2.20 Tensile Strength of 12-Micron Powders

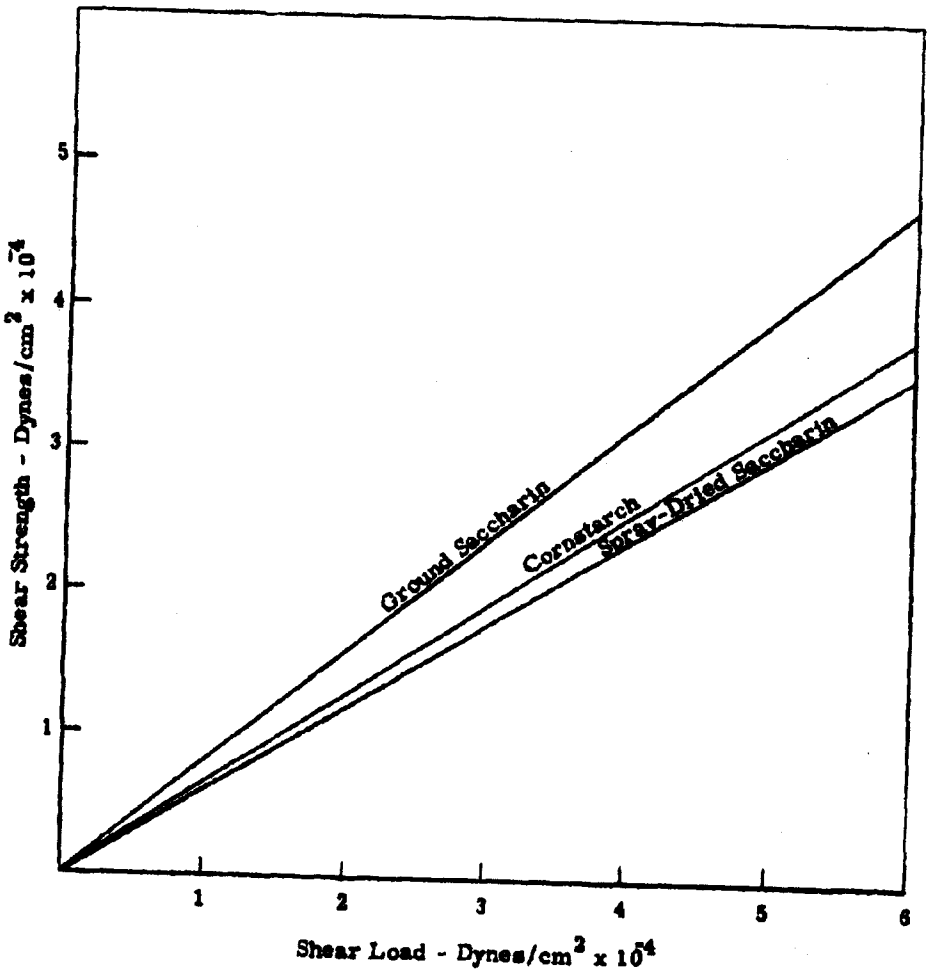

Figure 2.21 Compaction Shear Strength of 12-Micron Powders

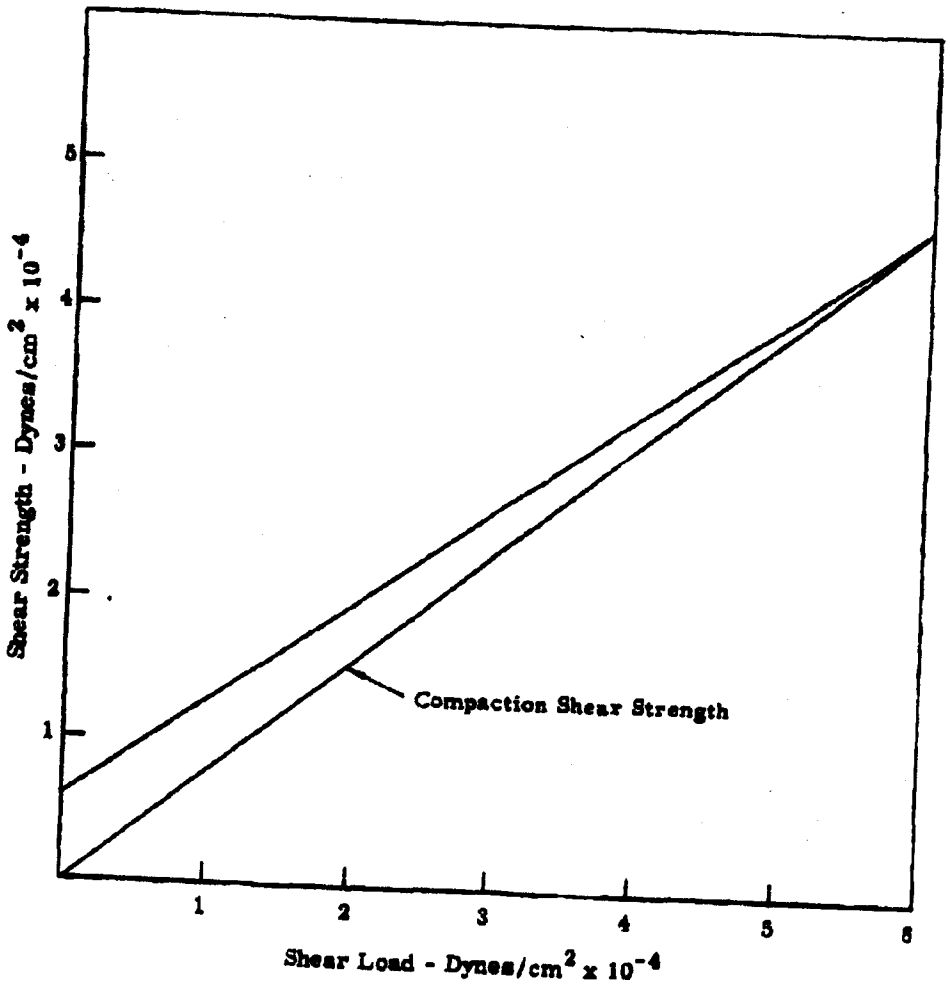

Figure 2.22. Shear Strength of Ground Saccharin (12)

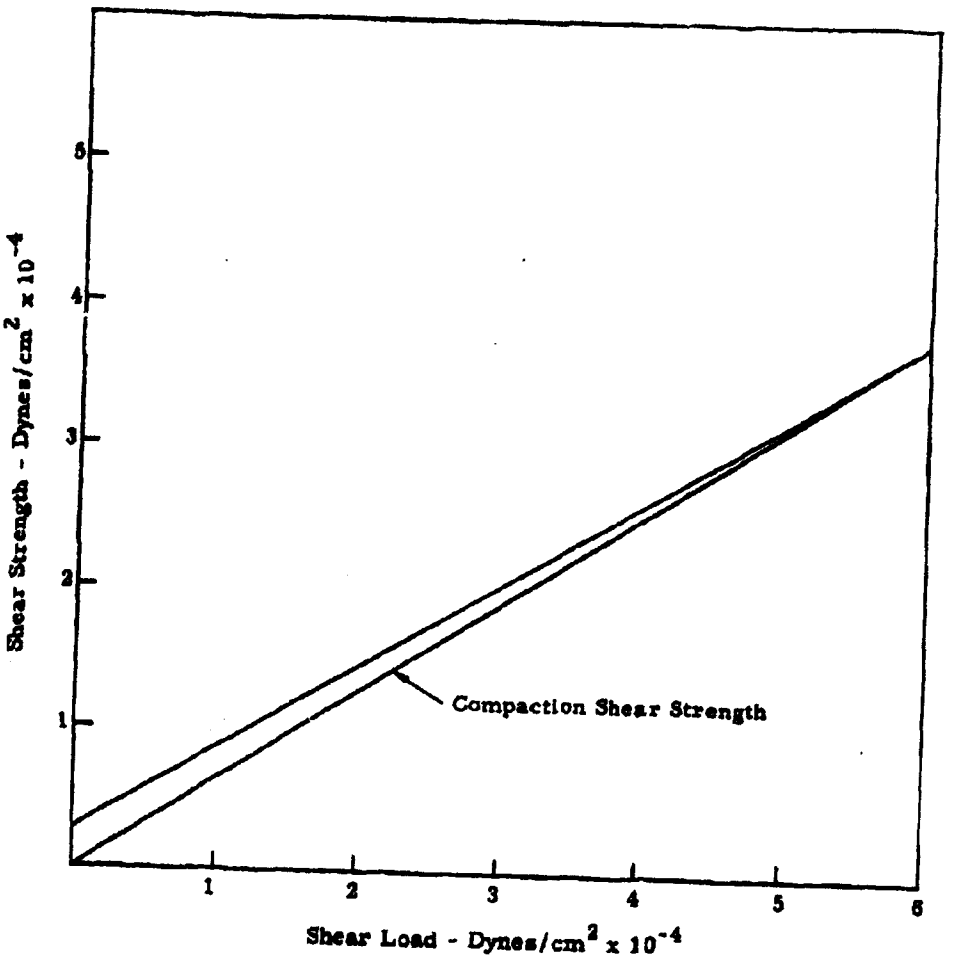

Figure 2.23 Shear Strength of Cornstarch (12μ)

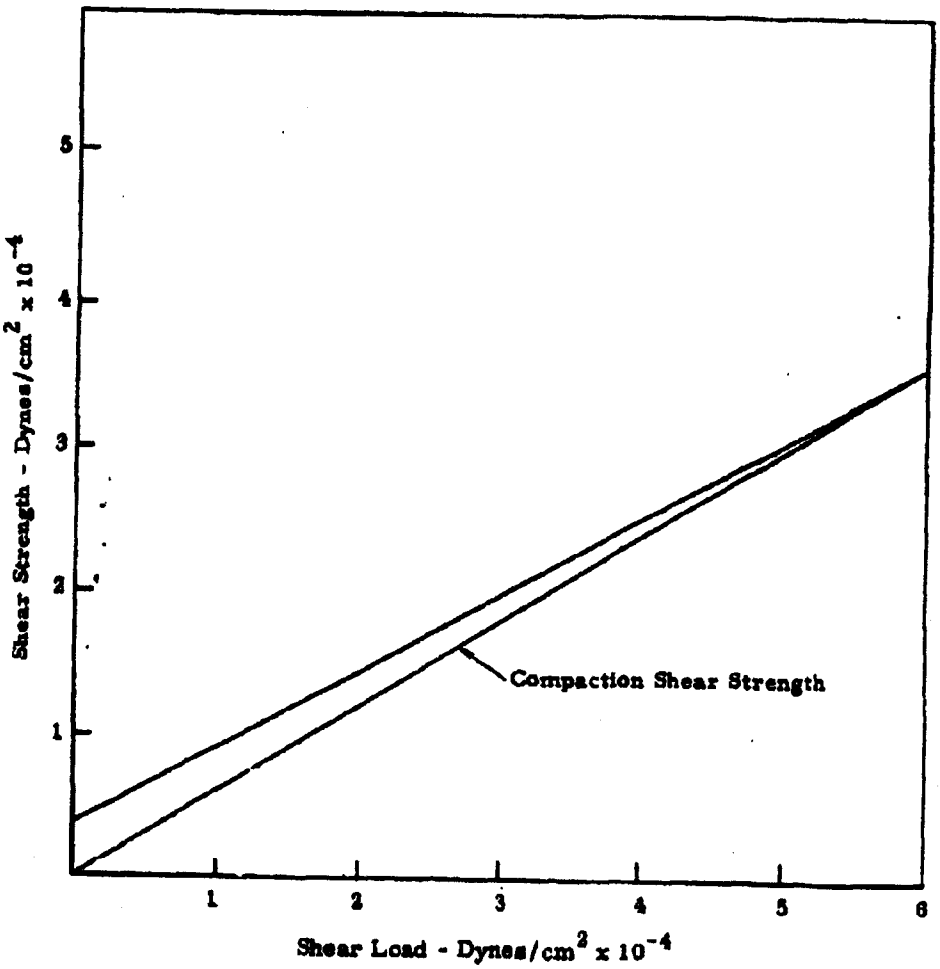

Figure 2.24. Shear Strength of Spray-Dried Saccharin (12 μ)

that the compaction forces to be compared with shear data are represented by the lower portion of the compaction graph.

2.2 Behavior of Powders in the Uncompacted State

The characteristic behavior of loose powders continues to be of interest in relation to the dissemination of solid agents. This information is of importance to predict the handling characteristics of the powder prior to compaction. In addition, some of the more fundamental powder properties are more readily evaluated in this state. A Powder Resistometer, recently designed and built in this laboratory, measures the interparticle resistance to flow in a bed of loose powder. The following sections describe our recent efforts in this area.

2.2.1 Powder Resistometer

The apparatus shown in Figures 2.25 and 2.26 utilizes a strain gauge and recording system to measure the resistance to uniform movement of a geometrical shape drawn through the bed of powder. As the probe moves through the bed, a wedge of powder (e.g., a cone if the probe is circular) quickly forms in front of the probe. Thus, the force measured is the resistance to flow of powder particle against powder particle.

The powder beds are contained in removable trays permitting the efficient study of a number of powders preconditioned simultaneously in a controlled environment. The dimensions of the powder bed were kept small to reduce the amount of powder required per run and to permit efficient operation of the apparatus within the confines of an isolation lab. The powder bed has a depth of 5 cm and a width of 10 cm. The probe travels a distance of about 50 cm at a uniform rate of 2 cm per second.

In a typical run, the force increases rapidly (5-10 sec) as the wedge of powder forms and then remains relatively constant for the remainder of the run. The rapid rise in force at the end of the run should be disregarded since it is a result of the powder being forced against the end of the tray. Amplitude-vs-time coordinates are then obtained directly from the recorder chart.

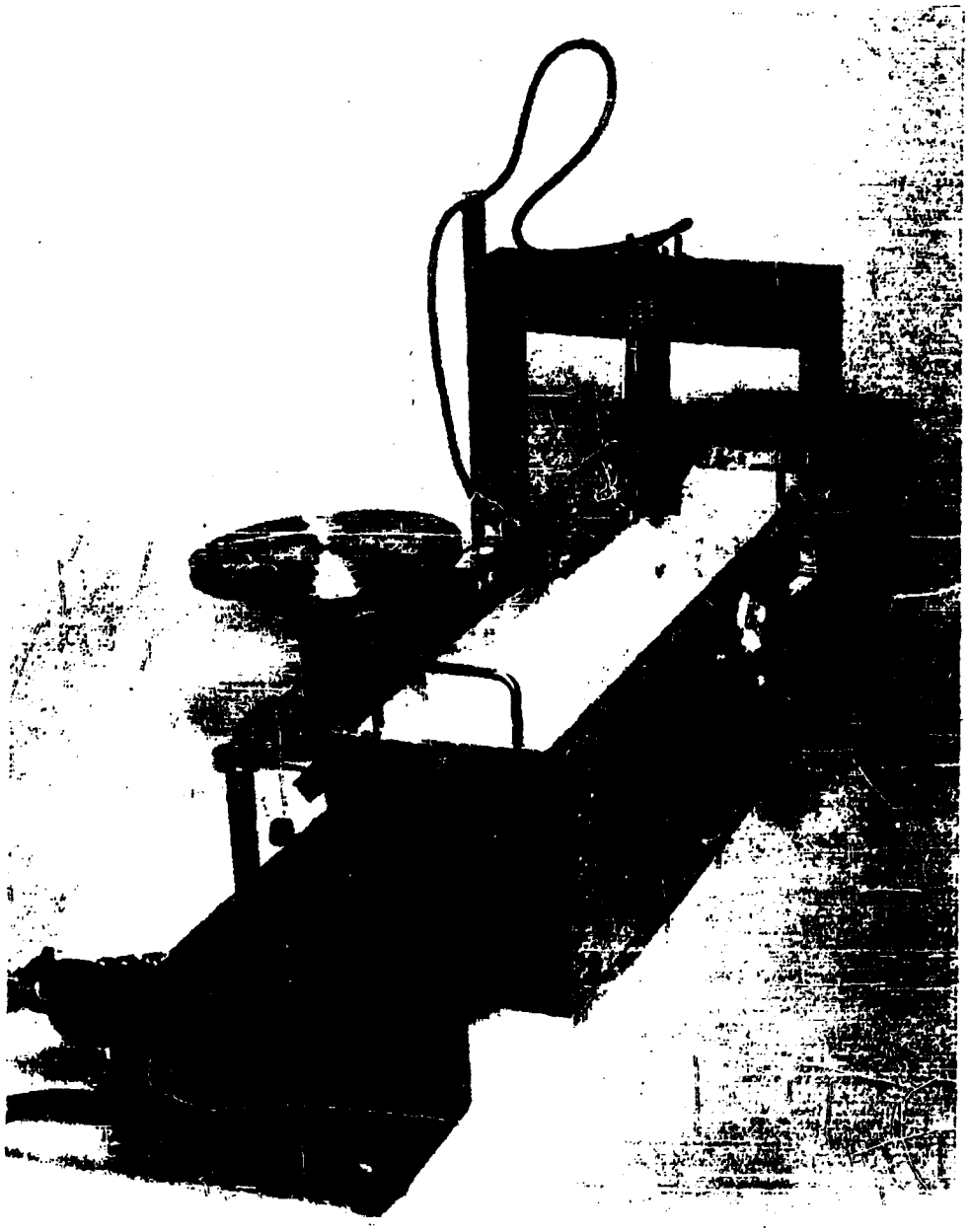

Figure 2.25 Powder Resistometer

Figure 2.26 Powder Resistometer - Closeup of Test Run

Since these coordinates are directly proportional to distance versus force, the selection is one of convenience of data handling.

An examination of the sample charts presented in Figure 2.27 reveals that the motion through the powder is not a continuing but rather a "slip-stick" effect. This effect is a function of the powder property and the nature of the force application via the cantilever beam. As the probe moves through the bed of powder, the force increases until the wedge of powder is caused to move through the bed. This yield point, of greatest interest to us, is represented by the upper envelope of points on the recorder chart. Since the probe momentarily moves forward at a rate faster than that of the carriage, the recorded force drops quickly. As the probe continues to move forward, the force again builds up to another yield point. The data recorded for each run include the equilibrium yield force and the frequency of oscillation.

2.2.1.1 Preliminary Tests

A series of preliminary tests was run to determine:

1. The criteria necessary to obtain reproducible results,
2. The differences which would result from changes in the geometrical shape of the probe.

In order to determine any effect of geometry, probes were constructed having circular, square, and triangular shapes, but with equal cross sectional areas. Two sets were made, one with four times the cross sectional area of the other.

As a result of this preliminary series, the following conclusions were made:

1. A bed of loose powder can be prepared in a reproducible manner for this test by simply stirring thoroughly with a glass rod.
2. A bed of powder can be used for more than one test.
3. Within experimental limits the forces measured are dependent upon the cross sectional area of the probe, but independent of its geometry.

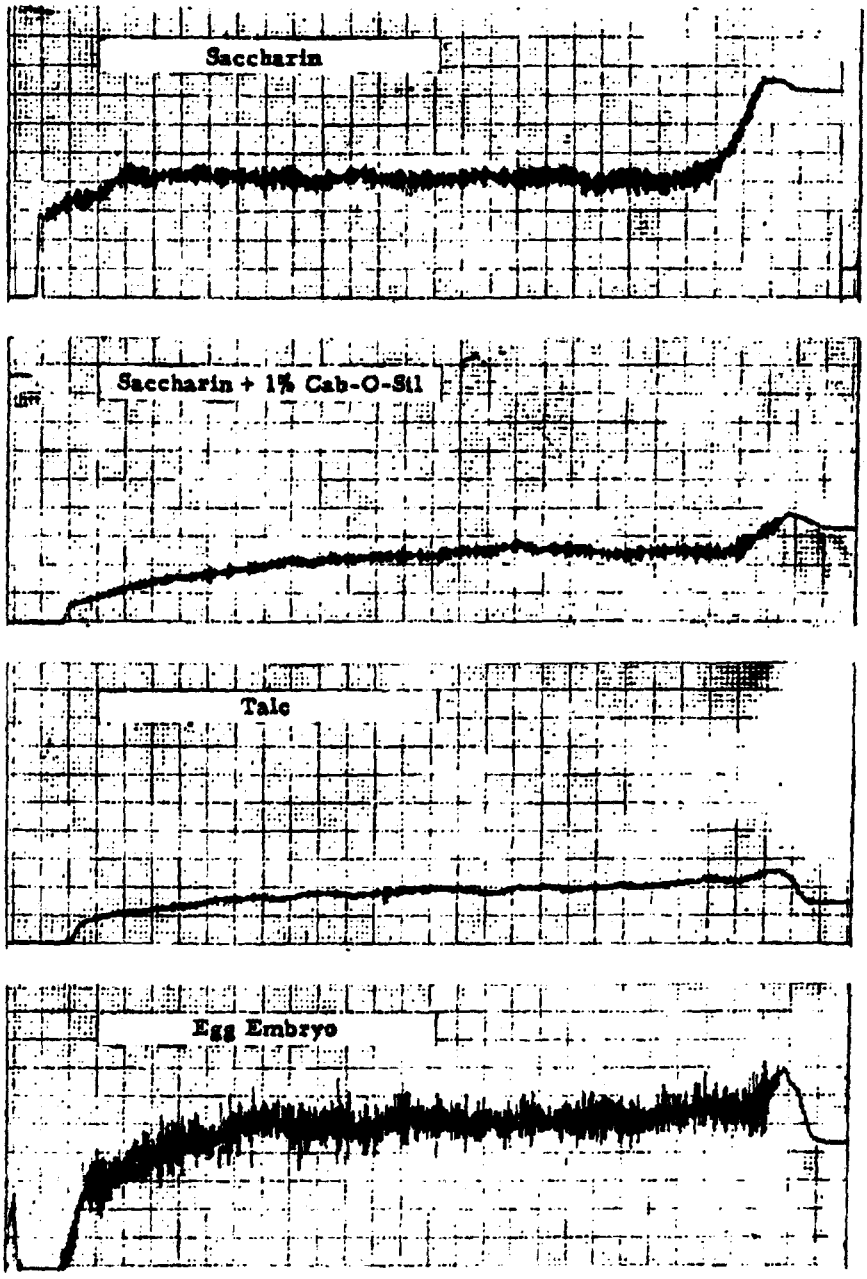

Figure 2.27 Sample Recorder Charts from Powder Resistometer

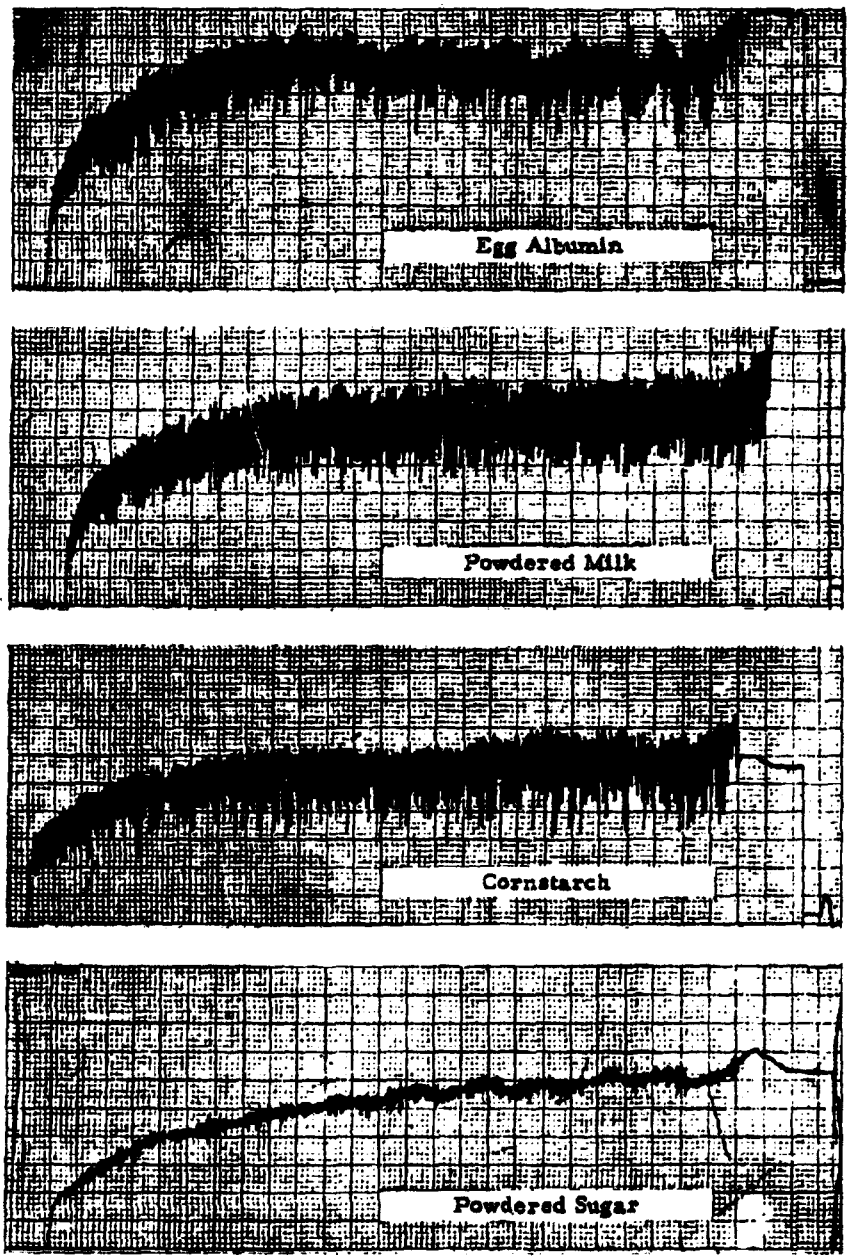

Figure 2.27 Sampler Recorder Charts

2.2.1.2 Experimental Results

In order to obtain accurate comparative data, the apparatus was enclosed in an isolator laboratory where precise environmental control is possible. The large circular probe (diameter = 3.4 cm) was selected for use for the entire series. The data are presented in Figure 2.28 and Tables 2.1 and 2.2. Figure 2.28, a graph of the resistive force versus time for a number of powders, shows the dramatic differences in flow resistance between the powders studied. Fourteen runs were made on each powder; the amplitude at corresponding times is shown in Table 2.1. For a measure of the reproducibility of the test series, the average deviations are listed at 1, 8, 16 and 24 seconds.

The equilibrium resistance R_{eq}, the yield frequency (f_y) and other pertinent data on the powders studied are summarized in Table 2.2.

2.2.1.3 Conclusions and Recommendations for Future Work

The powder resistometer shows great promise in measuring, with sensitivity, fundamental properties of bulk powders. In addition to yielding comparative information on a wide range of powders, the apparatus will be used to study the effects of varying degrees of agglomeration and precompaction of a given powder. Furthermore, the apparatus will be used to effectively measure the enhancement in flow characteristics accomplished by the use of additives (Cab-o-Sil, for example).

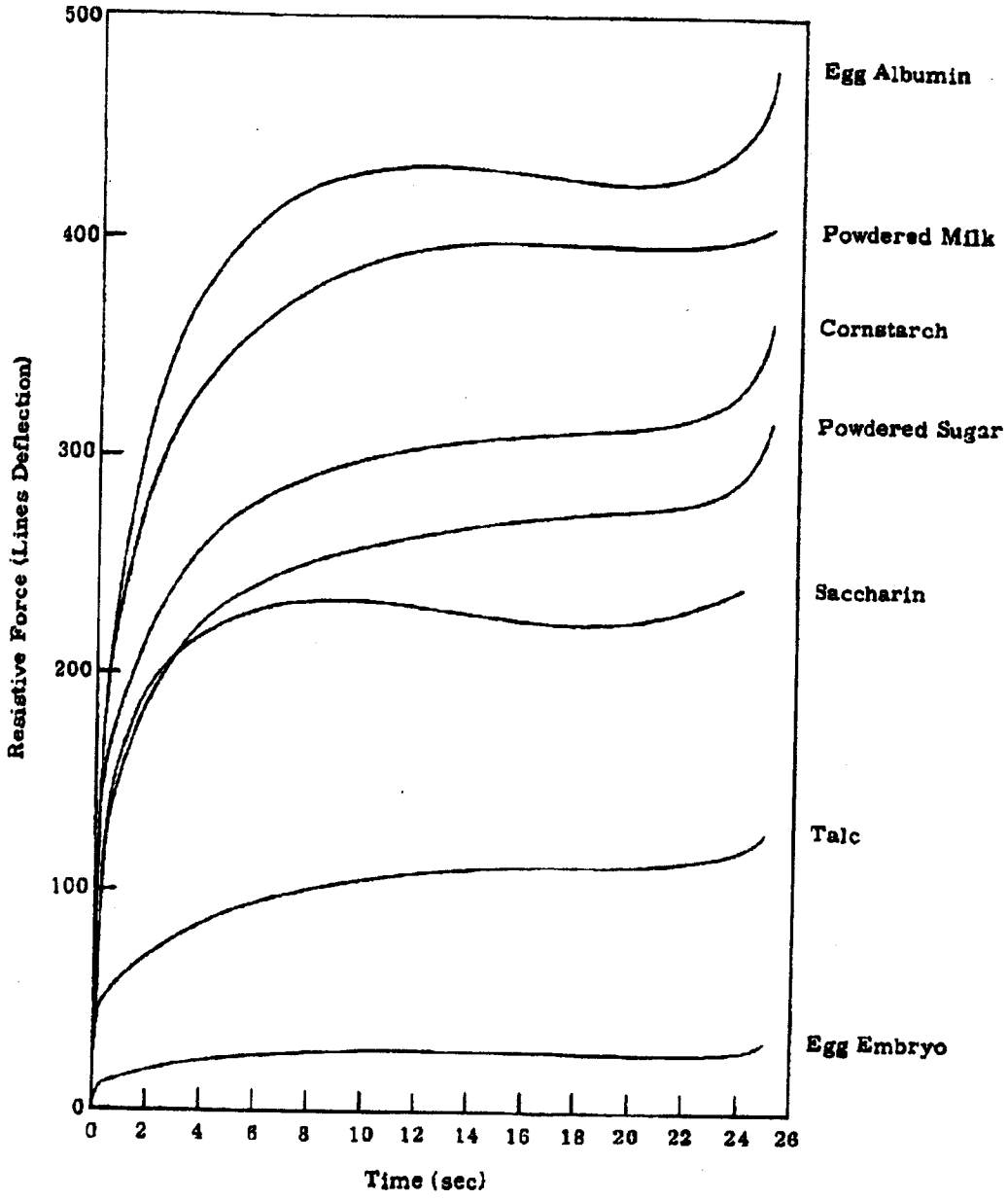

Figure 2.28 Interparticle Resistance to Flow Measurements Powder Resistometer

Table 2.1 Amplitude* versus Time Data from Powder Resistometer

Sec \ Powder	Egg Albumin	Powdered Milk	Cornstarch	Powdered Sugar	Saccharin	Saccharin 1% C-a-S	Talc	Egg Embryo
0.5	205	205	168	134	140	46	52	12
1	252 ± 30	241 ± 10	189 ± 5	154 ±10	167 ±13	55 ±5	60 ± 3	15 ± 1
2	311	283	220	189	195	64	70	19
4	377	335	259	225	219	84	85	23
6	407	362	280	240	230	95	94	25
8	428 ± 10	378 ± 10	291 ± 5	254 ±10	231 ±10	101 ±3	101 ± 2	27 ± 1
10	428	389	299	259	234	109	106	28
12	432	396	303	265	233	112	109	28
14	431	398	309	267	229	114	111	28
16	427 ± 15	399 ± 5	311 ± 10	273 ±10	226 ±10	115 ±3	113 ± 4	28 ± 1
18	428	398	313	274	225	116	113	27
20	425	398	315	277	225	117	114	28
22	429	394	319	280	233	116	115	28
24	446 ± 15	389 ± 7	331 ± 10	288 ±15	241 ±7	119 ±5	119 ± 5	29 ± 1
25	477	406	361	318	- -	131	128	33
26								

*Amplitude given is in units of lines deflection where one line is equal to 0.4 g.

Table 2.2 Summary of Data on Powder Resistometer Study

Powder	R_{eq}	f_y	Density (Bulk)	Density (Particle)	MMD*
Albumin	430	8.9	0.53	1.30	180
Powdered Milk	400	9.3	0.51	1.30	33
Cornstarch	315	10.9	0.43	1.50	12
Powdered Sugar	275	13.4	0.52	1.59	--
Saccharin	230	14.1	0.25	1.42	4.8
Saccharin 1% Cab-o-Sil	118	15.4	0.22	1.42	4.8
Talc	115	15.7	0.16	2.72	3.4
Embryo	28	17.9	0.06	1.50	8.2

*MMD data for egg embryo was furnished by Fort Detrich--all other MMD's were determined (Whitby Method) in this laboratory.

3. PHYSICAL AND CHEMICAL CHARACTERISTICS OF THE POWDER PARTICLE

The fundamental behavior of particulate material is determined by the nature of the inter-molecular forces existing at areas of contact between particles. The number and character of such contacts is directly related to the nature of the surfaces of the powder particles. During the current quarter, the total surface areas of egg albumin and three lots of Sm were determined, a method for determining the micropore structure of powders was explored, and the particle shape of a new egg embryo simulant was investigated by the use of an electron microscope.

3.1 Total Surface Area

The BET adsorption method was used to measure the total surface areas for egg albumin and three Sm samples: Sm 352, Sm 342 and Pool 7. By this method the quantity of gas necessary to form a mono-layer on the surface of the particle is determined. By assuming a value for the area covered by a single molecule, the area of surface covered by the adsorbed gas is then calculated. For this determination to be made accurately, it is necessary that all adsorbed impurities be removed from the particle surface. This is accomplished early in the procedure by a "degassing" process. Furthermore, the sample must remain stable under the degas conditions, otherwise the resultant decomposition leads to incorrect surface areas.

Like saccharin, when egg albumin and Sm are heated too high in a vacuum, some decomposition does occur. But unlike saccharin, egg albumin and Sm do not decompose in a simple manner (e.g., sublimation for saccharin), but by a complex process of protein fragmentation. Because of the complex structure of proteins, there is no distinct temperature at which decomposition begins, for such occurs, to some extent, at any heating temperature.

In the degassing process the major contaminant is water. Water is not only sorbed* on the surface but also absorbed throughout the entire particle.

* A non-committal term including both adsorption and absorption

Even the water on the surface is held by bonds varying from weak van der Waals' forces to strong hydrogen bonds. If the degas temperature is too high the hydrogen bonds in the protein molecule itself will begin to break down.

When the aforementioned criterion of instability is applied to "natural materials" which, in addition to the protein materials, includes materials like cornstarch and powdered milk, a false impression may be given of when the degassed state is reached. "Natural materials" degassed at given temperatures will reach a stable area when all the bonds corresponding to that temperature have been broken. Increasing the temperature will cause the area to stabilize at a new and higher value. Therefore, the surface area will stabilize at any given temperature when the surface area is proportional to the temperature.

With material of simple structure, the area will increase with temperature as more contaminants are removed. Eventually, however, a temperature will be reached when the surface area keeps increasing, thus showing that some decomposition is occurring. This phenomenon will continue until the material is entirely decomposed. In contrast, saccharin would disappear by sublimation.

The adsorption isotherm of water may give insight as to when the degassed state has been reached. As long as only absorbed water has been removed by the degassing procedure (not water that is part of the structure), the re-absorption isotherm will not change in shape -- only be displaced upward as more absorbed water is removed. Any decomposition or removal of water that is part of the structure will change the mechanism of absorption and, therefore, the shape of the isotherm. This concept is similar to the concept used by Makower et al.[1]

Thus the success of the BET method depends, in part, upon supplying enough energy to remove surface impurities but insufficient to decompose the sample. Usually there is sufficient difference in these energy levels that an effective operational range can be established. In our surface-area determinations of these natural materials, degas conditions of room temperature and under vacuum are satisfactory.

3.1.1 Egg Albumin

Figures 3.1 and 3.2 show the BET analysis and a complete isotherm for egg albumin. From Figure 3.1 the lack of hysteresis indicates a negligible pore structure. (The pore-size distribution shown in Figure 3.7 confirms this by showing only a small hump.) The egg albumin used had a Whitby MMD = 4.8μ and σ_g = 1.57. The BET surface area = 2.45 m^2/g ± 7 percent, corresponding to a rugosity of 2.30 (Table 3.1). Within experimental error, this corresponds to the rugosity of saccharin.

The temperature for degassing was 136 F and the degassing time had to be at least 24 hours. A degas temperature of 186 F increased the surface area to 2.9 m^2/gm. A test must be made at room temperature; however, little change in the area is expected, since increasing to 186 F produced such a small change.

3.1.2 Sm

The biological nature of Sm introduces another variable into surface area measurements. The correlation between change in surface with change in viability is uncertain. Nonetheless, tests are conducted to keep viability losses minimal. The high vacuum imposed may contribute to some loss of viability. Spoor-formers have been found to survive with little or no destruction after 35 days at 10^{-2} mm Hg at room temperature. Sm is not a spoor-former, but Bg is. Mesophilic aerobes, of which Sm is an example, were found in one study to have a 30.4-percent survival rate when exposed to high vacuums at 40 C for five days.[2] These conditions are much harsher than degassing at room temperature (25 C) for, at most, two days. Thus, survival rate should be much better than 30 percent during the degassing cycle. The adsorption cycle should have no effect on Sm inasmuch as cold storage is used to preserve it.

The treatment of Sm during the test is outlined as follows:

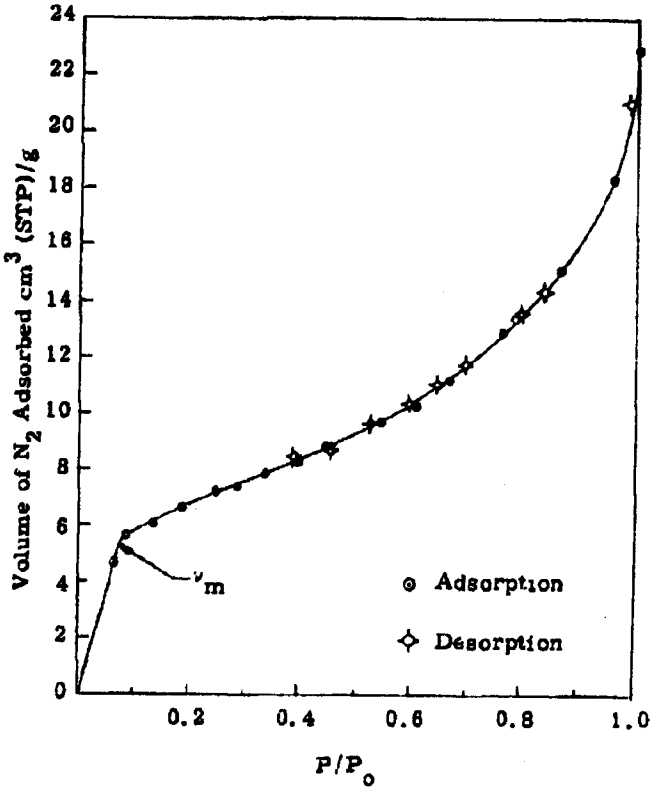

Figure 3.1 Nitrogen Adsorption Isotherm of Egg Albumin

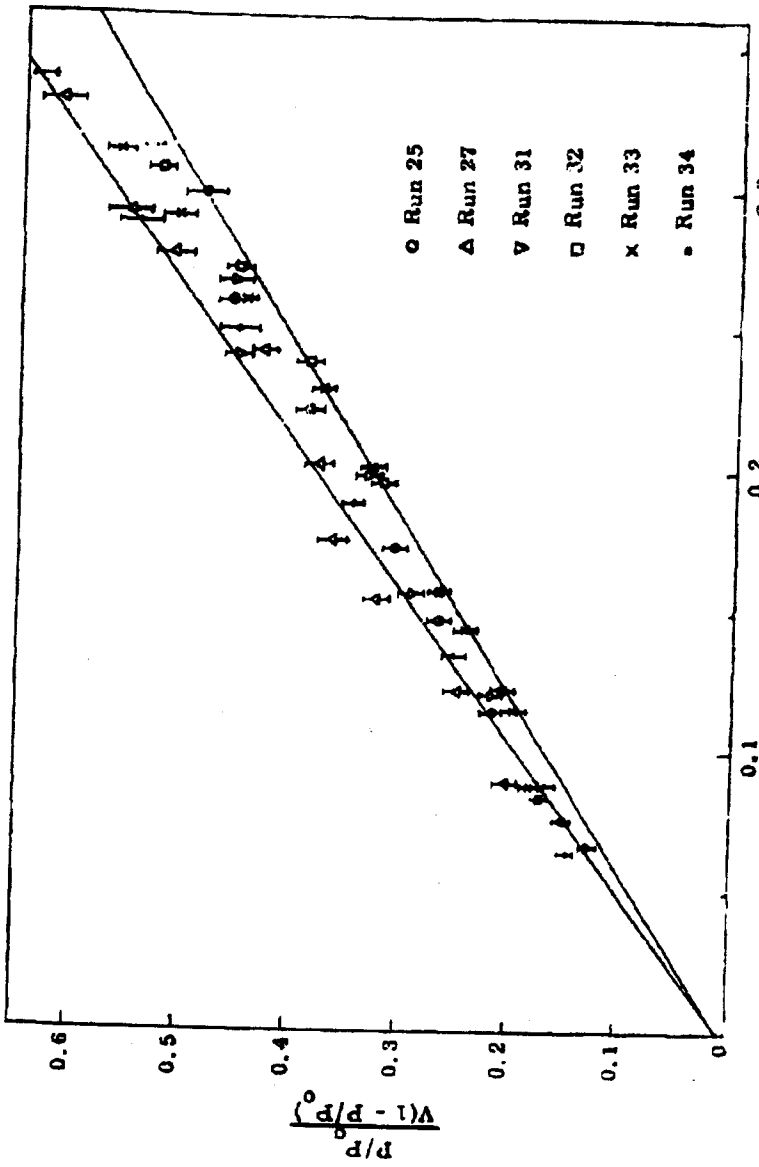

Figure 3.2 BET Plot for Various Egg Albumin Samples
Lines include normal errors

(1) Remove sample from freezer
(2) Place for 1 - 1-1/2 hours in warm-up to room temperature while sealed
(3) Withdraw approximately 0.5 g sample and reseal sample vial. (Time for step - 47 minutes)
(4) Transfer sample bucket to adsorption apparatus and start slow evacuation at room temperature
(5) Return sample vial to freezer (Total exposure 1-1/2 - 2 hours)
(6) Attain degassing vacuum in about 45 minutes
(7) Follow from here, normal adsorption procedure

Two Sm 352 and Sm 342 samples were tested but only one Sm Pool 7 sample. Although no definite trends were noted by a single warm-up, it is quite certain that repeated warm-ups will cause some uniform biological degradation.

Figures 3.3, 3.4, 3.5 and 3.6 show results of the BET analysis and the complete isotherms for the three Sm samples. Increasing surface area followed in order of decreasing particle size (Table 3.1): 7.4μ -- Sm 342 had an area = 1.99 m^2g, 6.4μ -- Pool 7 had an area = 2.34 m^2/g, and 5.0μ -- Sm 352 had an area = 3.14 m^2/g. The rugosities, in the order of increasing difficulty to compact,[3] are easiest -- Pool 7, rugosity = 2.93; medium -- Sm 342, rugosity = 3.01, and hardest -- Sm 352, rugosity = 3.08.

Theoretically, rugosity (which is a measure of particle roughness), should be proportional to the ease of compaction.

Table 3.1 Surface Data

Material	BET Area, m^2/gn	Particle Size MMD	σg	Rugosity
Sm 342	1.99 ± 8%	7.4	1.63	3.01
Sm 352	3.14 ± 5%	5.0	1.72	3.08
Sm Pool 7	2.34 ± 7%	6.4	1.75	2.93
Egg Albumin	2.45 ± 7%	4.8	1.57	2.30
Saccharin	1.53 ± 7%	6.9	1.45	2.30

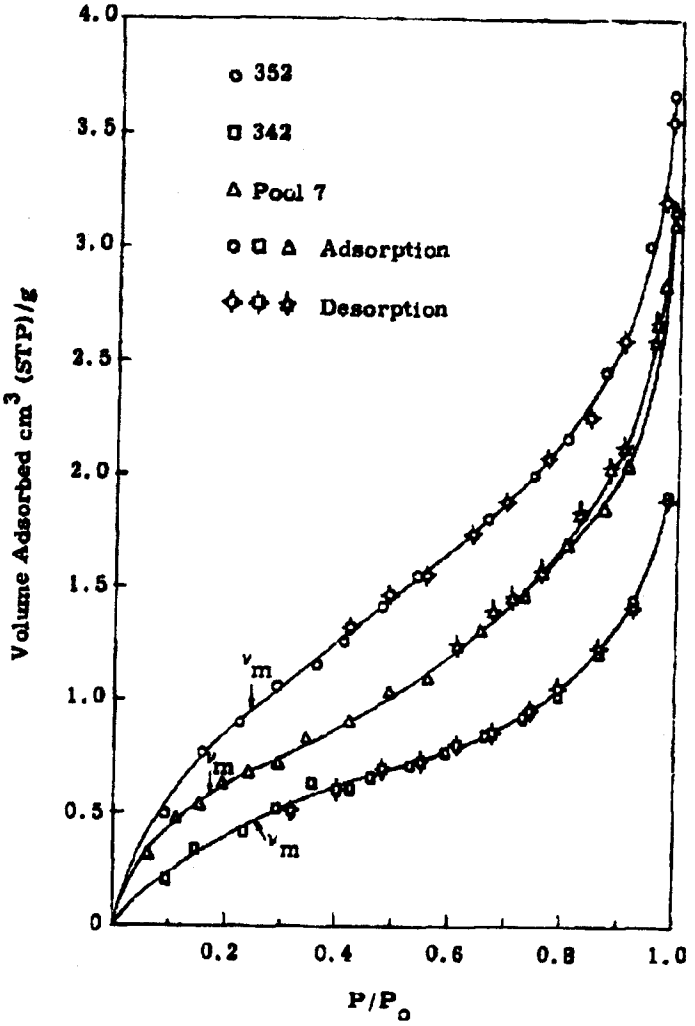

Figure 3.3 Nitrogen Adsorption Isotherm by Three Sm Samples

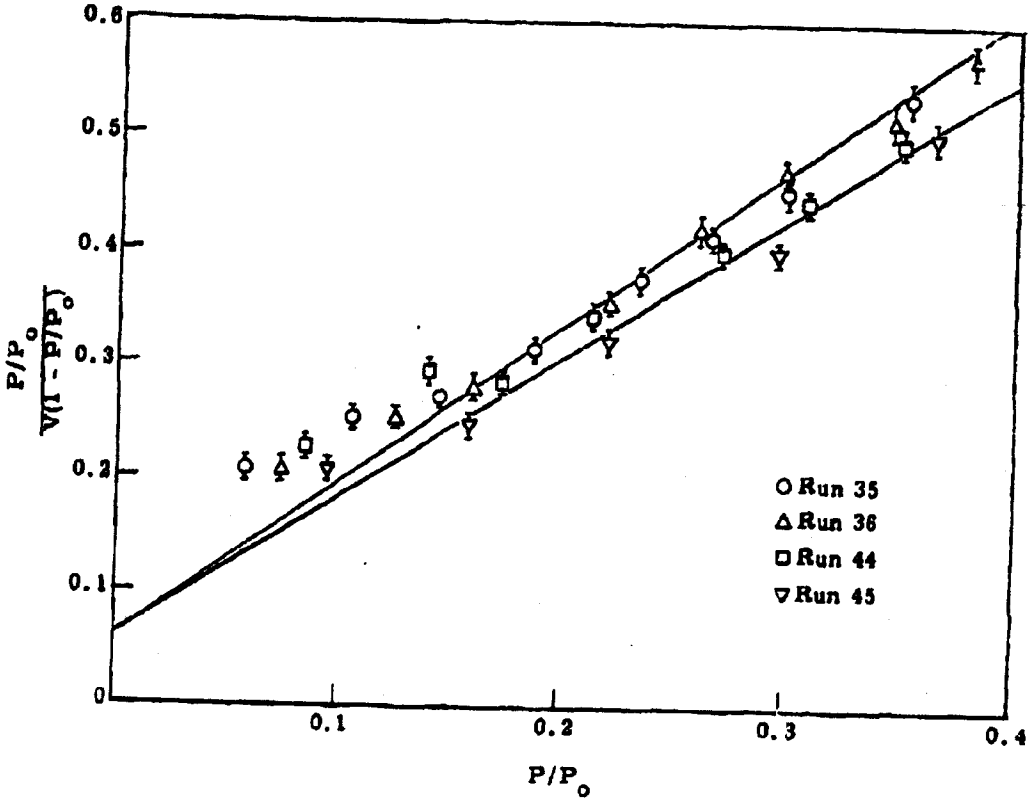

Figure 3.4 BET Plot of N_2 Adsorption on Sm 352

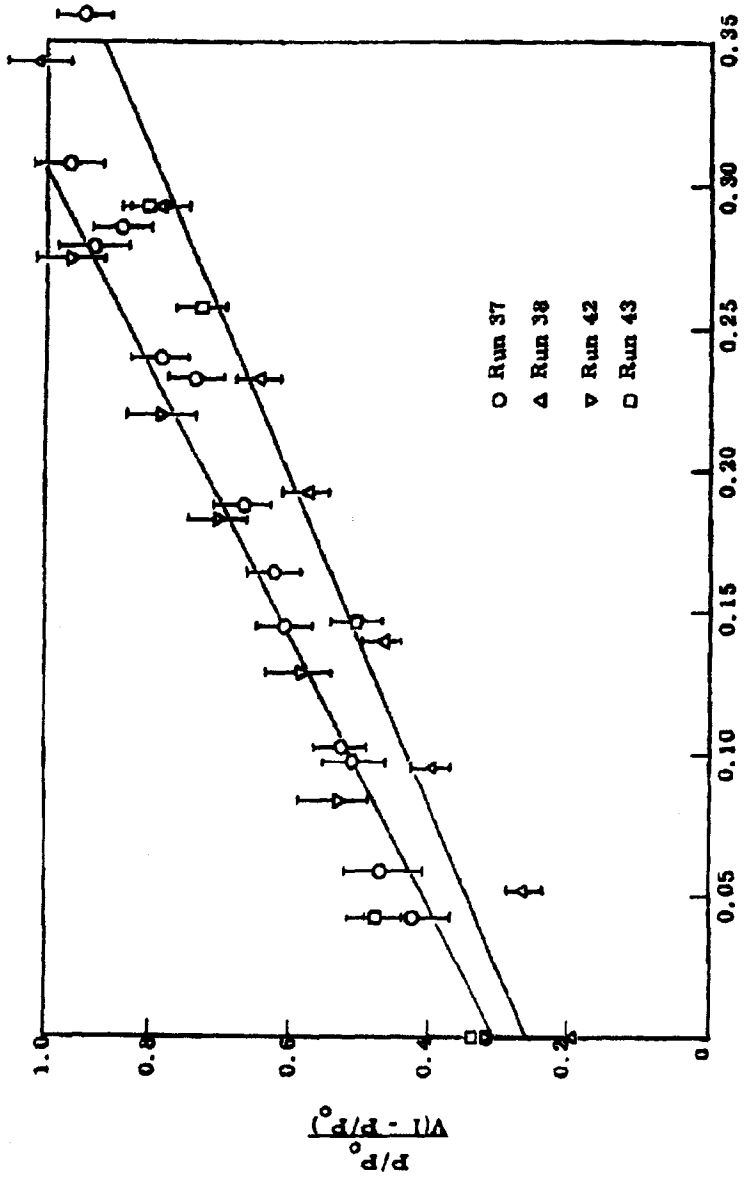

Figure 3.5 BET Plot of N_2 Adsorption on Sm 342

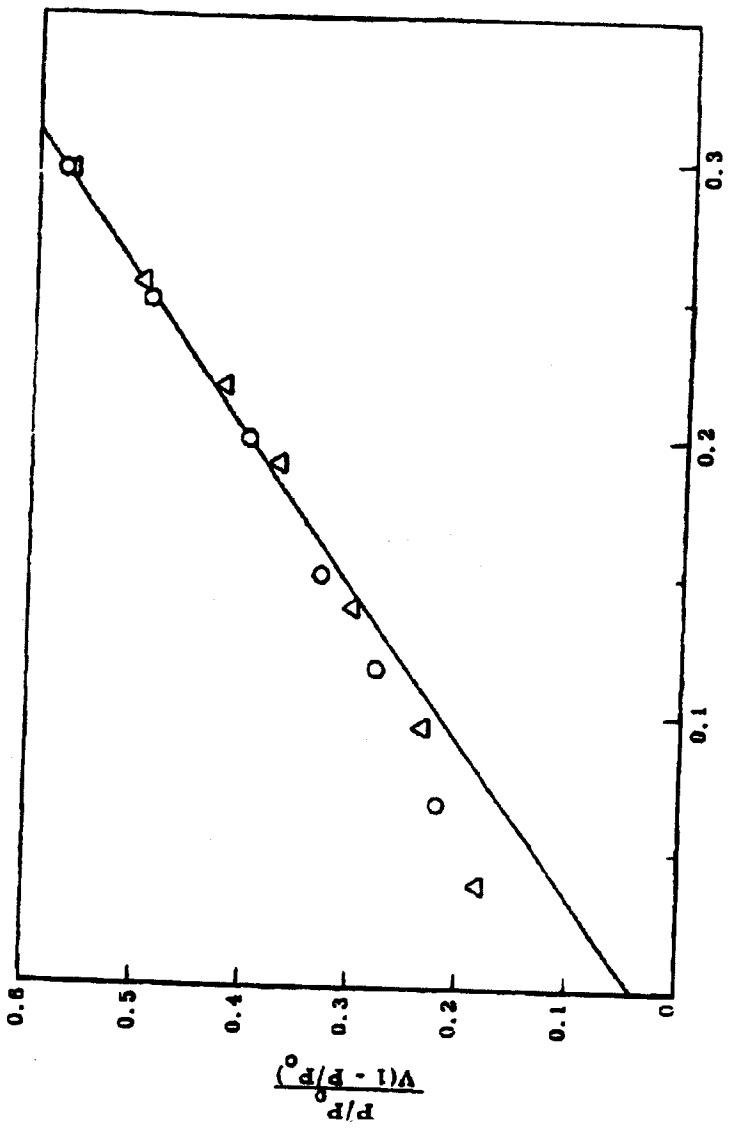

Figure 3.6 BET Plot for N_2 Adsorption by Sm Pool 7

The comparison of the Sm's to egg albumin and saccharin reveals some interesting differences. The rugosities for the Sm's are higher than the rugosity for egg albumin. Comparing the pore-size distributions, Figures 3.7 and 3.8 reveal only minor differences. This means that (1) the micro-pore structure of Sm is more extensive than egg albumin or (2) that Sm is more irregular or (3) Sm has more fines or (more likely) combines all three factors. The argument that Sm has more fine, receives some support from a comparison of σg -- a measure of the spread of particle sizes. Since Sm has a large σg, this means it has a wider range of larger and smaller particles and, since small particles contribute much to the surface area, it is expected that a particle-size distribution with the larger σg should exhibit the greater surface area.

From the BET plots, Figures 3.4, 3.5, 3.6 and Figure 3.2, we see another difference between Sm and egg albumin. The egg albumin is a typical plot with a small intercept (0.06) and the range of the BET equation is 0.1 to 0.3; whereas Sm has a large intercept (0.6) and the range of the BET equation is 0.18 to 0.36. If we look at the value of C from the BET equation:

$$\frac{P/P_o}{V(1-P/P_o)} = \frac{1}{V_m C} + \frac{C-1}{V_m C} P/P_o$$

which is related to the average heat of adsorption of the first layer, by

$$C = \exp \frac{|E_1 - E_2|}{RT}$$

where

E_1 = average heat of adsorption of the first layer

E_2 = heat of condensation

R = gas constant

T = temperature of adsorption

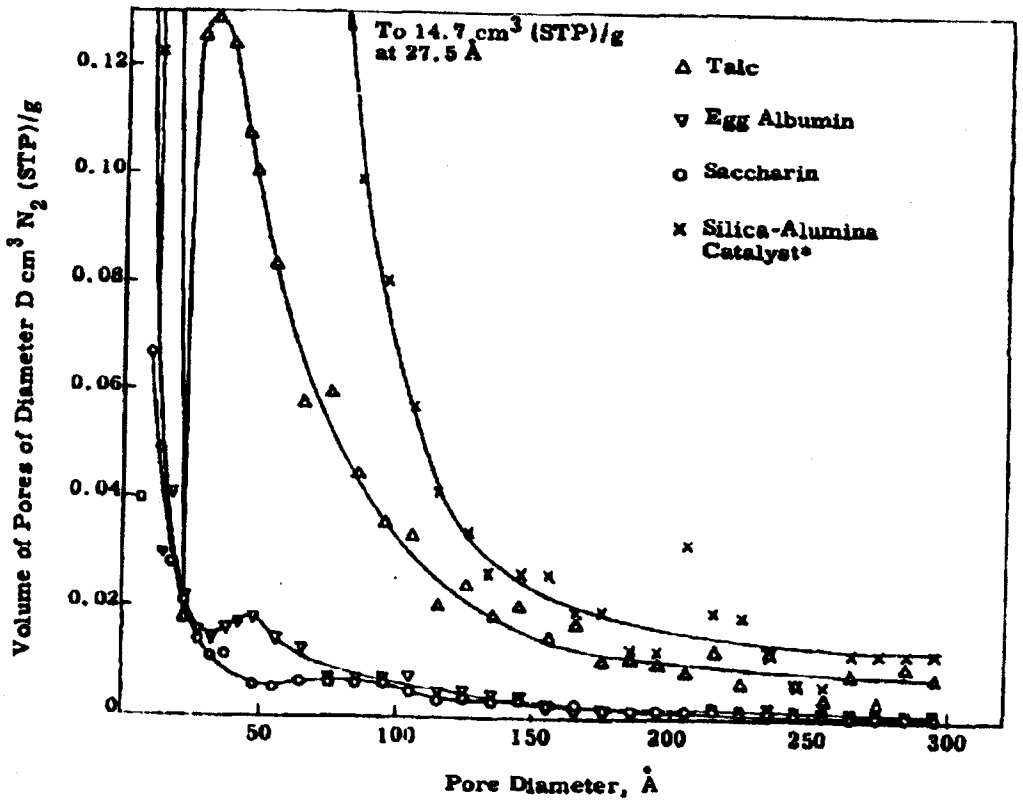

Figure 3.7 Pore Size Distribution of Various Materials

*Data from Cranston, R.W. and F.A. Inkley, Advances in Catalysis 9, pp. 143-54, 1957.

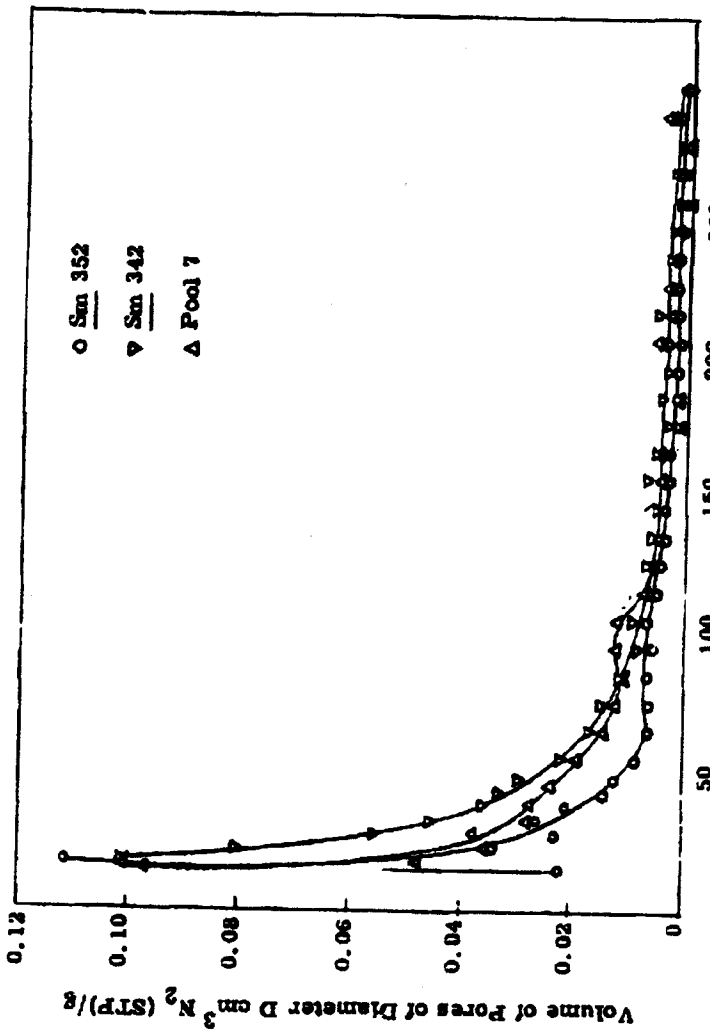

Figure 3.8 Pore Size Distribution for Various Sm Samples

For comparison purposes it is more convenient to use $E_{net} = E_1 - E_2$ and the equation in the form

$$C = E_{net}/RT$$

If we calculate C for egg albumin and Sm, we get approximate values

$$C_{EA} \sim 200 \text{ and, } C_{Sm} = 20$$

This means that E_{net} for egg albumin is approximately twice as large as E_{net} for Sm. Or, in other words, the Sm surface is only one-half as active towards adsorption as egg albumin. This explains why the Sm surface is so slow in becoming covered.

However, if egg albumin is freeze-dried,[4] it has the same general type of adsorption as freeze-dried Sm with V_m occurring at a $P/P_o = 0.2$ with a range extending much past 0.3). This indicates that mode of preparation has a great influence on surface characteristics.

3.2 Porosity of the Powder Particle

When total surface area measurements are made, the nitrogen monolayer forms not only on the external surface of the particle but on the internal pores, as well. Thus, to obtain an external surface area which can be related to the physical behavior of the powder, a measure of the pore volume of the powder must be obtained. In addition, the porosity of a powder is of interest with reference to kinetics of adsorption, as well as the structural strength of the powder particle. During this quarter, we have explored a method for determining the microporous structure of powders. Determination of macropore volumes will be investigated at a later date.

3.2.1 Micropore Structure

An investigation was conducted to determine the extent of microporous structure, pores with diameters up to 300 Å, in the materials under consideration in this study. The investigation did not include all the powders

but enough were studied to indicate trends. Of the powders studied, it was shown that only talc had some micropore structure and, for the most part, the other powders have negligible micropore structure.

Determining pore structure of catalysts has received much attention in industry. The history of the methods of application of adsorption isotherms of nitrogen to this problem has been reviewed by Wheeler.[5] The development presented here involves the Barrett, Joyner, and Hallenda method -- as modified by Wheeler[5] and the Cranston and Inkley[6] method.

At any point on an adsorption or desorption isotherm, the amount adsorbed, V_a, is composed of the amount adsorbed by capillary condensation, V_c, and the amount adsorbed on the walls of pores not filled by capillary condensation, by multilayer adsorption (V_m) or

$$V_a = V_c + V_m \tag{1}$$

Another way to say this is the total pore volume, V_g, not filled by adsorbed gases would be the volume of the pores with radii larger than filled by capillary condensation, R_c, not filled by the adsorbed multilayer or,

$$V_g - V_a = \int_{R_c}^{\infty} V(R)\, dR \tag{2}$$

where: V(R) is the volume of pores not filled by the adsorbed multilayer whose radius is R.

One method expressed V(R) in terms of the pore-size distribution L(R), the length of pores of radius R,[5] or:

$$V_g - V_a = \int_{R_c}^{\infty} \pi(R - t_{(R_c)})^2\, L(R)\, dR \tag{3}$$

where $t_{(R_c)}$ = thickness of adsorbed multilayer corresponding to the pressure needed to fill a pore of radius R_c by capillary condensation.*

Cranston and Inkley corrected the total pore volume of pores of radius R for the adsorbed multilayer to give the unfilled portion[6] or:

$$V_g - V_a = \int_{R_c}^{\infty} \left[\frac{R - t_{R_c}}{R}\right]^2 V_g(R)\, dR \qquad (4)$$

To solve, we have to differentiate with respect to R. Putting into differentials, Equation (3) becomes

$$d V_a = \pi \left[R_c - t_{(R_c)} \right]^2 L R_c\, d R_c - 2\pi\, d t_{R_c} \int_{R_c}^{\infty} \left[R - t_{(R_c)}\right] L_{(R)}\, d(R) \qquad (5)$$

and Equation (4) becomes

$$d V_a = \left[\frac{R_c - t_{R_c}}{R_c}\right]^2 V_g(R)\, dR - 2\, d t_{R_c} \int_{R_c}^{\infty} \frac{R - t_{R_c}}{R^2} V_g(R)\, dR \qquad (6)$$

These are "Volterra Equations of the First Kind" solved by iterative methods of assuming functions of $L(R)$ or $V_g(R)$.[7]

Various approximation methods have been employed in the past to circumvent the mathematical difficulties in such a development. The approximations of the Cranston and Inkley method are noted in the following sections.

Cranston and Inkley divided the isotherm into a finite number of steps stopping at an arbitrarily chosen largest pore diameter of 300 Å. At any interval, changing the pressure results in a change in the amount adsorbed, V_{12}, which is given by integrating Equation (6) from R_1 to R_2 -- the range of critical radii involved, or:

* The radius of the pore just filled at any pressure is composed of two terms: the radius calculated by the Kelvin Equation, and the thickness of the adsorbed multilayer, t, or $R_c = R_k + t$.

$$V_{12} = \int_{R_1}^{R_2} V_a \, dR = \int_{R_1}^{R_2} \left(\frac{R_c - t_{R_c}}{R_c} \right)^2 V_g(R_c) dR + \int_{R_1}^{R_2} dt_c \int_{R_2}^{\infty} \frac{2R - t_{R_1} - t_{R_2}}{R^2} V_g(R) \, dR \quad (7)$$

where $(2R - t_{R_1} - t_{R_2})$ is the average radius of the empty space as the thickness of the adsorbed layer decreases from t_{R_1} to t_{R_2}.

Then by assuming $V_g(R_c)$ as constant in each range of integration and equal to the average value $V_{12}/(R_2 - R_1)$, where V_{12} equals the total pore volume between pores of radius R_1 and R_2, and by replacing integration by summation up to R max using median values in each step, the working equation evolves

$$V_{12} = R_{12} \left[V_{12} - k_{12} \sum_{R_2 + 1/2 \Delta R}^{R \max} \frac{R - t_{12}}{2R^2} V_R \Delta R \right] \quad (8)$$

where

$$R_{12} = \frac{R_2 - R_1}{\int_{R_1}^{R_2} \frac{(R - t_{R_1})^2}{R^2} dR}, \qquad k_{12} = 4(t_2 - t_1), \qquad t_{12} = \frac{1}{2}(t_1 + t_2)$$

In terms of diameter

$$V_{12} = R_{12}\left\{V_{12} - k_{12}\sum_{D_2+1/2\Delta D}^{D_{max}}\left[(D-2t_{12})/D_2\right]V_D\Delta D\right\}. \qquad (9)$$

Equation (9) was applied to our desorption data for talc, saccharin, egg albumin, and three Sm samples using the Cranston and Inkley technique.

Results

Results of the micropore analysis for talc, saccharin, egg albumin, Sm 352, Sm 342, and Pool 7 -- together with the pore-size distribution for a catalyst from Cranston and Inkley -- are presented in Figures 3.7 and 3.8. Adsorption data for talc and saccharin were reported earlier.[8] Data for egg albumin and Sm appear elsewhere in this report.

From the curves, we see immediately that none of the powders, with the possible exception of talc, is porous when compared to a highly porous catalystic material. Even talc is not very porous when we compare the volume of the most common pores. Talc's volume of the most common pore is two orders of magnitude less than that for the catalyst. From these facts we can say the powders have negligible micropore structure when compared with highly porous catalytic materials.

If the powders had only a limited micropore structure, it would be expected that strange distributions would be obtained. This is the case for all powders, because the rapid upturn of the distributions indicates a large number of small pores. This would be significant were it not that the model begins to break down in the region of small pores, whereupon strange results are to be expected.

Since there is not a micropore structure sufficiently extensive to be measured by pore-size analysis methods, there surely are not enough

micropores to affect other physical properties, such as compaction. An indicator of the presence of micropore structure would be the roughness factor, $\frac{\text{BET area}}{\text{area from MMD}}$. If the roughness factor is not at least 10-15, it can be assumed that the micropore structure is negligible.

A roughness factor of 1.0 would be expected only for smooth spherical particles, such as glass spheres or ball bearings. Roughness factors, greater than 1.0 indicate that, in addition to being nonspherical, there may be some macropore structure. These are pores greater than 300 Å diameter. The largest macropores would be those affecting compaction characteristics. A possible method for investigation macropore structure would be the mercury porosimeter method of Rilter and Drake.[9]

Although care must be exercised in the interpretation of these curves, it should be noted that Pool 7 exhibits a small hump at about 100 Å, while talc and egg albumin exhibit humps in the 30-50 Å diameter range. In all cases it should be noted that the analysis fails soon after a hump has been reached. In the case of Sm's, it is sooner than for egg albumin, talc and saccharin. This fact is in direct relation when the monolayer formed; Sm's monolayer forms much later than that of talc, etc. Sm forms at a $P/P = 0.2$, while the others form at a $P/P \simeq 0.1$.

3.3 Particle Shape of Dried Egg Embryo Simulant

The electron microscope and light microscope were used to determine the particle shape of a new material, dried egg embryo simulant. This material is a mixture of silica, lactose, and the water-soluble extract of egg embryo that has undergone a freeze-drying process. Micrographs taken during this study are shown in Figures 3.9 to 3.13. Figure 3.13 is a light micrograph showing the general composition of the material. Figures 3.9 through 3.12 are electromicrographs of the darker particles shown in Figure 3.13. This simulant is a nonhomogeneous material consisting of a mixture of clear crystals, of clear and opaque, and some totally opaque particles. The particles shown in the electromicrographs are composed basically of submicron spheres. These spheres are probably silica, coated with lactose

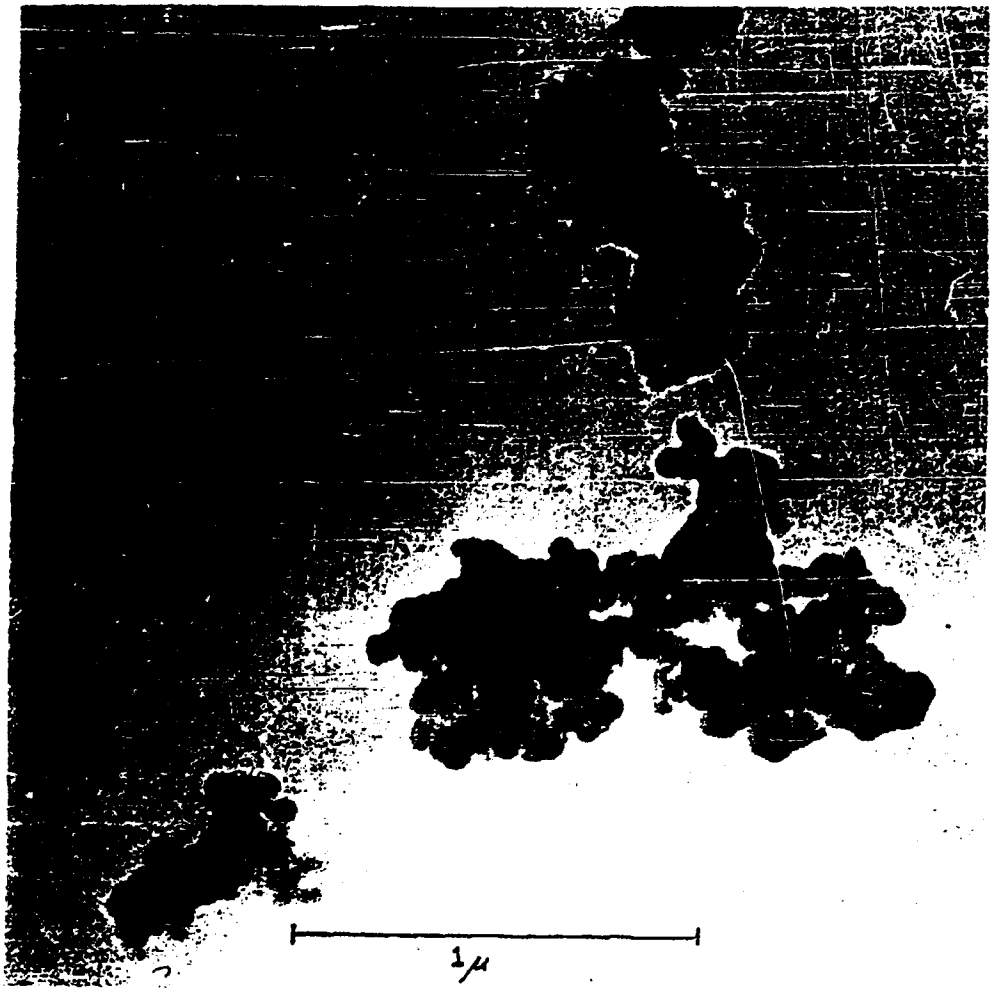

Powder Dried Egg Embryo

Method of Dispersion Ultrasonic Dispersion

Butyl Alcohol ≈ Spray Dispersed

Magnification See Scale

Micrograph No. 63-9-30 (Electron)

Figure 3 9 Electron Micrograph of Egg Embryo

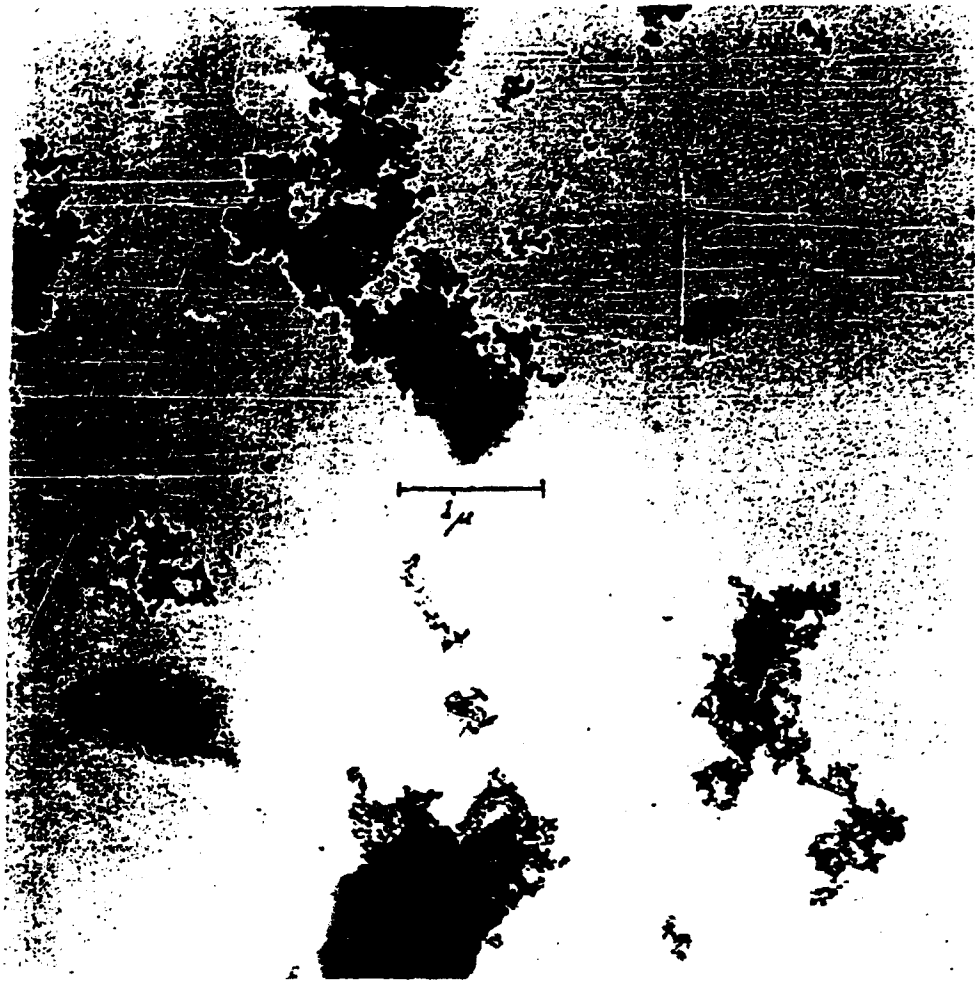

Powder Dried Egg Embryo

Method of Dispersion Ultrasonic Dispersion in Butyl Alcohol - Sprayed on Grid

Magnification See Scale

Micrograph No. 63-9-18 (Electron)

Figure 3.10 Electron Micrograph of Egg Embryo

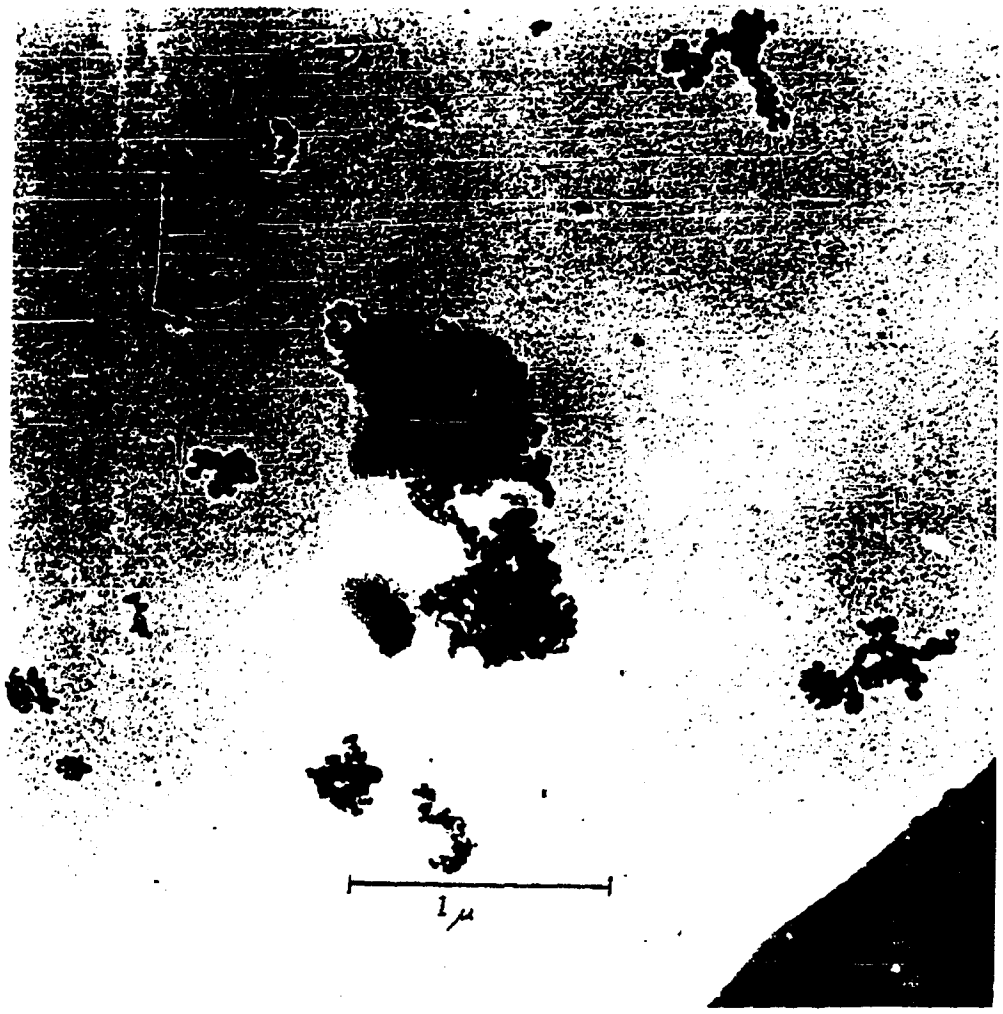

Powder Dried Egg Embryo

Method of Dispersion Ultrasonic Dispersion in Butyl Alcohol - Sprayed on Grid

Magnification See Scale

Micrograph No. 63-9-13 (Electron)

Figure 3.11 Electron Micrograph of Egg Embryo

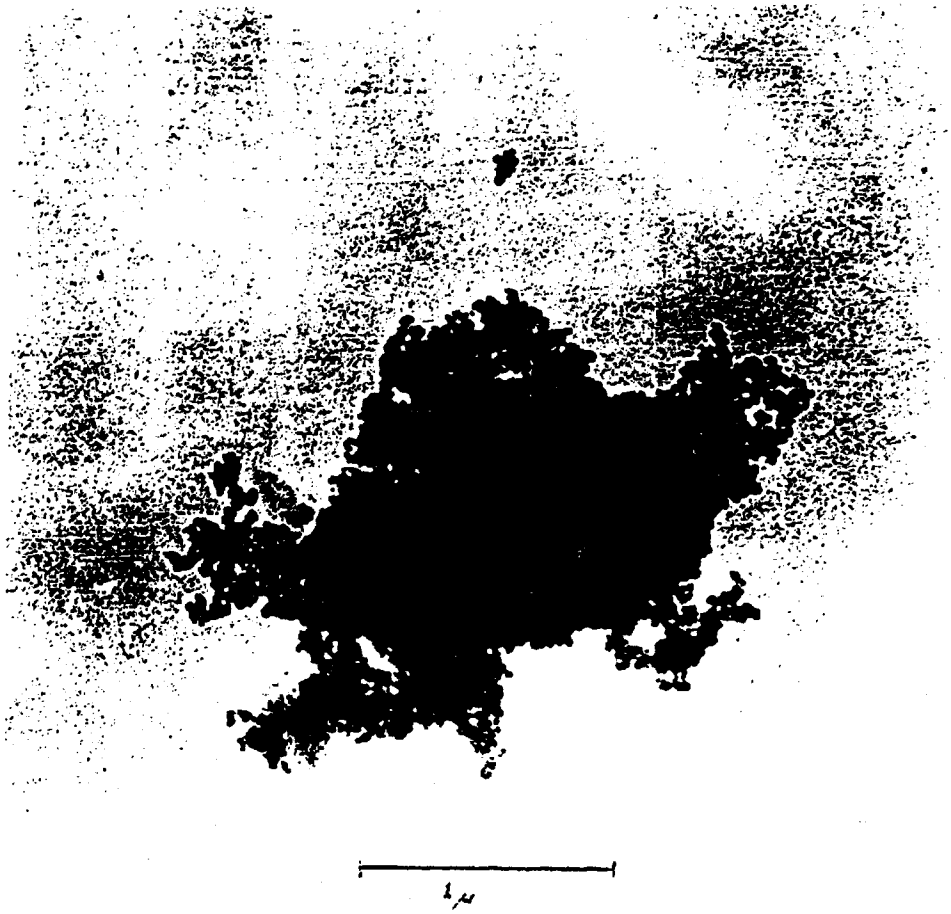

Powder Dried Egg Embryo

Method of Dispersion Ultrasonic Dispersion in Butyl Alcohol - Sprayed on Grid

Magnification See Scale

Micrograph No. 63-9-15 (Electron)

Figure 3.12 Electron Micrograph of Egg Embryo

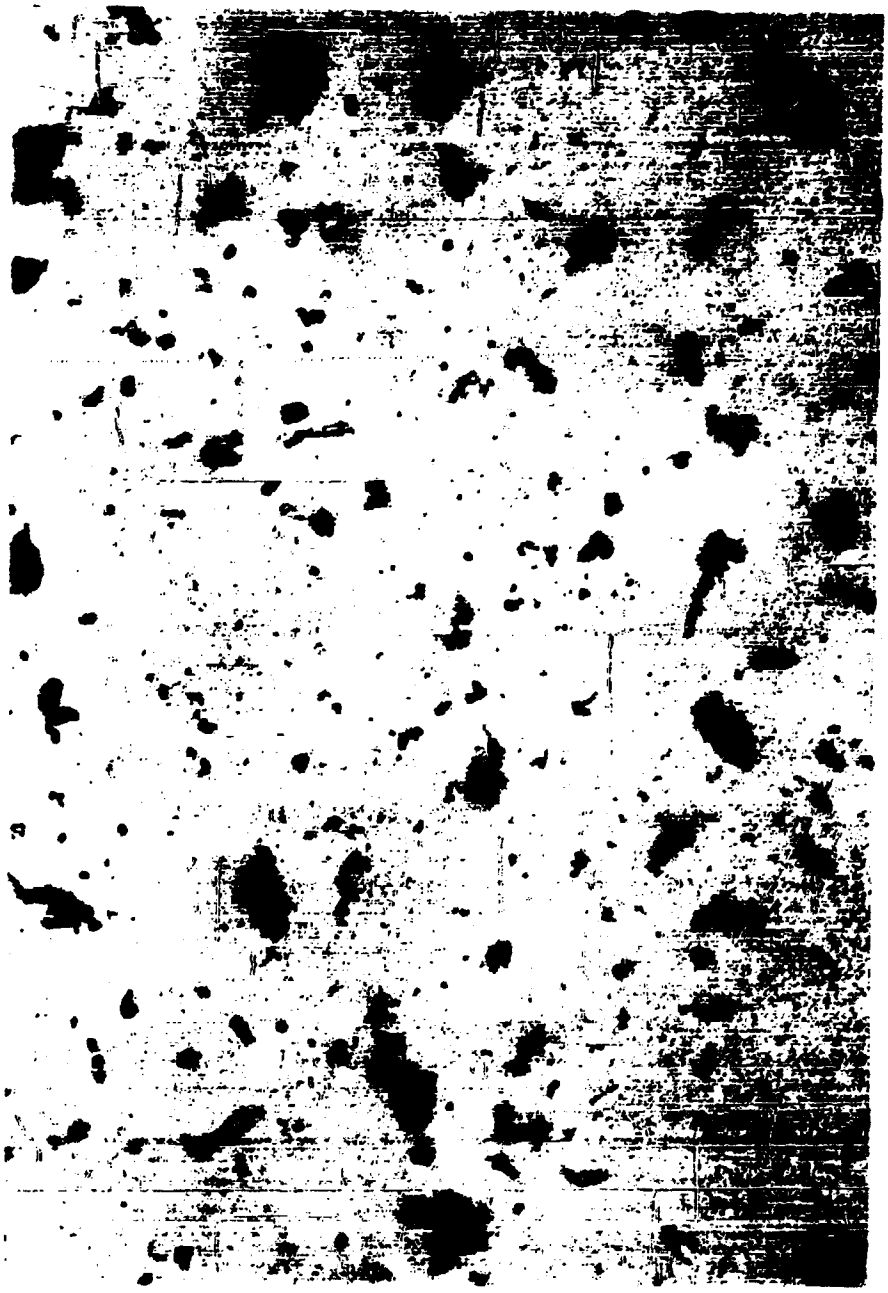

Figure 3.13 Light Micrograph of Egg Embryo

and/or egg embryo. This egg embryo simulant is a highly elastic material but appears to lose its elastic character when the sample is compacted to a high degree. This could be attributed to a possible breakdown of these submicron composites.

We are currently trying to determine, more specifically, the composition of these particles. In addition, a shadow-casting apparatus has just been installed which will aid in further elucidation of the particle structures.

4. AEROSOL STUDIES

In view of the importance of the effect of humidity conditions upon aerosol formation and decay, a new series of runs is underway.. The operating procedures are the same as those used previously except that considerably more emphasis has been placed on humidity control from the preconditioning of the powders to the precisely controlled chamber humidity and in our emphasis upon repetition of runs to supply a more secure data base. Also included in this report are the concluding runs in a series studying the effects of injected positive ions on aerosol formation and decay.

In the first section of this report, we discuss the operating procedure in detail. Many of the points of procedure will be familiar from previous reports. The data obtained from this quarter's work, and comments on these data, will be presented in the following sections.

4.1 Operating Procedure

4.1.1 Handling of the Powder Samples

Each of the aerosol runs conducted during this quarter involved 0.1-g sample of powder. These samples were prepared and conditioned in a standard manner as described below:

One-hundred ± 2 mg portions of powder were weighed out from stock and transferred to vials for humidity conditioning. The vials were stored in a glove box for at least two days before use. The humidity of the glove box is maintained continuously at 0.25 to 0.75 g H_2O/M^3. Prior to a given aerosol run, the swirl disperser was placed in the glove box and the powder sample transferred into it. The disperser was left in the glove box for one-half hour after which it was sealed by placing corks in the gas ports; thereafter, it was removed from the glove box, and mounted on the aerosol chamber. The dry-nitrogen supply line was then cleared by a short burst of the gas and was subsequently connected to the disperser. The cork in the outlet port of the disperser was left in place until pushed out by pressure of the gas when the disperser was operated.

The amount of powder lost in transfer is estimated at less than 5 mg; thus it is insignificant. It should be mentioned that the weighing of powder samples takes place at room humidity conditions so that a certain part of the 100 ± 2 mg sample weight is moisture; however, this is removed in the subsequent humidity conditioning.

4.1.2 Aerosol Chamber Humidity

A careful account was kept of the humidity in the aerosol chamber. For the electrostatic-charge runs, which were conducted with the chamber at room humidity, the procedure was to leave the chamber door open for one-half hour prior to each run so that the chamber was well flushed with room air. The room humidity was then read from an infrared hygrometer and the chamber was sealed for running.

The humidity runs were conducted in the same fashion as in earlier work. Runs were made both at room humidity and at low humidity. The latter chamber condition was obtained, as before, by placing about 200 g of fresh molecular-sieve dessicant in the chamber and sealing. A copper tube was run from the chamber to the hygrometer, so that the chamber air could be sampled directly. To prevent a depletion of air in the chamber while sampling, dry nitrogen was admitted at a rate equal to the sampling rates (5 liters/min). The connection of the hygrometer to the chamber also permitted a more relevant measurement of the humidity when operating at room conditions. The humidity measurements were made just prior to each aerosol run.

4.1.3 Standard Setting for Light Source and Photomultiplier Amplifiers

The procedures used to ensure constant-intensity light source and constant amplifier gain will be described briefly. To check the amplifier gain, a radioactive standard light source is placed in the aerosol chamber in a standard position so that it illuminates the phototube. The amplifier gain is then adjusted to yield a prescribed output (5.0 units). The working light-source intensity is then checked by placing a Blake culture bottle filled with distilled water in a standard

position in which it scatters some light from the bulb into the phototube. The lamp voltage is then adjusted to yield a prescribed output (0.5 units) at the amplifier. These checks were made at least once a day.

It is found that, after several days of warm-up, both the amplifier gain and the light-source intensity are quite stable. The combined stability of the two units is about ±2 percent.

4.1.4 Powder-Dispersing Procedure

The sequence of steps in starting an aerosol run has been described in earlier reports, but will be reviewed here for completeness. In the electrostatic-charge runs, dry nitrogen is jetted into the aerosol chamber from two diametrically opposed points - the one jet being the powder-dispersing jet and the other being the carrier gas for the ions. The ion carrier gas is started first and is adjusted to 30 psi (flow rate 0.16 l/sec). It is run for 1 minute. The disperser was operated at 130 psi for a 5-second interval starting 10 seconds subsequent to the start of ion-carrier gas flow. The disperser flow rate is 1.4 l/sec. The above sequence, where the high voltage was not applied (so that only dry nitrogen emerged from the ionizer), was called mode A. In mode B, the gas flow sequence was the same as in mode A, but the high voltage was applied for a 10-second interval starting 5 seconds prior to operation of the disperser. Thus, in mode B, the powder sample was dispersed into an atmosphere which had an abnormally high concentration of positive ions. In mode C, the gas-flow sequence was again the same but the high voltage was applied for a 10-second interval, starting 30 seconds after operation of the disperser. In this 30-second interval the powder becomes uniformly dispersed in the aerosol chamber so that the ions are injected into a preformed aerosol. The free ion current was approximately 0.3 microampere for these runs.

The humidity runs differed from mode A of the electrostatic-charge runs in that the ion carrier gas was not turned on. Thus the runs of this category were initiated by operating the powder disperser for a 5-second interval. The dispersing pressure here was 125 psi and the disperser flow rate was 1.44 l/sec.

The background light-scattering signal was checked between each run. The residual aerosol from the preceding run was removed, either by allowing several hours for settling or by flushing the aerosol chamber with room air. The background was typically 0.010 to 0.025 units.

4.1.5 Data Reduction

The raw data from each aerosol run consist in a trace of the light-scattering signal on a Brown recorder chart. The scattered light rises sharply from background sometime during the 5-second interval when the disperser is operated. An initial time is thus defined to within a few seconds. The signal at this initial time, however, is often not clearly defined. In fact, it is clear from the traces that many aerosols do not achieve a thorough dispersion until 15 to 30 seconds have elapsed. Therefore, for purposes of data reduction, we have taken the initial time as 1 minute after the operation of the disperser. The data to be presented, then, pertain to the decay of those aerosols which existed in the chamber 1 minute after operation of the disperser.

The raw data from the Brown recorder charts were replotted in logarithmic normal form. It was found that, with a few exceptions, the data so plotted could be fit well with a straight line. The reduced data presented later in this report for each aerosol run consist of the following three items:

1. The initial signal amplitude (that is, the signal amplitude 1 minute after operation of the disperser),
2. The aerosol half-life (the time required for the signal to fall to 50 percent of the initial signal), and
3. A measure of the slope of the log-normal plots -- obtained by dividing the time corresponding to 16 percent, into that corresponding to 84 percent.

4.2 Experimental Work and Results

4.2.1 Powders

The powdered materials studied in the present work were:

1. Talc, miatron vapor
   mass median diameter - 1.75 μ geometric standard deviation - 1.99 μ
2. Saccharin, 81524 stock
   mass median diameter - 6.9 μ geometric standard deviation - 1.58 μ
3. Powdered Sugar (ground)
   mass median diameter - 5.8 μ geometric standard deviation - 1.74 μ
4. Cornstarch
   mass median diameter - 12.2 μ geometric standard deviation - 1.28 μ

4.2.2 Humidity Runs

As mentioned, some of the earlier work on the effects of chamber humidity on aerosol decay has been repeated. The procedure was improved in that the powder samples were carefully humidity-conditioned in a dry box (relative humidity 1 percent to 3 percent) before dispersing and that more careful measurements were made of chamber humidity. The powders used in this study were talc, powdered sugar, and cornstarch. The reduced data from these runs are shown in Figures 4.1, 4.2, and 4.3. Most of these aerosol runs were done in triplicate and the data points in Figures 4.1, 4.2, and 4.3 are collected into corresponding groups of three. Considerable scatter is in evidence, although remarkably, the runs performed at low-chamber humidity show better reproducibility than those at room humidity.

Average values from the humidity runs are shown in the table below.

	Chamber Humidity, (g H_2O/M^3)	Initial Signal Amplitude (arbitrary units)	Aerosol Half-Life (min)	Slope Index
Powdered Sugar				
average of 3 runs	0.12	0.979	3.69	27.0
average of 3 runs	10.28	1.086	5.62	33.0
Talc				
average of 3 runs	0.19	0.759	4.1	33.0
average of 3 runs	11.44	1.038	8.2	39.3
Cornstarch				
average of 3 runs	0.4	0.091	1.04	12.8
average of 2 runs	10.7	0.067	1.12	13.1

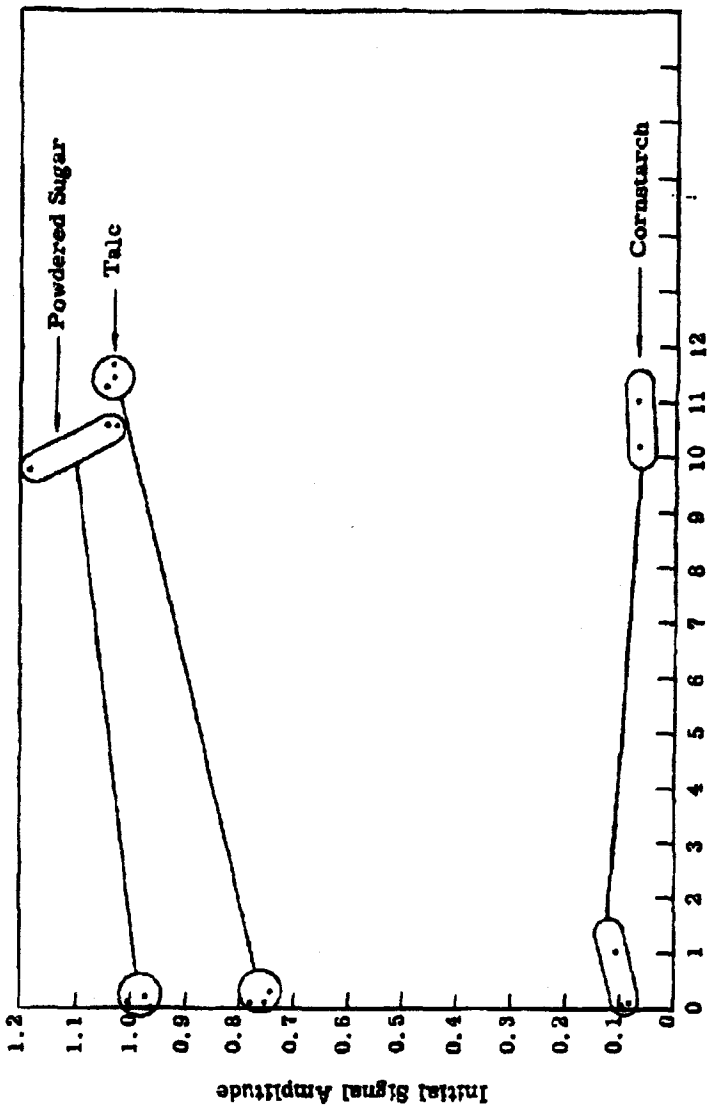

Figure 4.1 Plot of Initial Amplitudes for Humidity Runs

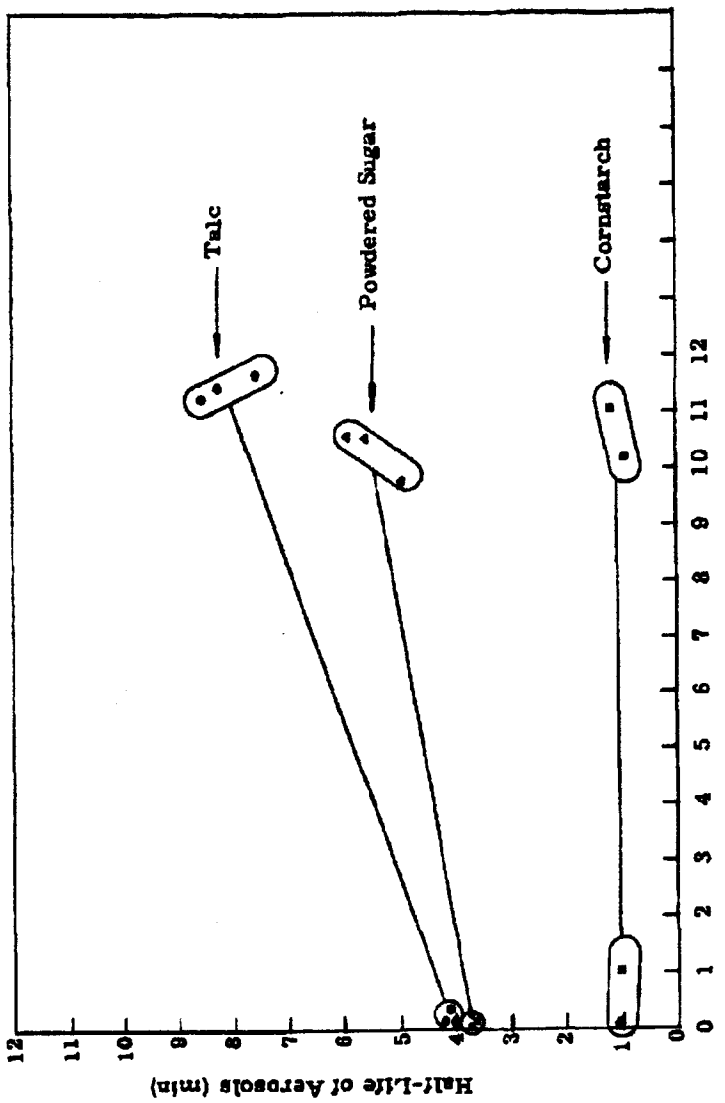

Figure 4.2 Plot of Aerosol Half-Life for Humidity Runs

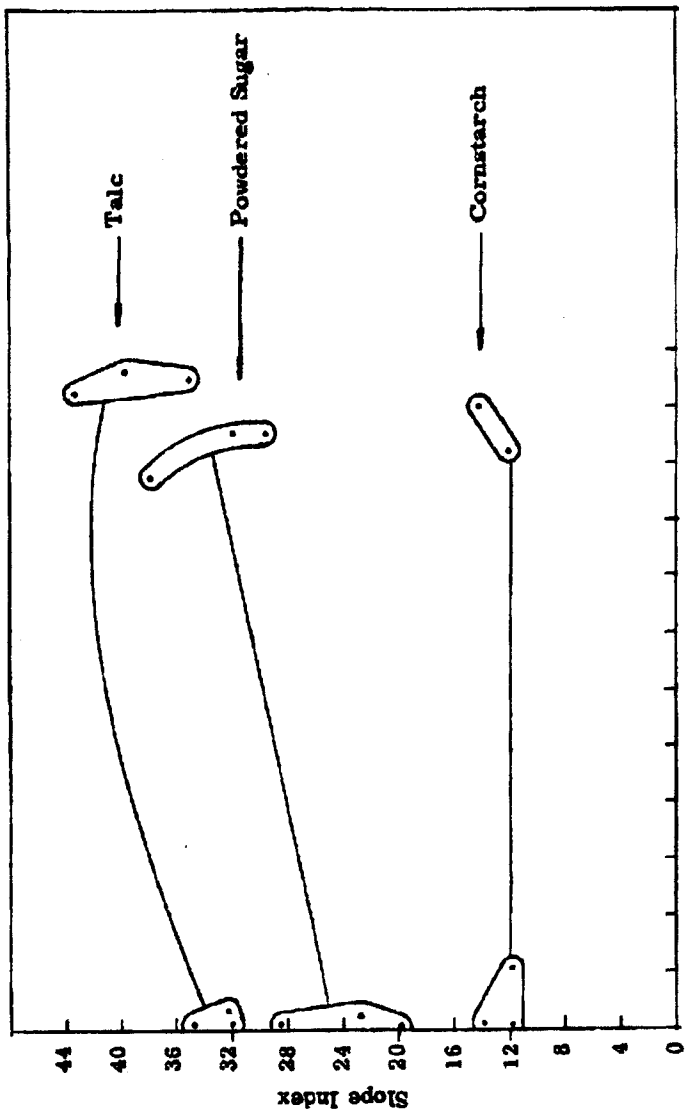

Figure 4.3 Plot of Slope Index for Humidity Runs

It is seen that talc is strikingly affected by chamber humidity. The half-life is doubled in passing from low-chamber humidity to medium-chamber humidity. The initial signal and the slope index are also considerably increased. The same changes, though less marked, occur for powdered-sugar aerosols. In the case of cornstarch, the half-life and slope index are barely affected by change of humidity condition, but the initial signal amplitude changes considerably and in a manner opposed to that of the other aerosols.

4.2.3 Electrostatic-Charge Runs

Electrostatic-charge runs were conducted on talc, saccharin, powdered sugar, and cornstarch. Only in certain cases, however, were duplicate runs made. These data are shown in Figures 4.4, 4.5, and 4.6. Averages computed from these data are shown in the accompanying table.

	Aerosol Chamber Humidity, ($g H_2O/M^3$)	Initial Signal Amplitude (arbitrary units)	Aerosol Half-Life (min)	Slope Index
Powdered Sugar				
mode A (average of 6 runs)	11.0	0.975	7.23	27.2
mode B (average of 3 runs)	10.8	0.979	8.9	28.3
mode C (average of 3 runs)	10.7	0.972	5.7	30.7
Talc				
mode A (average of 2 runs)	10.9	1.187	11.3	38.6
Saccharin				
mode A (average of 2 runs)	10.1	0.780	8.3	37.6
Cornstarch				
mode A (average of 3 runs)	10.7	0.082	1.52	15.0

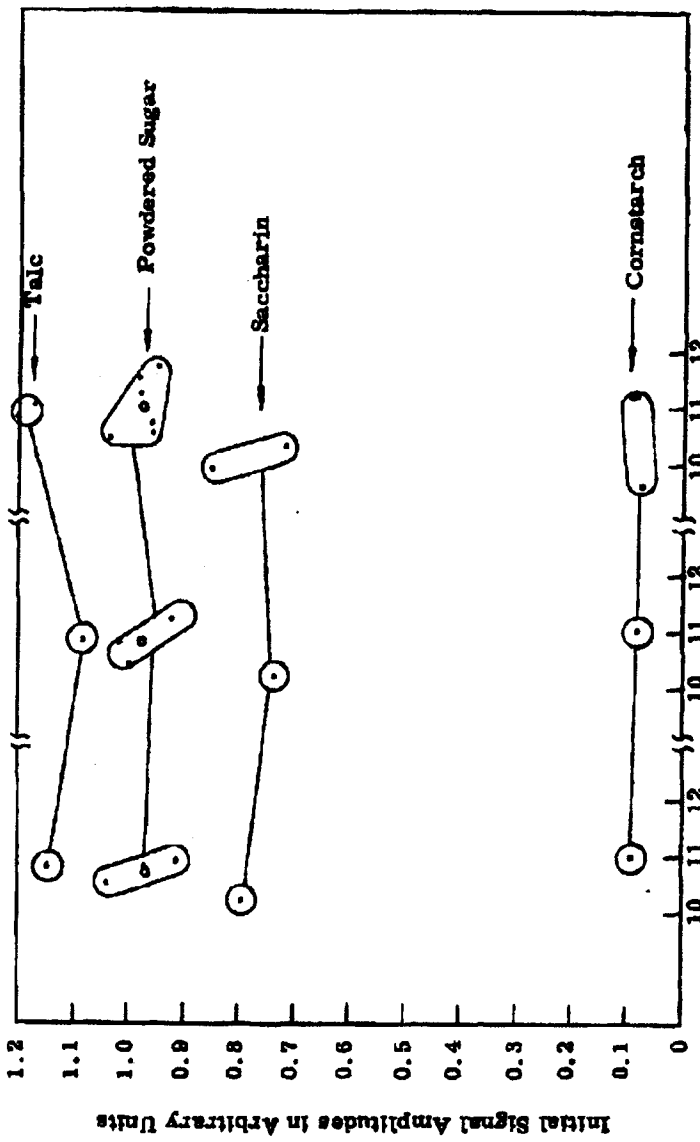

Figure 4.4 Plot of Initial Amplitudes for Electrostatic Charge Runs

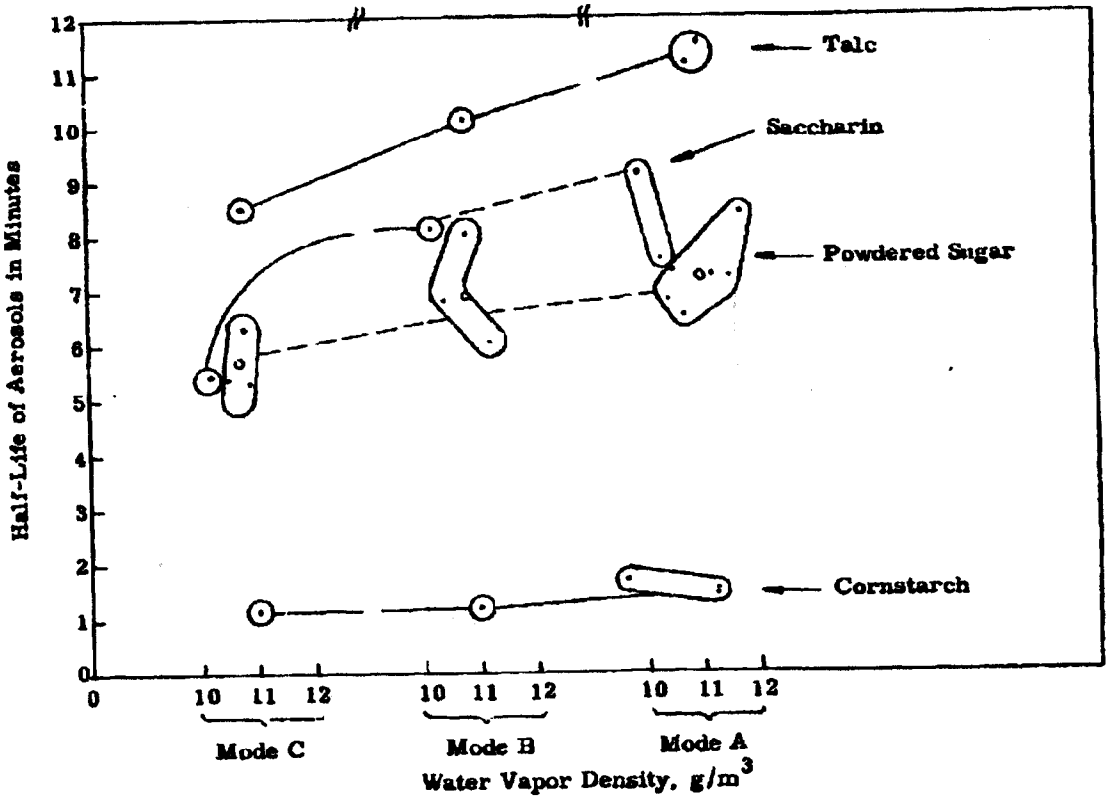

Figure 4.5 Plot of Aerosol Half-Life for Electrostatic Charge Runs

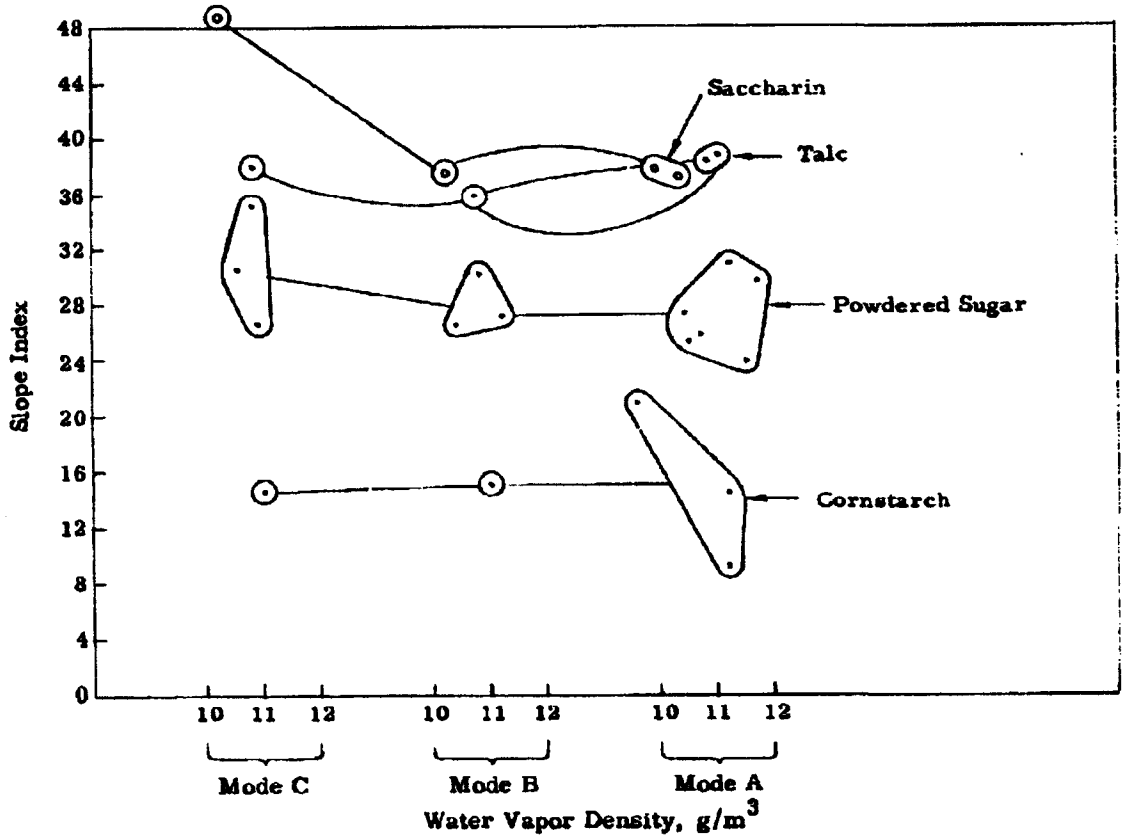

Figure 4.6. Plot of Slope Index for Electrostatic Charge Runs

Consider the powdered sugar data. It is seen that the initial signal amplitudes are the same for all modes of charge injection -- A, B, and C. This is one indication that the actual dispersing process is not affected by the injection of positive ions, either during the dispersing process (mode B) or just subsequent to it (mode C). (It should be recalled that the initial signal is read 1 minute after operation of the disperser, subsequent to the charge injection of either mode B or mode C.) Furthermore, the mode-B aerosols had half-life slightly lower than mode A, while that of mode C aerosols was substantially less.

4.3 Comments on Present Results and Correlation with Previous Results

Several significant points are suggested by the data of the present report. In examining these data, we shall keep in mind the hypothesis that the state-of-charge of the aerosol particles is strongly related to humidity conditions, so that the two series of runs reported herein may, in some sense, be two facets of the same phenomenon -- that of particle charge.

4.3.1 Electrostatic-Charge Series

It has already been mentioned that, in the electrostatic-charge runs, the initial signal amplitude seems unaffected by injection of charge, while the aerosol half-life is thereby markedly decreased (particularly in mode C). The former observation indicates that the aerosols which enter the decay phase of each run have identical degrees of monodispersity, so the changed half-lives cannot be due to changed particle size. These changes in half-life must then be due to attachment of injected positive ions to the aerosol particles, so that the aerosol cloud acquires net positive charge. This space charge increases the rate of migration of aerosol particles to walls.

4.3.2 The Humidity Series

It has also been mentioned that in the humidity runs, depression of chamber humidity prior to dispersing the powder resulted in aerosols with lower half-life and lower initial signal (cornstarch excepted). The conclusion to be drawn here

is that aerosol which survives the dispersing phase of each run has fewer independent particles per unit volume and larger average particle size in the dry case than in the medium-humidity case. This behavior has two possible explanations which, though essentially distinct, have the same practical effect in our experiment. First, the dry atmosphere may in some way inhibit the initial breakup of particles in dispersing or, second, the dryness may promote reagglomeration of the aerosol particles during the first 1-minute period.

The first of the two possible explanations is not very reasonable. One feels that the particle breakup is accomplished with sufficiently violent turbulence in the dispersing jet, that the humidity in the receptacle should have no effect. The second alternative, in which reagglomeration of considerable proportions takes place before the full dilution of the initial cloud, seems more tenable. In the event that the second alternative is operative, then we must ask why a dry atmosphere is more conducive to coagulation than a moderately humid one. In this connection, particle static charge comes to mind.

It may be supposed that the powder particles acquire some electric charge, through the triboelectric effects, in the process of being expelled from the dispersing unit. It is likely that there would be large quantities of particles of both signs. This charging process would be a common feature of all runs conducted during this quarter and since all runs started from common initial conditions, the extent of charging should be the same. Thus, if a particular condition of the receptacle atmosphere is to affect the dispersing phase of an aerosol run, it must be through the rapid alteration of the charge pattern of the forming aerosol. Our humidity results might then be explained by saying that the "abundant" water vapor present in a moderate humidity atmosphere causes rapid neutralization of particle charge and, thereby, of interparticle forces responsible for coagulation.

It may also be noted from Figure 4.3 that depressing the humidity of the receptacle atmosphere depresses the slope index. This indicates that a smaller variety of particle sizes is present in an aerosol formed in a dry atmosphere than in a humid one. We may imagine this as a tendency of small particles to attack to larger ones. The significance of the slope index is less clear in the case of the electrostatic-charge runs.

4.3.3 Relationship between Humidity Runs and Electrostatic-Charge Runs

In the two preceding sections the humidity series and the electrostatic series have been discussed separately. Interpretations with some degree of inner consistency have been advanced for both series in terms of static charge. When the implications of one series on the other are considered, however, contradictions arise which place interpretations in jeopardy.

In Section 3.2 we proposed that

1) Powder particles leave the disperser in a highly charged condition (both signs being copiously present) which caused rapid coagulation, unless
2) Water vapor is present in the receptacle atmosphere and is capable of rapidly discharging particles.

However, in Section 3.1, it was proposed that

3) Injection of copious amounts of positive ions, even at the most crucial moments, had no effect on the dispersing process, but that
4) There was considerable attachment of positive ions to aerosol particle.

Since the electrostatic-charge series was conducted at medium humidity, statements 2) and 4) are not entirely compatible. Statements 1) and 3) also tend in opposite directions. In the latter case, however, one may ask if the injected ions actually had opportunity to affect the dispersing process early enough.

An indication that the injected ions had early opportunity to interact with the powder particles may be had by comparing the mode A runs of the electrostatic series to the medium-humidity runs of the humidity series. These runs were conducted under conditions which were identical except that the mode A had a jet of dry nitrogen opposing the powder-dispersing jet.

The data compare as follows:

	Chamber Humidity ($g H_2O/M^3$)	Initial Signal (arbitrary units)	Half-Life (min)	Slope Index
Powdered Sugar				
mode A	11.0	0.975	7.2	27.2
medium humidity	10.3	1.086	5.5	33.0
Talc				
mode A	10.9	1.187	11.3	38.6
medium humidity	11.4	1.038	8.2	39.3
Cornstarch				
mode A	10.7	0.082	1.52	15.0
medium humidity	10.7	0.067	1.12	13.1

It is reasonably clear from the half-lives that better breakup of particles was achieved in mode A than in the medium-humidity runs. Among other things, this indicates a strong interaction between the jet of air from the ionizer and the developing aerosol cloud. It might, therefore, be expected that when ions are carried by the ionizer jet (as, particularly, in mode B), there is ample opportunity for ions to attach to aerosol particles.

While the half-life clearly gives the edge of mode A as a more thorough dispersing mechanism, the other data are not so clear. Normally, one would expect better breakup in dispersing to give a higher initial signal. This is not uniformly observed.

There is the possibility that the increased half-life in mode A over that of the medium-humidity runs is due to a more rapid dilution of the initial aerosols cloud; that is, the jet from the ionizer prevents reagglomeration, rather than facilitating breakup of particles. This, if true, would help to relieve the situation with regard to the inconsistencies mentioned earlier. Further information could be had by running experiments hybrid between the two series worked on this quarter. For example, if the humidity runs were done with the dispersing procedure of mode A, a better idea of the role of the additional gas jet in dispersing should evolve.

4.4 Summary and Future Work

The preceding sections have described our current state-of-the-art in the control and measurement of aerosol formation and decay. Considerable progress has been made in recent months in obtaining an experimental setup sufficiently precise to obtain accurate and reproducible results. Concurrently we have increased our depth of knowledge of the general behavior patterns of powders undergoing dispersion and decay. The dependence of the dispersibility and decay properties of powders upon such variables as atmospheric humidity, electrostatic-charge, particle size, shape, and composition is frequently complex. This emphasizes the need to eliminate as many variables as possible in our study in order to define basic behavior patterns.

With this in mind, the next step will be to study the dispersibility and decay properties of a single powder throughout the range of 0 to 100 percent relative humidity. Our experimental techniques are now sufficiently accurate to do this in a meaningful way. This will then provide us with basic information concerning operational and nonoperational regions with respect to effective dissemination of powders as a function of sample and aerosol exposure to atmospheric humidity.

5. DISSEMINATION AND DEAGGLOMERATION STUDIES OF STORED Sm

During this quarter, we continued to store samples of Sm in the compacted condition (bulk density 0.57 and 0.61 g/cm^3) at temperatures of -2 and -23C. At the present time, dissemination tests have been conducted for storage periods to 30 days. The results indicate that there is no significantly detrimental effect of storage on the physical deagglomeration efficiency for dissemination based on the principles used in the E-41 type disseminator. For this reason, we have deviated from the original test plan and omitted the 91-day storage period. In the near future, evaluations will be made of the 6-month samples.

Laboratory studies of the effects of storage on the viability of this material have continued with assays of the 2-month and 4-month samples. Again, the results to date indicate that there is no significant difference between the viability of compacted and uncompacted Sm in the range investigated.

6. E-41 SPRAY TANK

Work relating to the E-41 spray tank continued through the reporting period. Some of the effort was devoted directly to fabrication and test of the second unit which was completed during this quarter. Additional effort was expended in areas relating to the use of the two units in field evaluation programs.

6.1 Status of the Second E-41 Spray Tank

In August, 1963 the second E-41 spray tank was completed and tested in the laboratory at General Mills, Inc. This unit is scheduled to be used in flight tests with the "Mohawk" airplane at the Patuxent River Naval Air Test Center. It has been filled with compacted talc and is ready for shipment to the Grumman Aircraft Engineering Corporation, Bethpage, New York for fit tests prior to the Patuxent River flight program.

This second unit has been assembled with a tail section having four fins as shown in Figure 6.1. A similar tail section is also now available for the first E-41 spray tank so that both units can be flown in either the two- or four-finned configuration. There is only one set of internal components for each E-41 and these components must be transferred from one tail section to the other when a change in configuration is necessary. The drive unit and a bulkhead carrying several electrical items are the essential components which must be transferred but the effort required is minimal.

The tail section with 4 fins weighs 8 pounds more than the tail with 2 fins; therefore, the total empty weight of the E-41 with four fins is 726 pounds. There is also a small shift in the location of the center of gravity. The station locations of the center of gravity for empty and loaded conditions for the 2- and 4-fin configurations are as follows:

	2 fins	4 fins
Empty	Station 81.3	Station 82.2
Loaded with 300 lb payload plus 12 lb N_2	Station 81.9	Station 82.5

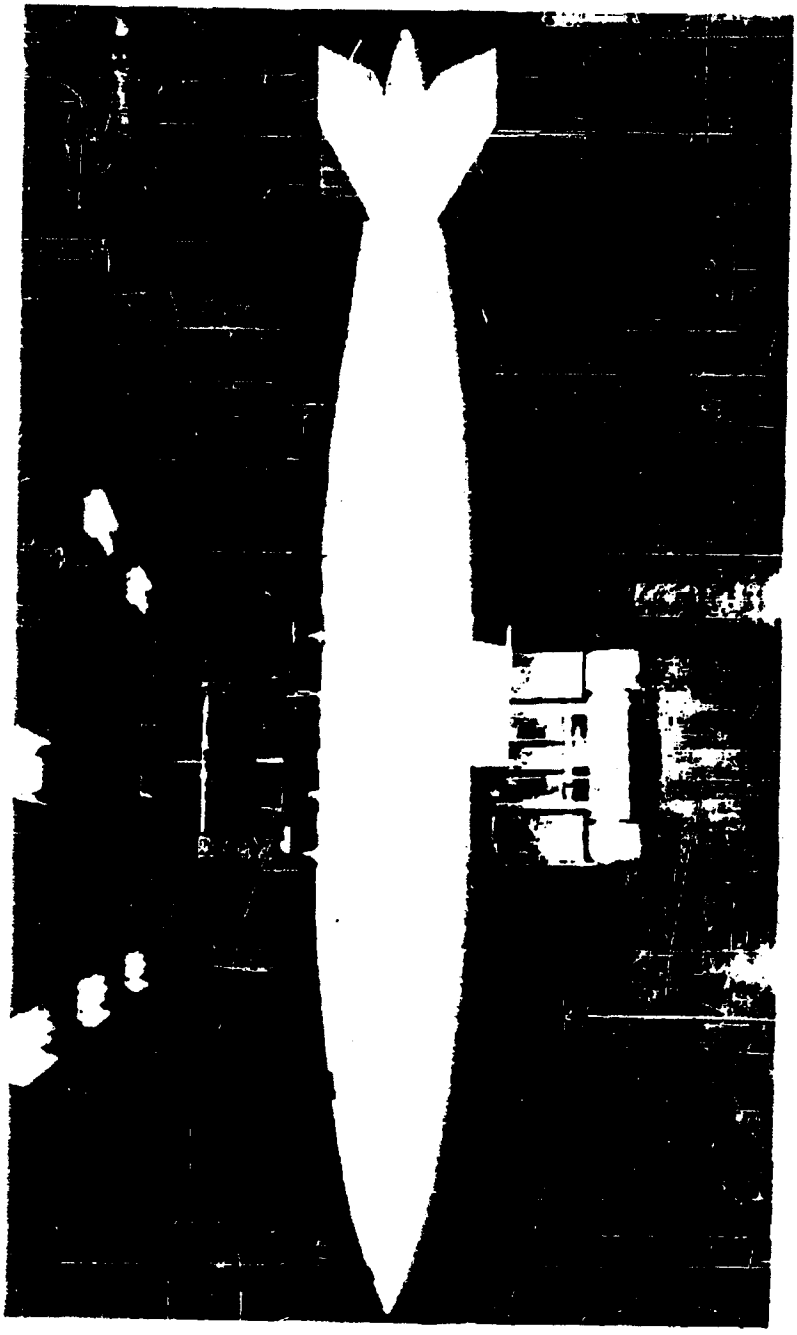

6-1 E-61 Spray Tank, Tail Section with Four Fins

With the existence of two E-41 spray tanks it now becomes possible to run concurrent field tests at widely separated locations. In fact, it appeared that the tests scheduled for Eglin Air Force Base and those scheduled for Patuxent could coincide or overlap. Therefore, essential items of support equipment such as the ground check out boxes and the gas charging equipment were fabricated or procured for the second unit. However, duplication of the filling equipment and the tail and nose handling carts is not contemplated at this time.

6.2 Preliminary Operating Procedures Manual

During this quarter work was initiated on an operating procedure manual for the E-41 spray tank. This manual will contain a description of the unit and detailed instructions for operating and servicing the unit.

6.3 Compaction and Discharge Tests of Talc in the Full-Scale Experimental Unit

Tests of compaction using the internal screw piston mechanism and subsequent discharge through normal operation were made with talc in the full-scale experimental unit. The compaction process consisted of disengaging the disaggregator from the screw (so that the disaggregator would not rotate while advancing the pistons to compact powder), filling the disseminator with loose talc, and driving the pistons inward with the screw advance mechanism until the powder was packed to the desired density. The process was repeated until the disseminator was filled with the desired amount of compacted powder. Attempts to disseminate in the normal fashion were then made. The features to be tested in this experiment are represented by the questions:

1) Can the screw piston be used with a reasonable torque to compact the powder?

2) Does internal compaction cause a wall force on the powder too large to allow advance of the compacted plug during the discharge operation?

3) Does internal compaction fill the screw threads so thoroughly that the screw piston mechanism cannot operate?

4) Can the powder entering the center section be removed so that the normal discharge operation can be begun?

5) Will the disengagement mechanism between the disaggregator and the screw be constrained by packed powder?

It was thought that the powder could be compacted with the internal screw-piston mechanism but that three negative influences exist: (1) the torque required might be excessive, (2) the powder might leak around the piston, and (3) the air in the powder might not escape sufficiently well to allow compaction. Felt-faced pistons with an array of air vents drilled through the pistons were used. The object of this arrangement was to allow air to escape through the felt and air vents to the back of the pistons; the object of the felt was to provide a seal between the piston and the cylinder wall. This arrangement worked: the air escaped as planned and there was virtually no leakage of the powder past the piston.

In the compaction operation a torque of 60 ft-lb was used; the powder packed to a density of .57 g/cc. The torque was steady during compaction. No difficulty with the powder in the screw threads occurred during compaction. For these experiments the pistons had thread cleaners of the design described in a previous report.[10]

It was determined that the powder which enters the disaggregator section during the compaction operation could be removed easily by introducing gas through the jets in the normal fashion.

The device used to engage and disengage the disaggregator discs consisted of a movable key in the center hub which mated with a slot in the power screw. A special screw driver was installed through the wall of the unit to advance or retract the key.

It was anticipated that powder might be forced into the mechanism during the compaction operation and disturb the function so felt seals were provided on the shaft to restrict the entrance of the powder through the clearance

between the shaft and the disaggregator hub. This disengagement mechanism functioned adequately for the tests but would have to be improved if used in an airborne unit.

In the first attempt to discharge the compacted powder, no difficulty was encountered. The torque was steady at less than 50 ft-lb. The second test yielded the same result. During the third test, the torque became prohibitively high (200 ft-lb) and the test was stopped. After the piston was backed off several inches, the test was resumed and the function was satisfactory with a torque of 100 ft-lb. In all tests, comparable densities were used (about .57 g/cc). The reason for the failure of the third test is not known, although the reasonable belief is that forces of the packed powder in the screw or the force of the powder against the wall caused the problem. Current plans are that further tests will be made in which the forces either at the screw or at the wall will be reduced so that difficulties can be isolated.

6.4 Experiments with Methods to Reduce Side Wall and Screw Friction

In anticipation of high forces on the screw and wall, concurrent tests have been made on means to reduce these forces. In an attempt to reduce the force between the wall of a cylinder and the plug of compacted powder, a group of dry lubricants have been applied to test cylinders to determine the affect of the lubricants on the wall force. These lubricants include molydenum disulfide, graphite, and Teflon powder. In order to reduce forces due to powder compacting in the screw threads, it has been considered that the threads could be filled with a material that would break away dependably without compacting as the hub is advanced along the screw. At this time, parafin and sodium silicate have been tried in qualitative tests and both appear to have potential applications. Quantitative tests have been made with the dry lubricants on the cylinder walls.

[redacted]

6.4.1 Use of Dry Lubricants to Reduce Side Wall Friction

Preliminary tests with graphite as the lubricant were discussed in the Twelfth Quarterly Report.[11] Data were presented which showed that graphite caused a significant reduction in the side-wall friction of compacted talc and powdered sugar.

Subsequent tests using six-inch diameter aluminum tubes treated in various manners and using the test method previously reported have shown that the effects of graphite are not as pronounced as was first reported. It appears that rather minor changes in surface roughness can change the wall friction sufficiently so that comparative tests are valid only for identical surface conditions.

The results obtained in these experiments are presented in Tables 6.1 and 6.2. Each value reported represents a single test and the variability inherent in the test method is evident. Table 6.1 gives the test data for compacted powder sugar where the reduction in friction resulting from the use of graphite is clearly evident. The data obtained with talc is contained in Table 6.2. Here, the wall friction on the smooth, bare aluminum surface was not reduced by the application of graphite. The bare aluminum surface, sanded so that scratch marks ran lengthwise of the tube, was as good as the smooth surface. For other surface conditions where roughness was a factor, the application of graphite generally caused a small reduction in wall friction.

By way of explanation, the Poxylube is a molybdenum disulfide-in-plastic dry film which is sprayed on. The film surface is comparatively rough. The Fluoro Glide is a powdered Teflon suspended in a vehicle which evaporates after spraying.

[redacted]

Table 6.1 Comparative Tests on the Effects of Graphite on the Wall Friction Force for Compacted Powdered Sugar in Six-Inch Diameter Aluminum Tube

Surface Condition	Compressive Force, lb	$\frac{L}{D}$ Ratio	Ejection Force, lb
Bare Aluminum	124	0.99	10
	124	1.40	20
	124	1.81	38
	246	0.94	32
	246	1.33	55
	246	1.71	99
	370	0.92	53
	370	1.29	108
	370	1.65	163
Dry Graphite	124	1.04	8
	124	1.39	16
	124	1.83	18
	246	0.97	17
	246	1.33	29
	246	1.71	42
	370	0.93	22
	370	1.29	52
	370	1.28	37
	370	1.28	37
	370	1.67	50

Table 6.2 Comparative Tests on the Effects of Surface Condition on the Wall Friction Force for Compacted Mistron Vapor Talc in Six-Inch Diameter Aluminum Tubes. (A Compaction Force of 100 lb Used in All Cases.)

Surface Condition	$\frac{L}{D}$ Ratio	Ejection Force, lb
Bare Aluminum	1.50	46
	2.06	68
	2.46	112
Dry Graphite	1.52	45
	2.10	75
	2.49	104
Graphite in Alcohol	1.53	42
	2.08	75
Graphite in Water	1.52	33
	2.10	75
Graphite in Trichloroethylene	1.48	33
	1.52	38
	2.06	66
	2.09	65
	2.43	115
	2.48	87
Vapor-Blasted Aluminum	1.50	51
	2.06	87
	2.47	125
Vapor-Blasted + Dry Graphite	1.50	41
	2.10	72
	2.47	110
Bare, Sanded Circumferentially	1.52	46
	2.04	84
	2.47	120

Table 6.2 Comparative Tests on the Effects of Surface Condition on the Wall Friction Force for Compacted Mistron Vapor Talc in Six-Inch Diameter Aluminum Tubes. (A Compaction Force of 100 lb Used in All Cases.) -- Continued

Surface Condition	$\frac{L}{D}$ Ratio	Ejection Force, lb
Sanded Circumferentially + Dry Graphite	1.50	39
	2.10	80
	2.47	115
Bare, Sanded Lengthwise	1.50	38
	2.08	69
	2.47	115
Poxy Lube 440	1.52	80
	2.10	200
	2.47	265
Poxy Lube 440 + Dry Graphite	1.52	67
	2.10	150
	2.47	205
Poxy Lube 440 Sanded	1.52	60
	2.10	135
	2.47	210
Poxy Lube 440 Sanded + Dry Graphite	1.52	40
	2.10	110
	2.47	180
Bare, Sanded and Buffed	1.52	45
	2.10	90
	2.47	115
Sanded and Buffed + Dry Graphite	1.52	20
	2.10	115
	2.47	115

Table 6.2 Comparative Tests on the Effects of Surface Condition on the Wall Friction Force for Compacted Mistron Vapor Talc in Six-Inch Diameter Aluminum Tubes. (A Compaction Force of 100 lb Used in All Cases.) -- Continued

Surface Condition	$\frac{L}{D}$ Ratio	Ejection Force, lb
Poxy Lube 330	1.38	90
	2.08	160
	2.38	245
Poxy Lube 330 + Fluoro Glide	1.50	65
	1.96	130
	2.42	245
Poxy Lube 330 + Dry Graphite	1.38	75
	1.96	130
	2.38	210
Fluoro Glide	1.45	65
	1.96	160
	2.42	220

6.4.2 Experiments with Filled Threads of Power Screw

Experience has shown that filling the E-41 spray tank by a procedure which packs the power screw threads with powder results in high thread friction between the screw and the piston nut. High thread friction is not experienced when the compacted charge is prepared with a central hole just large enough to accommodate the screw as is done with the presently used loading technique. This observation led to the conclusion that low thread friction should be obtainable in a direct filling procedure if the screw thread is pretreated so that the threads are filled with a substance which prevents entry of the powder and yet does itself not cause binding.

Two experiments were conducted to investigate the feasibility of such a scheme: one with parafin wax, the other with sodium silicate. A short length of the screw was filled with the substance and the piston nut was advanced over this portion of the screw. The piston nut had the thread cleaning feature. It was observed that both materials were effectively removed from the thread. However, a film of parafin remained whereas none of the sodium silicate stuck to the threads. The frictional torque was determined only comparatively and was observed to be higher with the parafin than for the dry threads. There was no appreciable increase when the sodium silicate was used. Both experiments were conducted without powder.

6.5 Flight Tests at Eglin Air Force Base

On 12 July 1963, an E-41 spray tank and associated support equipment were shipped to Detachment 4, ASD, Weapons Laboratory (ASQWC), Eglin Air Force Base for flight tests to demonstrate the compatibility of the spray tank with the F-100D and the F-105 airplanes. Because of circumstances attending the use of airplanes for tests, the E-41 has not yet been flown at Eglin. However, the unit has successfully passed fit tests on both aircraft and is ready for use whenever airplanes can be scheduled.

The E-41 spray tank was filled with compacted talc for the Eglin tests. Plans initially called for reloading with talc at Eglin and support equipment was shipped with the unit. Because of delays in the Eglin Program and the impending tests with the Mohawk airplane at the Patuxent River Naval Air Test Center, it was necessary to return the support equipment to General Mills, Inc., Minneapolis, so that the second E-41 spray tank could be prepared for the Mohawk tests. Dr. Joe Farmer of the Weapons Laboratory agreed to adjust the flight plans so that it will not be necessary to reload with talc at Eglin Air Force Base. There are approximately 200 lb of material presently in the unit to be disseminated during the tests. The support equipment for reloading is now at General Mills, Inc., Minneapolis.

7. FLIGHT TESTS OF THE E-41 ON THE MOHAWK AIRPLANE

On 12 July 1963, a planning meeting was held for the forthcoming flight tests of the E-41 spray tank on the OA-1 "Mohawk" airplane. This meeting was held at the Navy Department in the Bureau of Weapons with the following personnel present.

Mr. Jack P. Qualey, U. S. Army Biological Laboratories
Lt. Col. V. L. Ulery, BuWeps, RA 524
Mr. John Coursen, Grumman Aircraft Engineering Corporation
Mr. Gordon Whitnah, General Mills, Inc.
Mr. Joseph McGillicuddy, General Mills, Inc.
Mr. Don Harrington, General Mills, Inc.

As a result of this meeting, action was initiated to provide funding for the modifications to be performed by the Grumman Aircraft Engineering Corporation on the specific airplane to be used in the flight tests at the Patuxent River Naval Air Test Center. General Mills, Inc. was requested to provide Grumman with the necessary engineering data to permit them to proceed with a quote on costs to perform the required aircraft work.

A tentative date of 7 September 1963 was set for tests to commence at Patuxent. General Mills, Inc. was to ship the E-41 to Grumman by 15 August 1963 to allow them to check the unit on the airplane prior to shipment to Patuxent. It was definitely decided that the E-41 be provided with the tail section having four fins.

There has been a delay in scheduling the airplane modification work and, consequently, the E-41 spray tank has not yet been flown on the Mohawk airplane. The spray tank is presently at General Mills, Inc. and is ready for shipment to Grumman when they require it.

It is planned that two series of tests will be made with the Mohawk airplane flying out at Patuxent River Naval Air Test Center. The first flights will be made to demonstrate general compatibility of the E-41 on the Mohawk. Talc will be disseminated during these flights. The E-41 will then be reloaded with compacted Bg and a series of biological flight tests will be flown. It is planned that the Bg will be disseminated at Carrols Island at Edgewood Arsenal using a sampling tower to determine dissemination efficiency.

[redacted]

8. SUMMARY AND CONCLUSIONS

The work for the Thirteenth Quarter has been completed and is summarized in the following sections.

The segmented-column method was used to study the tensile strength of powders as a function of bulk density and of particle size. Data on powdered sugar and egg albumin are presented typifying behavior of the powders currently under study (Section 2).

The sliding-disk shear-strength method was studied in depth to determine the possible effects of preshearing, or not preshearing, the powder preparatory to the measurement of shear strength. Meaningful data were obtained for both conditions. It was concluded that preshearing the powder would yield data which could be related more logically to the compaction process (Section 2).

Two new powders, dried egg embryo simulant and a low-density Bg simulant, were incorporated into our study. The egg embryo simulant has been characterized as a nonhomogeneous rough-surfaced crystalline product that is highly elastic and difficult to compact. The Bg material appears to present no unusual problems (Section 2).

The fundamental behavior of two categories of powders was studied in depth to demonstrate that the techniques developed on this project will, in fact, characterize the behavior of powders in a meaningful way so that the various powder properties may be intelligently interrelated. The two categories were (1) different lots of the same sample, Sm, and (2) three different powders all having the same MMD. The powders were (a) ground saccharin, (b) spray-dried saccharin and (c) cornstarch. Data on shear strength, tensile strength, compaction characteristics, size analysis, particle shape, particle rugosity, etc., are presented and compared. The resulting comparative data correlate the powder properties in a self-consistent and logical manner (Section 2).

To study the behavior of the powders in the uncompacted state, the Powder Resistometer (recently designed and built in this laboratory) was used to measure interparticle resistance to flow in a number of powders. This apparatus has been shown to measure small differences in powder behavior with great precision and sensitivity (Section 2).

[redacted]

The BET adsorption method was again used to measure the surface area of a number of powders, including the three Sm samples mentioned earlier. In addition, a mathematical determination was made utilizing these data to determine the micropore structure of the powders under study. (Section 3).

The electron microscope was used to obtain information on the shape and structure of the egg embryo simulant. In addition, a shadow-casting apparatus is being installed in order to obtain greater definitions of the surface structure of the powder particles (Section 3).

The current aerosol studies emphasize the effects of electrostatic charge and humidity conditions upon aerosol formation and decay. Considerable progress has been made during recent months in obtaining an experimental set-up sufficiently precise to obtain accurate and reproducible results. We are now in a position to define operational and nonoperational regions in the relative humidity range of 0 to 100 percent (Section 4).

The storage of samples of compacted Sm (bulk densities 0.57 and 0.61 g/cm^3) at -2 and -23 C was continued. The original schedule calling for deagglomeration studies after 91 days has been altered and such studies will next be made after 6 months storage. Viability determinations on 2-month and 4-month samples showed no significant difference between compacted and uncompacted Sm during these periods (Section 5).

A second E-41 spray tank was completed in August 1963 and made ready for use in the flight test program with the "Mohawk" airplane. Tail sections with four fins are now available for both E-41 spray tanks. An operating procedure manual for the E-41 was started. Tests were conducted with the experimental model in which talc was successfully compacted within the unit using the piston-screw mechanism to accomplish compaction. Problems were encountered in subsequent operation of the unit to disseminate the talc. Experiments using dry lubricants to reduce side wall friction of compacted talc have shown that the gains are small but that surface roughness of small magnitude is an important factor. Parafin wax and sodium silicate were successfully

removed from a section of the power screw intentionally filled with these materials as a possible technique for keeping powders off the threads. The unit at Eglin Air Force Base has successfully passed fit tests on the F-100D and F-105 airplanes and is now awaiting flight tests (Section 6).

A meeting was held at the Navy Department to plan the tests using the E-41 spray tank on the Mohawk airplane. Grumman Aircraft Engineering Corporation was to prepare cost estimates for the airplane wiring modifications. General Mills, Inc. is to provide the E-41 fitted with a tail section having four fins. Flight tests will be conducted first with talc and then with Bg. The airplane will be based at the Naval Air Test Center, Patuxent River, Maryland (Section 7).

9. REFERENCES

1. Makower, B., S. M. Chastain and E. Nielsen. Moisture determination in dehydrated vegetables: vacuum oven method. Ind. Eng. Chem. 38: 725-31 (1946); and Stitt, F. Moisture equilibrium and the determination of water content of dehydrated foods. In Fundamental aspects dehydration foodstuffs, Papers Conf. Aberdeen, 1958. pp. 67-88.

2. Massachusetts Institute of Technology. Department of Nutrition and Food Science. Contribution no. 547, by G. J. Silverman and N. S. Davies (1963).

3. General Mills, Inc. Electronics Division. Report no. 2411. Dissemination of solid and liquid BW agents, by G. R. Whitnah. Contract DA-18-064-CML-2745. 12th Quart. Progress Report (March 4-June 4, 1963). Figure 2.13, p. 2-17. Confidential

4. Benson, S. W. and D. A. Ellis. Surface areas of proteins. I. Surface areas and heats of adsorption. J. Am. Chem. Soc. 70: 3563-69 (1948).

5. Wheeler, A. Reaction rates and selectivity in catalyst pores. In Catalysis II, Fundamental principles (Part 2), ed. by P. H. Emmett. N. Y., Reinhold, 1955. pp. 105-23 (1955).

6. Cranston, R. W. and F. A. Inkley. The determination of pore structures from nitrogen adsorption isotherms. Advances in Catalysis 9: 143-54 (1957).

7. Hildebrand, F. B. Methods of applied mathematics. Englewood Cliffs, N. J., Prentice-Hall, 1952. p. 439.

8. General Mills, Inc. Electronics Division. Report no. 2395. Dissemination of solid and liquid BW agents, by G. R. Whitnah. Contract DA-18-064-CML-2745. 11th Quart. Progress Report (December 4, 1962-March 4, 1963). p. 3-10; and Report no. 2411 (Op. Cit.). 12th Quart. Progress Report (March 4-June 4, 1963). p. 3-7. Confidential

9. Drake, L. C. and H. L. Ritter. Macropore-size distributions in some typical porous substances. Ind. Eng. Chem. Anal. Ed. 17: 787-91 (1945).

10. General Mills, Inc. Electronics Division. Report no. 2300. Dissemination of solid and liquid BW agents, by G. R. Whitnah. Contract DA-18-064-CML-2745. 7th Quart. Progress Report (December 4, 1961-March 4, 1962). pp. 6-7 and 6-8. Confidential

11. Op. Cit., General Mills, Inc., Report no. 2411. pp. 5-1 thru 5-9.